

**Development of a Waste Rock Simulation Model Including Placement Techniques to
Minimize Environmental Impacts of Acid Rock Drainage**

by

Rebecca Ramona Hurtubise

A thesis submitted in partial fulfillment of the requirements for the degree of

Master of Science

in

Geoenvironmental Engineering

Department of Civil and Environmental Engineering
University of Alberta

ABSTRACT

This research aims to develop a model using a systems dynamics approach that can be coupled with TMSim to account for the deposition of waste rock at hard rock mines at the feasibility stage of mine planning. The model includes waste rock placement techniques to minimize the environmental impacts of acid rock drainage at many hard rock mines. The GoldSim software was used to develop the model, with two aspects, the deposition of waste rock based on mine processes to create the “pile”, and the environmental conditions and associated variably saturated flow of water within the waste rock pile.

The conceptualization of the waste rock in the pile was constructed in four lifts. These four lifts were divided into 15 rows and 16 columns to create a pseudo 3-D structure of 240 1-D columns. The model includes waste rock deposition, precipitation, snowmelt, evaporation, runoff, infiltration, and seepage. The variably saturated system was modelled using a modified version of the variably saturated flow sub-model for a tailings cover. Modifications of the model included potential evaporation calculation, snow accumulation and meltwater calculation, and simplification of runoff.

The model was run using a case study for a mine site at the feasibility stage to demonstrate the application of the model. Overall, the model behaved as expected with general pile water balance behaviour observed over the course of construction and long-term behaviour. The models clearly show the benefits of paddock dumping versus end dumping with reduced water storage volumes within the pile.

ACKNOWLEDGEMENTS

This thesis could not have been completed without the support of my partner Taylor, my grandmother Emily, and my cats Peggy, Wilhelm, and Bing Bong. Taylor for patiently helping me visualize real world scenarios and brutal honesty when I needed it; my grandmother for always being only a phone call away to listen, even when she had no clue what I was talking about; and my cats for the many forced snuggles to get me through the day.

I would like to thank my supervisor Dr. Nicholas Beier for his guidance through this thesis, and patience over these last few years as I inched towards the finish line.

I would like to thank NSERC for funding this project through TERRE-CREATE, without which I would not have been able to complete this work.

TABLE OF CONTENTS

1	INTRODUCTION.....	1
1.1	Background.....	1
1.2	Scope and Objectives.....	2
1.3	Organization of Thesis.....	3
2	LITERATURE REVIEW.....	4
2.1	Introduction.....	4
2.2	Construction of Waste Rock Piles.....	4
2.3	Geotechnical Characteristics of Waste Rock.....	6
2.3.1	Particle Size Distribution.....	6
2.3.2	Water Content.....	7
2.3.3	Void Ratio and Density.....	7
2.4	Fluid Transport Through Waste Rock Piles.....	8
2.4.1	Liquid Transport Through Waste Rock Piles.....	8
2.4.2	Gas Transport Through Waste Rock Piles.....	12
2.5	Acid Rock Drainage Generation.....	13
2.6	Acid Rock Drainage Prevention and Mitigation Methods.....	14
2.7	Acid Rock Drainage Models.....	15
3	GENERAL MODEL DEVELOPMENT.....	20
3.1	Introduction.....	20
3.1.1	Model Objective.....	20
3.1.2	System Dynamics.....	20
3.1.3	Model Conceptualization.....	21
3.2	Simulation Model Components.....	23
3.2.1	Waste Rock and Overburden Management.....	24

3.2.1.1	Model Selection and Setup	24
3.2.1.2	Model Calibration	30
3.2.2	Snowmelt.....	30
3.2.2.1	Model Selection and Setup	30
3.2.2.2	Model Calibration	32
3.2.3	Evaporation.....	32
3.2.3.1	Model Selection and Setup	32
3.2.3.2	Model Calibration	34
3.2.4	Hydrogeology.....	34
3.2.4.1	Model Selection and Development.....	34
3.2.4.2	Model Calibration	37
3.2.5	Runoff	38
3.2.5.1	Model Selection and Development.....	38
3.2.5.2	Model Calibration	40
4	DEMONSTRATION OF MODEL APPLICATION	41
4.1	Introduction	41
4.2	Mining Inputs	41
4.2.1	Mine Plan	41
4.2.2	Stockpile Design.....	41
4.3	Waste Rock Inputs	44
4.3.1	Unsaturated Soil Parameters	44
4.3.2	Unsaturated Soil Parameters for Compacted Surface Layer	47
4.4	Climate Inputs	48
4.4.1	Weather Data	48

4.4.2	Evaporation.....	48
4.4.3	Snowmelt.....	52
4.5	Modelling Results	53
4.5.1	General Model Behaviour	54
4.5.2	Dumping Method Comparison.....	55
4.5.3	Mitigation Method Comparison	57
4.5.4	All Scenarios Comparison.....	58
4.6	Discussion	62
4.6.1	General Model Behaviour	62
4.6.2	Dumping Method Comparison.....	62
4.6.3	Mitigation Method Comparison	63
4.6.4	All Scenarios Comparison.....	63
5	CONCLUSIONS AND RECOMMENDATIONS	65
5.1	Conclusions.....	65
5.2	Recommendations for Future Work.....	66
	REFERENCES	68
	APPENDIX 1 – GOLDSIM ELEMENTS AND FUNCTIONS	79
	APPENDIX 2 – GOLDSIM MODEL DETAIL	83
	Model Overview	83
	Input Container	85
	Climate Container	89
	Mining Waste Container	93
	Saturated/Unsaturated Flow (End_Dump Container)	93
	Output Container	98
	APPENDIX 3 – MODEL USER GUIDE	99

APPENIDX 4 – RESULTS FROM MODEL APPLICATION 105

LIST OF TABLES

Table 2-1. Comparison of multi-component multi-phase reactive transport models	18
Table 3-1. Required information to determine heat content of snowpack (NRCS 2004)	31
Table 3-2. Coefficient of Determination	38
Table 4-1. Geometry of Modelled Pile.....	42
Table 4-2. Waste Rock Soil Parameters	44
Table 4-3. Soil parameters for Diavik waste rock (modified from Barsi, 2017).....	45
Table 4-4. Correlations of soil parameters normalized to soil D	45
Table 4-5. Unsaturated soil parameters for five waste rock soil types used in model.....	46
Table 4-6. Daily average precipitation and potential evaporation.....	49
Table 4-7. Calibration parameters after model optimization.....	52

LIST OF FIGURES

Figure 1-1. Classifications of Models (from Zheng and Beier 2018)	2
Figure 2-1. Waste rock pile configurations (from Hawley and Cuning 2017)	4
Figure 2-2. Waste Rock Pile Structure and Processes (from INAP 2009)	5
Figure 2-3. Proposed Waste Rock Pile configuration, built in benches with inclined compacted layers (from Broda et al. 2014, adapted from Maknoon and Aubertin 2013)	6
Figure 2-4. Typical particle size distribution ranges for waste pile rockfill materials (from Hawley and Cuning 2017).....	7
Figure 2-5. Effect of waste rock pile height on geotechnical parameters (from Hawley and Cuning 2017).....	8
Figure 2-6. Conceptual model for waste rock piles proposed by Herasymuik (1996) (from Wilson et al. 2011).....	9
Figure 2-7. Effect of hysteresis on the SWCC (from Fredlund et al. 2012).....	9
Figure 2-8. Typical soil water characteristic curve showing major zones of desaturation (Taken from Fredlund et al. 2012).....	10
Figure 2-9. Example soil water characteristic curves for waste rock piles.....	11
Figure 2-10. Type 1 Test Pile Benched with Herasymuik Classified Zones (from Barsi 2017)	11
Figure 2-11. Relationship between SWCCs and permeability function for sand and clayey silt (from Fredlund et al. 2012)	12
Figure 2-12. Factors that affect sulphide oxidation and transport (from INAP 2009).....	13
Figure 2-13. Stages in the formation of ARD (Modified from INAP 2009).....	14
Figure 2-14. ARD mitigation options and effectiveness with time (from INAP 2009).....	15
Figure 3-1. Conceptual Model.....	22
Figure 3-2. Causal Loop Diagram of Unsaturated Water Flow in Waste Rock Pile	23
Figure 3-3. Pseudo 3D Structure	25
Figure 3-4. Plan Layout of the Model Waste Rock Pile	26
Figure 3-5. Decision tree impacting construction of waste rock pile.....	27
Figure 3-6. Decision tree of PAG and NAG material flow	28

Figure 3-7. Conceptual set-up of the hydrogeology model (modified from Zheng, 2019).....	34
Figure 3-8. Geometric setup of the GoldSim model (modified from Zheng, 2019)	35
Figure 3-9. Comparison of Cumulative 1D Seepage to Base Case	37
Figure 3-10. Runoff prediction for a typical rainfall event (from Jubinville 2013, after Wilson 2006)	39
Figure 3-11. Direction of Runoff from Batter (Slope)	40
Figure 4-1. Waste Rock Pile Design.....	42
Figure 4-2. Area (m ²) of each cell of waste rock pile	43
Figure 4-3. Waste Rock Pile ARD Mitigation Options Design	44
Figure 4-4. Soil water characteristic curves for five waste rock soil types used in model.....	46
Figure 4-5. Soil water characteristic curves for compacted soil types used in model.....	48
Figure 4-6. Cumulative evaporation over one year of scenario modelled.....	50
Figure 4-7. Comparison of the cumulative evaporation modelled using GoldSim and Hydrus .	50
Figure 4-8. Cumulative 1-D seepage over one year of scenario modelled.....	51
Figure 4-9. Comparison of the cumulative 1-D seepage modelled using Goldsim and Hydrus .	51
Figure 4-10. 36-year mean modelled and measured snowpack depth in GoldSim.....	53
Figure 4-11. 50 Year Water Balance for Scenario 1: End Dumping with PAG Separation	54
Figure 4-12. 6 Year Water Balance for Scenario 1: End Dumping with PAG Separation	55
Figure 4-13. Comparison of normalized 1D water storage for each dumping method.....	56
Figure 4-14. Comparison of seepage for each dumping method	56
Figure 4-15. 1-D Water Storage for ARD mitigation methods with End Dumping	57
Figure 4-16. 1-D Seepage for PAG mitigation methods with End Dumping	58
Figure 4-17. Long-term Global Pile Precipitation.....	59
Figure 4-18. Long-term Global Pile Evaporation.....	59
Figure 4-19. Long-term Global Pile Runoff from Lift 1 Batter	60
Figure 4-20. Long-term Global Pile Runoff from Surface.....	60
Figure 4-21. Long-term Global Pile Water Storage	61
Figure 4-22. Long-term Global Pile Seepage	61

LIST OF SYMBOLS AND ACRONYMS

%	Percent
°C	Degrees Celsius
α	Constant in Thornthwaite method
α , DDF	Degree-day factor for snowmelt ($\text{cm } ^\circ\text{C day}^{-1}$)
a	van Genuchten model fitting parameter (m^{-1})
AE	Actual Evaporation
AEV	Air Entry Value
ARD	Acid Rock Drainage
c, SWE	Snow Water Equivalent ($\text{cm snow/cm precipitation}$)
cm	Centimetre
e	Void ratio
f_i	Transmission rate (m/s)
G_s	Specific weight of solids
H	Heat content of the snowpack
H_g	Conducted heat from underlying ground
H_l	Latent heat of vaporization from condensation or evaporation/sublimation
H_p	Advection heat from precipitation
H_{rs}	Net solar radiation
H_{rt}	Net thermal radiation
H_s	Sensible heat transfer from air
i	Heat indices
I	Sum of 12 monthly heat indices
INAP	International Network for Acid Prevention
K	Latitude correction factor for total sunlight hours in a month
K	Unsaturated hydraulic conductivity of the soil layer (m/s)
kg	Kilogram
kPa	Kilopascals
Ksat	Saturated hydraulic conductivity (m/s)
m	Metre
m	van Genuchten model fitting parameter
MEND	Mine Environment Neutral Drainage Program
mm	Millimetre
n	van Genuchten model fitting parameter
NAG	Non Acid Generating
NRCS	National Resources Conservation Services

PAG	Potentially Acid Generating
PE	Potential Evaporation
Ph	Pressure head within the soil layer, as a positive number (m)
Ps	Precipitation as snowfall identified by T_{crit} (cm day^{-1})
q, θ	Volumetric Water Content
Q_R, θ_R	Residual Volumetric Water Content
Q_S, θ_S	Saturated Volumetric Water Content
R^2	Coefficient of determination
s	Second
S	Water in snow storage (m)
SD	System Dynamics
S_e	Normalized effective volumetric water content
S_i	Amount of water stored in the soil layer (m)
S_s	Specific surface of solids (m^2/kg)
S_T	Total water storage within all soil layers (m)
SWCC	Soil Water Characteristic Curve
T	Daily mean temperature ($^{\circ}\text{C}$)
T_a	mean monthly air temperature ($^{\circ}\text{C}$)
T_{crit}	Critical Temperature where below it, precipitation occurs as snow
Thk	Thickness of the soil layer (m)
TMSim	Tailings Management Simulation Model

1 INTRODUCTION

1.1 Background

One of the main environmental concerns with hard rock mines is acid rock drainage (ARD) generation in waste rock piles. The process occurs when sulphurous rock reacts with atmospheric oxygen and water. The rate of sulphide oxidation in waste-rock piles is slow initially, but if oxygen and water continuously enter the waste rock pile, the rate of acid generation increases rapidly as the pH decreases (Bussi re 2007). One of the current accepted ARD management techniques is the construction of cover systems that limit oxygen and/or water infiltration (Johnson and Hallberg 2005). This strategy is often implemented once the entire waste rock pile has been constructed. However, the operation and construction of a waste rock pile can occur over many years or decades. The process of ARD generation starts the moment water and oxygen are introduced to sulphide materials within the waste rock (Wilson 2011). To minimize the generation of ARD, it is important to decrease the oxygen or water present within the pile during construction (Johnson and Hallberg 2005). ARD mitigation strategies that can be implemented during construction include encapsulation, layering, progressive capping, blending, and co-disposal (INAP 2009).

Modeling techniques in the field of mine waste management are predominately process-based approaches that typically study only one aspect of the mining and waste interactions (e.g., water balance, ARD, tailings dewatering, storage embankments, etc.). Each of these processes are typically modelled separately using complex analytical tools and are focused on one detail of the mine design, not the overall mine waste management plan performance. Decisions regarding ARD mitigation strategies made during the early stages of mine planning can irrevocably affect successful mine waste management over the life of the mine and post closure. There is a need for the ability to predict long-term behaviour of the entire life of mine to aid in the development of mine waste management plans. There are few available models or approaches that look at the whole system of mine waste management over the mine lifespan. One such tailings management simulation model (TMSim) uses a system dynamics approach to evaluate tailings dewatering

technologies on their ability to meet reclamation and closure goals (Beier 2015; Beier et al. 2020). System dynamics philosophy allows the user to simulate large complex inter-related systems that cannot be modelled with a traditional process-based software. When modelling systems, there must be a balance between the level of detail and the breadth, or scope of a model. As seen in Figure 1-1, as the level of detail and number of processes increase, the breadth of the model decreases. In system dynamics modelling, simplifications are necessary in order to model large scale systems. TMSim and the other models, however, do not incorporate ARD and related rock overburden waste management strategies specifically encountered at hard rock mining operations.

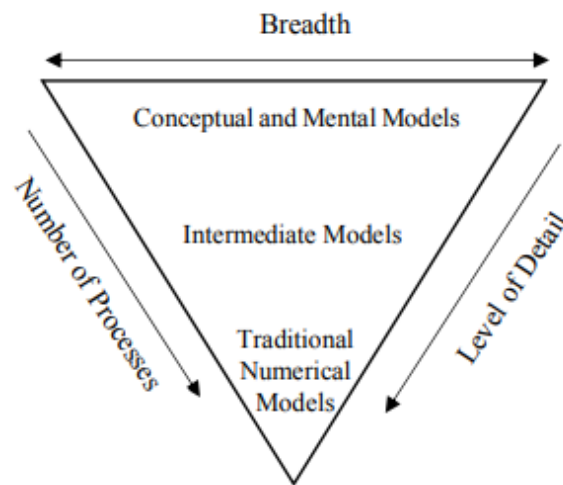


Figure 1-1. Classifications of Models (from Zheng and Beier 2018)

1.2 Scope and Objectives

The research aims to develop a model using the same approach as TMSim to account for ARD phenomena in mine operations. This will be done by incorporating a waste-rock deposition and mass balance sub-model using the GoldSim software to account for the development and configuration of waste-rock piles to evaluate the water balance. Water balance information from the waste rock pile would subsequently be used to support geochemical predictions of water quality. The flow of air (oxygen) can have a significant impact on the rate of geochemical reactions; however, the flow of air and geochemical modelling are not within the scope of this thesis.

This thesis will outline the conceptual model and approach to developing the waste rock sub-model that could be coupled with TMSim in future. The waste rock model will be broken down into two separate components, mine related, and environment related. The mine related calculation will consist of a series of arrays based on the mine plan that will dictate the input conditions into the 1-D variably saturated environment component. Specific strategies to be incorporated into the model include traditional end dumping of waste-rock (base case), paddock dumping to prevent segregation, encapsulation or layering of potentially acid generating (PAG) material with non-acid generating (NAG) material, and compaction of the surface layer to limit seasonal infiltration, these will be discussed further in section 3.2.1. The model will output water balance information that, coupled with geochemical predictions, can be used to evaluate the specific waste management strategies.

1.3 Organization of Thesis

This thesis contains five chapters. Chapter 1 introduces the research objective and background information. Chapter 2 presents a review of relevant literature outlining previous studies into hard rock mining, construction of waste rock piles, geotechnical characteristics of waste rock, fluid transport through waste rock piles, ARD generation, prevention, and mitigation, and ARD models. Chapter 3 discusses how the model was developed in GoldSim and how each component was setup and validated. Demonstration of the model using a case study is presented in Chapter 4 including a comparison of the water balance for several waste management strategies. Finally, Chapter 5 presents the conclusions of the research study as well as recommendations for future work on the GoldSim model. Appendix 1 includes details on GoldSim elements and their uses, Appendix 2 includes the GoldSim Model detail, Appendix 3 provides a user guide to setting up the inputs for the model, and Appendix 4 includes the results of the GoldSim modelling completed.

2 LITERATURE REVIEW

2.1 Introduction

The process of mining is the extraction of ores and minerals from the earth's crust for resources and/or economic value (Bussière 2007). There are two main material streams as a result of mining, (i) material with a high enough grade or value to be profitable and (ii) waste. Economic material is processed through physical (e.g., crushing, grinding, gravity, magnetic, or electrostatic separation) and chemical (e.g., heap leaching, vat leaching, or in situ leaching) processes to concentrate the metal or mineral for distribution (Lottermoser 2010). The waste stream includes earthen materials such as overburden, low grade ore, and waste rock excavated during mining activities and a slurry waste (tailings) produced during mineral processing. Current practice in mine waste management is to store these materials separately. The overburden may be stockpiled to be used during reclamation activities for the mine site. There is a chance that with changing markets and technology, the low-grade ore could become profitable in future and can be stored separate from waste rock and overburden. The tailings stream begins as a slurry which may be further processed to reduce the water content and must be stored in containment areas (Bussière 2007). The properties of waste rock will be discussed in further detail in the following sections and is the focus of this thesis, the other waste streams will not be discussed further.

2.2 Construction of Waste Rock Piles

The configuration, or layout of a waste rock pile (or dump) is dictated by the topography surrounding the mine site. Waste rock pile configurations consist of valley-fill, cross-valley fill, sidehill fill, ridge crest fill, and heaped fill; these are illustrated in Figure 2-1.

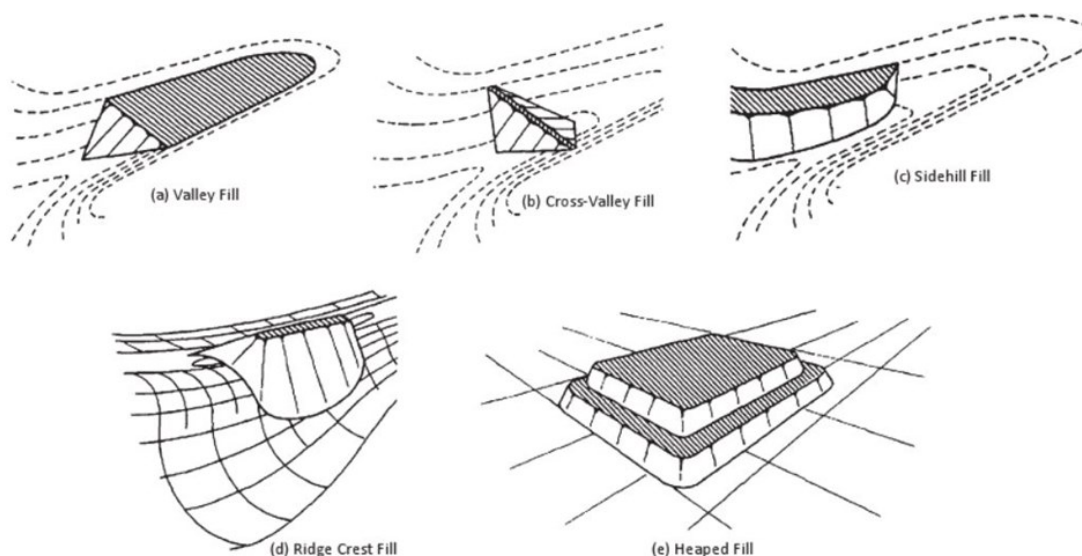


Figure 2-1. Waste rock pile configurations (from Hawley and Cuning 2017)

Valley fills partially or completely fill a valley and are constructed in the downstream direction. Cross-valley fills are a variation of the valley fill where the structure spans the valley, but material is not placed up-gradient. Cross-valley fills are sometimes constructed to create causeways for haul roads, light vehicle access roadways, and rail embankments. Sidehill fills are constructed on

sloping terrain with slopes inclined in the same direction as the topography. The ridge crest fill is a variation of sidehill fill where the structure straddles the crest of a ridge and material is placed on both sides of the ridge. Heaped fills are created on relatively flat areas with no topographical restraints and are constructed from the bottom up in lifts with fill slopes on all sides. Water diversion channels or rock drains may be needed for water flow control depending on topography and particularly needed for valley, cross-valley, and sidehill fills (Darling 2011, Hawley and Cunning 2017).

There are two main construction methods for waste rock piles, end-dumped and paddock dumped, with push-dumped being a combination of the two (Pearce et al. 2016). These methods refer to how the waste rock is placed within the pile using mechanical equipment. End-dumping is the most common method used in the mining industry, as it is quick, easy, and cost effective. End-dumping is when material is tipped off a truck from the crest of the waste rock pile, allowing the material to flow down the slope and rest at or near the angle of repose (35° to 40° ; Darling 2011). The resulting pile structure consists of gravity segregated particles, with fining upwards and a coarse rubble zone at the bottom; as well as inclined interbedded layers of coarse- and fine-grained material (Herasymuik 1996; Smith et al. 2004), as seen in Figure 2-2. This structure creates an ideal reactor for ARD generation (Wilson 2011), that will be discussed further in section 2.4.

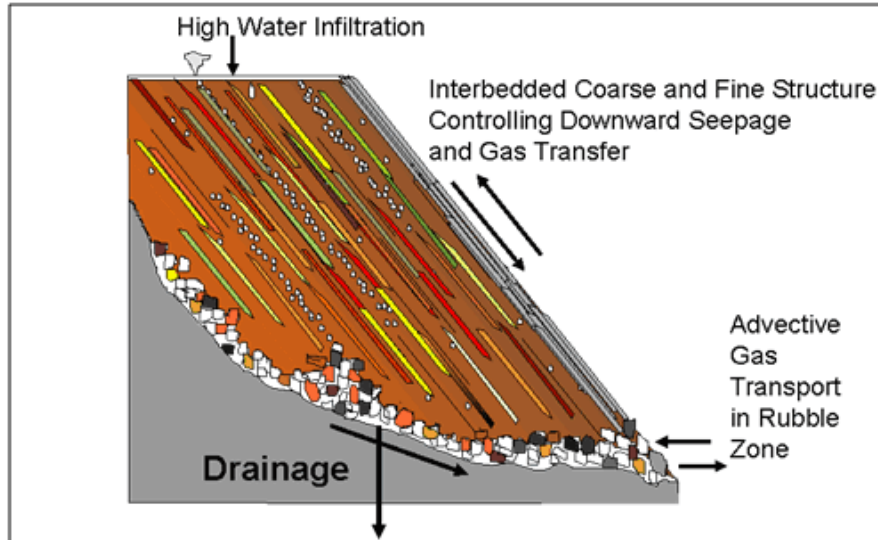


Figure 2-2. Waste Rock Pile Structure and Processes (from INAP 2009)

In contrast, paddock dumping requires more effort, time, and cost. Paddock-dumped piles are constructed from the bottom up with each lift being compacted, which increases the strength and stability of the pile (Darling 2011). This method reduces heterogeneity in the vertical direction from the reduction in gravity segregation, Wilson (2011) demonstrated that lifts less than 4-6 m in height had little fines segregation. As well, the method reduces the occurrence of preferential flow paths. With end-dumping, thin layers of alternating coarse and fine material can be deposited creating preferential flow paths, whereas paddock dumping creates a more homogenous porosity within the placed material.

An additional method of construction that has gained recent interest is to construct the pile with the pile constructed in benches with inclined compacted surface layers as depicted in Figure 2-3. The addition of the layer within each bench reduces infiltration into the waste rock, with the following mechanisms (Broda et al. 2014, Dawood and Aubertin 2014, Maknoon 2016, Martin et al. 2017): 1) the compaction decreases the hydraulic conductivity, thereby reducing infiltration rates; 2) the compacted material is finer than the coarse waste rock below, creating a capillary barrier effect (Nicholson et al. 1989; Akundunni et al. 1991; O’Kane et al. 1998; Bussiere et al. 2003; Aubertin et. al. 2009), whereby the low saturation of the coarse layer inhibits the unsaturated flow, and the fine layer retains moisture; and 3) the slope of the incline promotes gravity drainage to the outer edges of the pile. The use of this construction method can be helpful for prevention of ARD as the moisture content of the central waste rock remains low, and the fines layer, if sufficiently saturated can inhibit the flow of oxygen to the waste rock (Broda et al. 2014). ARD generation and mitigation is further discussed in Section 2.6.

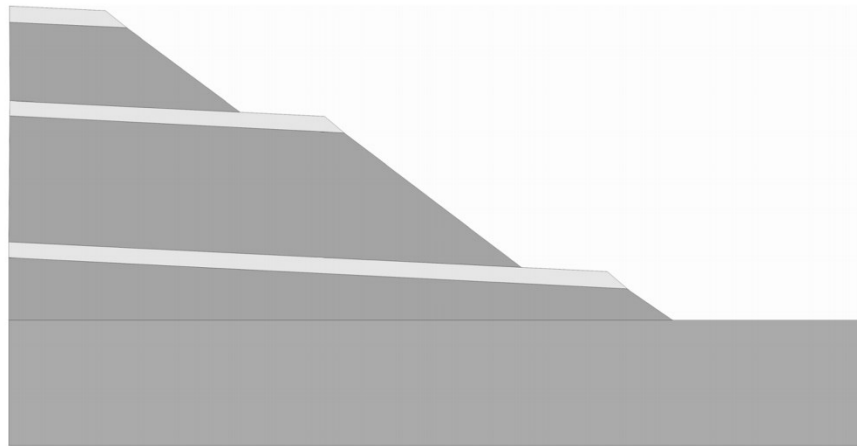


Figure 2-3. Proposed Waste Rock Pile configuration, built in benches with inclined compacted layers (from Broda et al. 2014, adapted from Maknoon and Aubertin 2013)

2.3 Geotechnical Characteristics of Waste Rock

Due to the inherent heterogeneities within a waste rock pile, the geotechnical characteristics also have wide ranges in particle size, water content, void ratio, and density.

2.3.1 Particle Size Distribution

The particle size of material within a waste rock pile can range from particles less than 1 mm up to particles greater than 1 m. The range of particle size distributions of waste rock can vary significantly, as seen in Figure 2-4 (Hawley and Cuning 2017). The material within a waste rock pile can usually be split up into two differently behaving materials, the fine fraction, and the coarse fraction. The fine fraction is defined as particles passing the No. 4 sieve (<4.75 mm; sand, silt, and clay) and exhibits matrix flow under negative (suction) pressure. Whereas the coarse fraction is the particles greater than the No. 4 Sieve (>4.75 mm; gravel, cobbles, and boulders), which exhibits preferential flow paths under positive pressure (Amos et al. 2015). The study undertaken by Yazdani et al. (2000) demonstrated that the hydraulic properties of a waste rock pile are driven by the fine fraction undergoing matrix flow if the fine fraction makes up at least

35% of the material by volume. The hydraulic properties determined by the fine fraction are the soil-water characteristics curve (SWCC), air-entry value, and the residual saturation. While the volumetric water content and residual saturation were reduced based on the proportion of the coarse fraction (>4.75 mm).

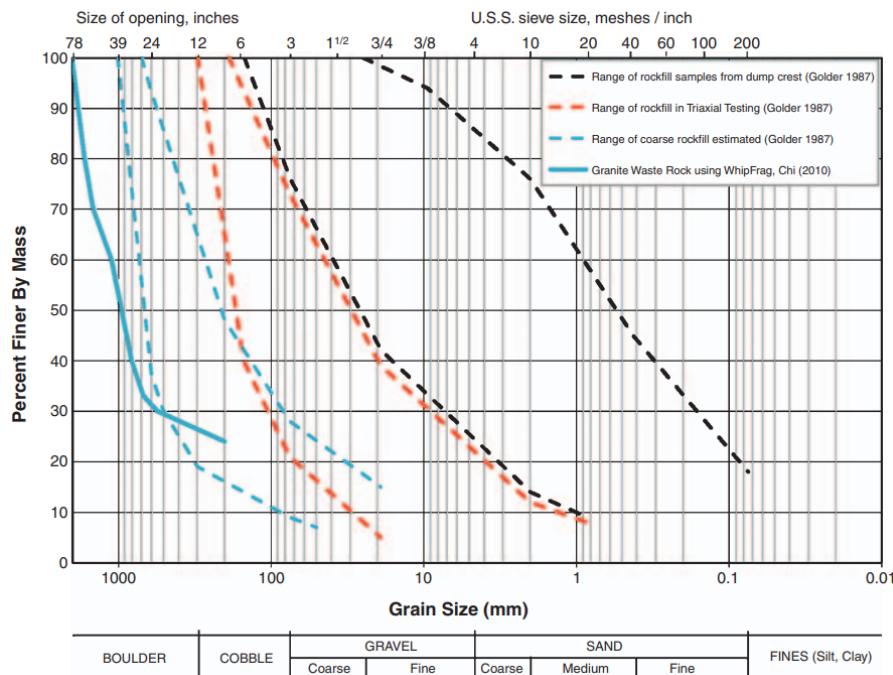


Figure 2-4. Typical particle size distribution ranges for waste pile rockfill materials (from Hawley and Cuning 2017)

2.3.2 Water Content

The water content within a waste rock pile is dominated by the granular fraction that passes the No. 4 sieve (<4.75 mm; Yazdani et al. 2000). The gravel fraction between 4.75 mm and 19 mm will contribute, and all particles larger than 19 mm are assumed to have a negligible water content (Hawley and Cuning 2017). Common in-situ water contents range from approximately 2-25% by volume. Fines (2006) investigated two waste rock piles in South Carolina and Northern Ontario with in-situ water contents of 4-23% by volume and 3-7% by volume respectively. Azam et al. (2007) investigated the Golden Sunlight Mine in Montana and found an in-situ water content of 2-14% by volume.

2.3.3 Void Ratio and Density

The void ratio is the relationship between the volume of voids and volume of solids. The void ratio is directly related to the hydraulic conductivity of a soil, the larger the pore space, the greater amount of fluid flow. The void ratio can vary based on a number of factors and causes wide variances between published values. Void ratio can range from 0.1 to 0.9; Azam et al. (2009) reported samples with a void ratio of 0.76-0.78, Azam et al. (2007) reported samples from the Golden Sunlight Mine (Montana) with a void ratio of 0.3-0.36, Linero et al. (2006) reported a void ratio of 0.46 for the Andina Mine (Chile), Dawson et al. (1998) reported values between 0.4-0.9 for a heaped waste rock pile, and Golder Associates Ltd (1987) reported field measurements of 0.25-0.3. Valenzuela et al. (2008) investigated the relationship between void ratio, dry density,

and effective mean stress with respect to the height of waste rock piles. As seen in Figure 2-5, as the height of pile increases, the dry density increases, and the void ratio decreases (Valenzuela et al. 2008). This decrease in void ratio is due to particle breakage from the high stresses within the pile. Literature values of dry density can vary as well, Azam et al. (2009) reported 1500-1600 kg/m³ for a semi-arid base metal mine, Azam et al. (2007) reported 1500-2100 kg/m³ for the Golden Sunlight Mine (Montana), and Fines (2006) reported a range of 1200-1800 kg/m³ for a mine in South Carolina.

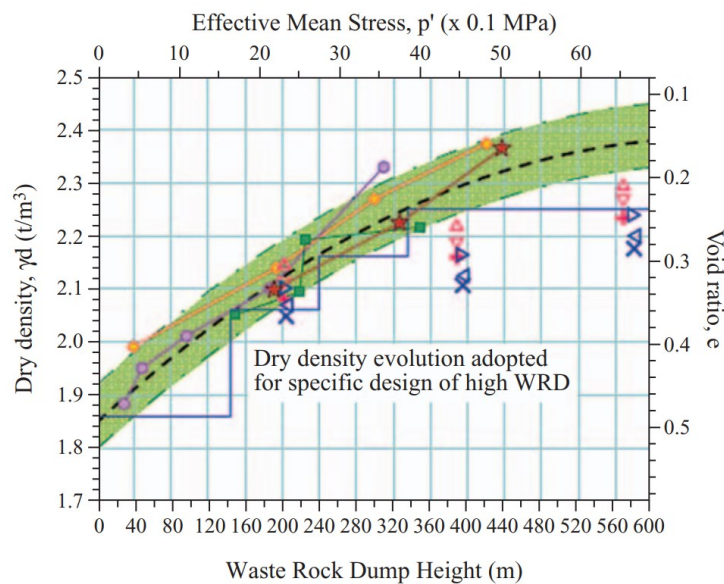


Figure 2-5. Effect of waste rock pile height on geotechnical parameters (from Hawley and Cunning 2017)

2.4 Fluid Transport Through Waste Rock Piles

The flow of water and air through waste rock piles is governed by the internal structure, which is influenced by blasting, rock properties, physical and chemical weathering, construction techniques, and climate (Herasymuik 1996). There are two main types of liquid flow through unsaturated waste rock piles, matrix flow, where the water is driven by capillary forces, or macropore flow, where flow is rapid and channelized and driven by gravity. Peterson (2014) found that macropore flow was based on the presence of large boulder sized materials, the test pile that was dominated by boulders, cobbles, and gravel exhibited the most fluctuating seepage, attributed to macropore flow. Whereas the test pile with no boulders and finer grained particle size distribution exhibited a more stable seepage due to matrix dominated flow. The degree to which each flow mechanism contributes is dependent on the particle size distribution and hydrological conditions (Amos et al. 2015).

2.4.1 Liquid Transport Through Waste Rock Piles

In the model proposed by Herasymuik (1996) for end dumped waste rock piles, the fine-grained layers maintain moisture and exhibit matrix flow, whereas the coarse-grained layers remain relatively dry under normal conditions and allow macropore flow during large precipitation events.

This can create the perfect “reactor” for the development of ARD within the waste rock pile where the fine-grained layers provide a source of water, and the unsaturated coarse-grained layers provide a source of oxygen available for reaction, further discussed in Section 2.5.

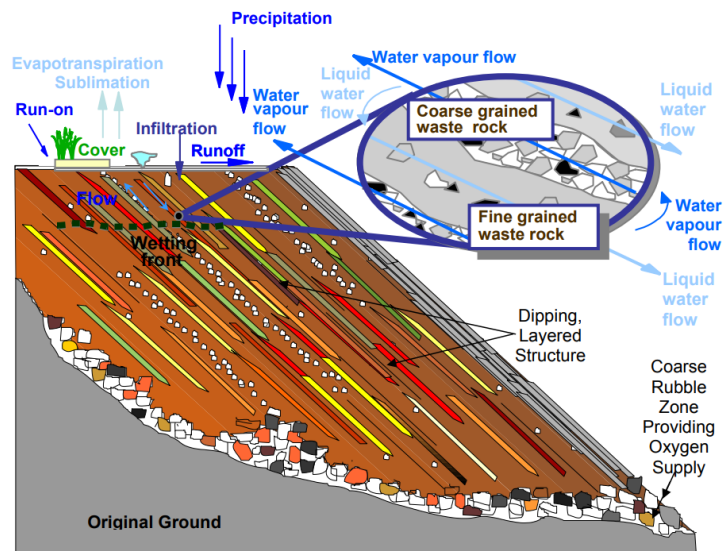


Figure 2-6. Conceptual model for waste rock piles proposed by Herasymuik (1996) (from Wilson et al. 2011)

Matrix fluid flow through an unsaturated waste rock pile is dependent on the amount of air voids within the soil; as the air content increases, the number of connected pathways for drainage to occur decreases and the matric suction increases (Barsi 2017). This relationship is referred to as the soil water characteristic curve (SWCC), where the volumetric water content is a function of the matric suction within the soil. The SWCC is determined by starting with a completely saturated sample and taking measurements as the soil is desaturated (drying curve), or by slowly adding water to a desiccated soil sample (wetting curve). An example of the drying and wetting SWCCs are shown in Figure 2-7, these two curves are significantly different, this difference is known as hysteresis. In practice, it is not always possible to obtain both the drying and wetting curves, since determining the drying curve in the laboratory is simpler, it is the curve more often used in practice (Fredlund et al. 2012).

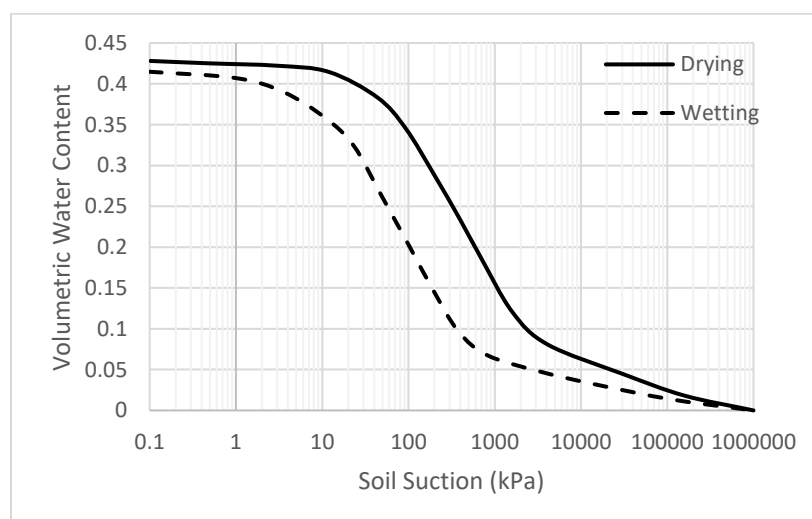


Figure 2-7. Effect of hysteresis on the SWCC (from Fredlund et al. 2012)

There are three zones of behaviour for the SWCC, the “boundary effect” zone, the “transition” zone, and the “residual” zone (Figure 2-8). In the boundary effect zone, the upper boundary is the saturated volumetric water content (θ_s). The curve is relatively flat until the intersection of the boundary effect and transition zone is met; this point is known as the air-entry value (AEV) that represents the moment the largest pores begin to drain. The water content continues to decrease with increasing suction until the residual volumetric water content (θ_R) is reached at the intersection of the transition and residual zones (Fredlund et al. 2012).

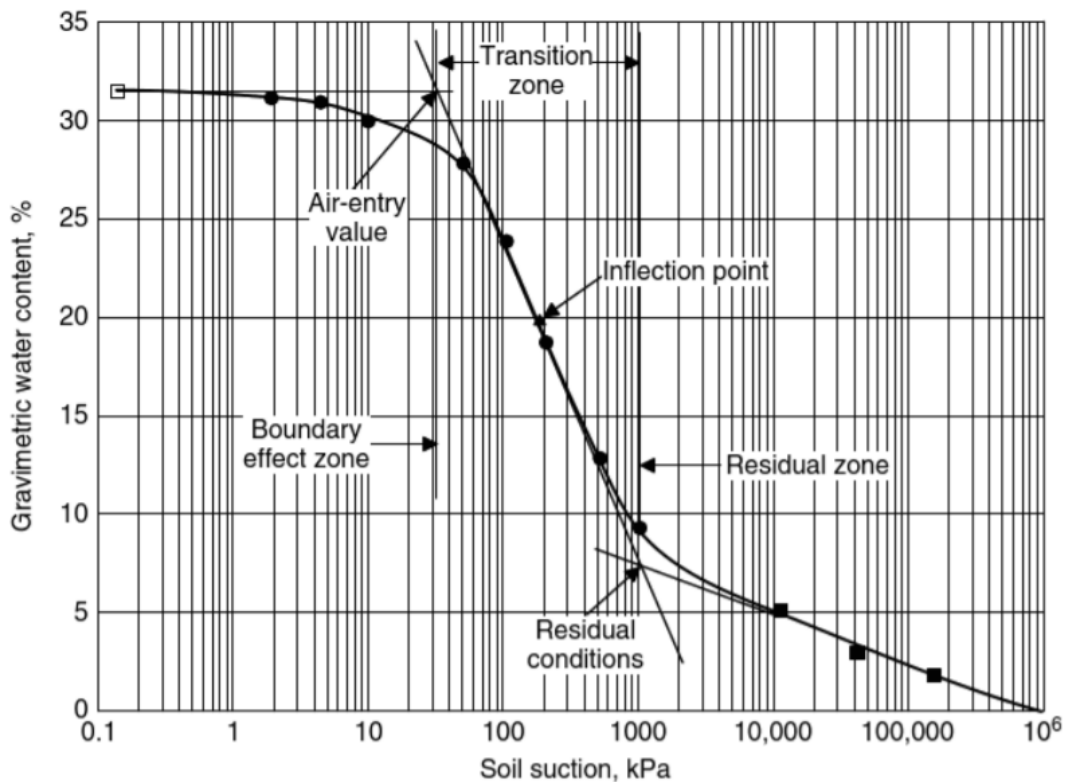


Figure 2-8. Typical soil water characteristic curve showing major zones of desaturation (Taken from Fredlund et al. 2012)

Figure 2-9 contains a number of SWCCs for waste rock piles in North and South America. Azam et al. (2009) reported a saturated water content of 0.44, residual water content of 0.26-0.3 and an AEV of 0.2-0.8 kPa for a semi-arid base metal mine. At the Golden Sunlight Mine in Montana, Azam et al. (2007) reported a saturated water content of 0.22-0.34, residual water content of 0.12-0.19 and AEV of 0.02-3.42 kPa. At the Diavik mine in the Northwest Territories, Barsi (2017) reported a saturated water content of 0.25, residual water content of 0.04-0.11, and AEV of 0.1-1.23 kPa. Cash (2014) reported a saturated water content of 0.2-0.41, residual water content of 0.02-0.14 and AEV of 0.2-5.4 kPa for a mine in South Carolina.

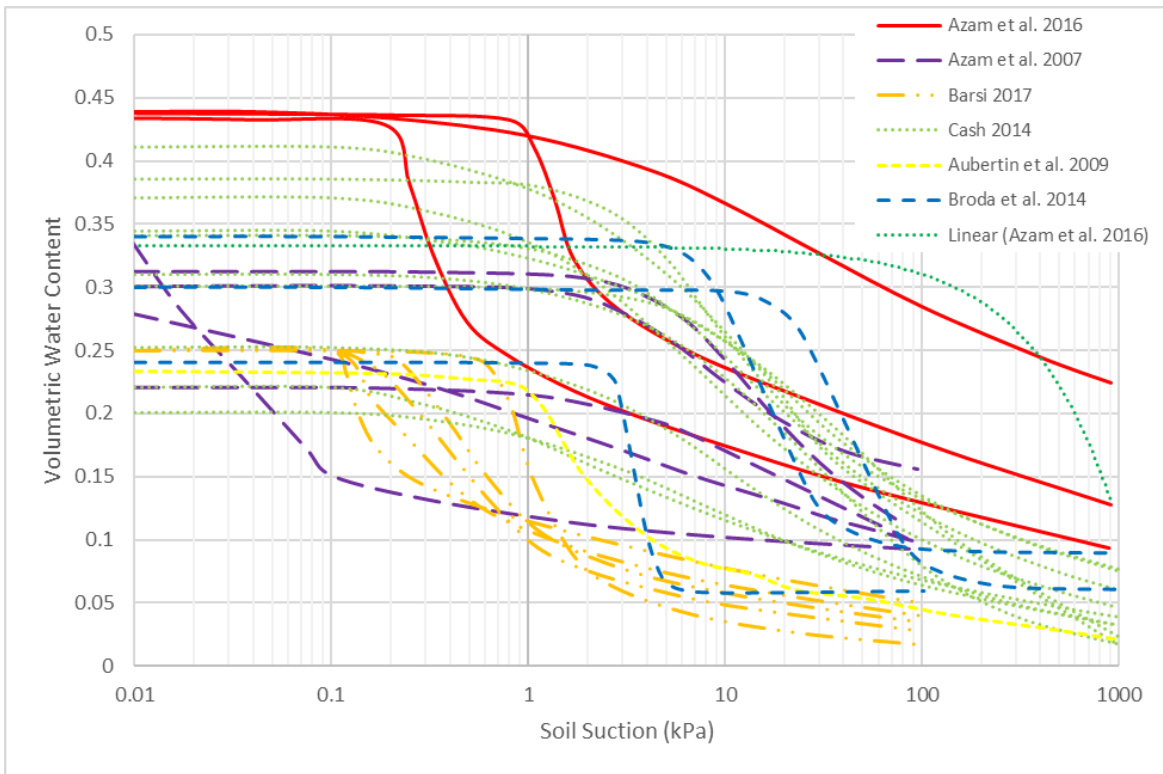


Figure 2-9. Example soil water characteristic curves for waste rock piles

The heterogeneity within a waste rock pile makes the determination of the unsaturated flow behaviour difficult as the SWCC could vary significantly laterally and by lift within the pile. Barsi (Barsi 2017; Barsi et al. 2019) demonstrated this by categorizing blocks within the Diavik test pile based on the percentage passing the No.4 sieve (Figure 2-10). The variation of particle size distributions within the pile directly relate to differing SWCCs and unsaturated flow behaviour.

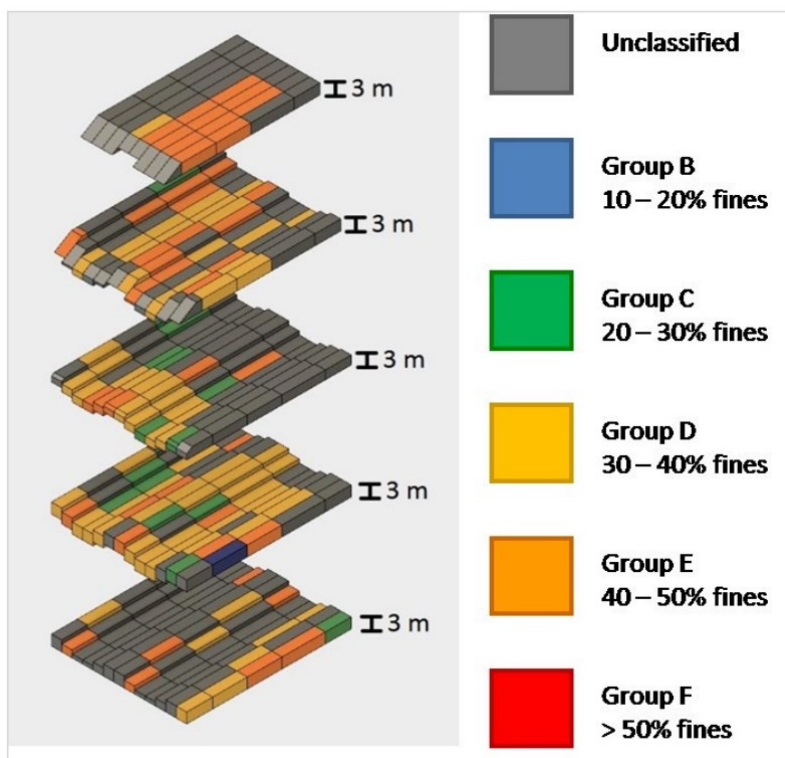


Figure 2-10. Type 1 Test Pile Benched with Herasymuik Classified Zones (from Barsi 2017)

Once the SWCC is determined, curve fitting parameters can be obtained, and the permeability function (hydraulic conductivity as a function of matric suction) can be created using various methods; one widely used method is Fredlund and Xing (1994). Fredlund and Xing (1994) uses

the shape of the SWCC, saturated volumetric water content, residual suction, and saturated hydraulic conductivity to determine the permeability function. Figure 2-11 depicts the relationship between the SWCC and the permeability function, the curves follow the same general behaviour with both water content and hydraulic conductivity decreasing once the AEV is reached. Measurements of the matrix fraction in-situ and laboratory saturated hydraulic conductivity are usually in the range of 10^{-6} - 10^{-3} m/s (Barsi 2017, Azam et al. 2009, Amos et al. 2015, Cash 2014, Neuner et al. 2013, Fines 2006).

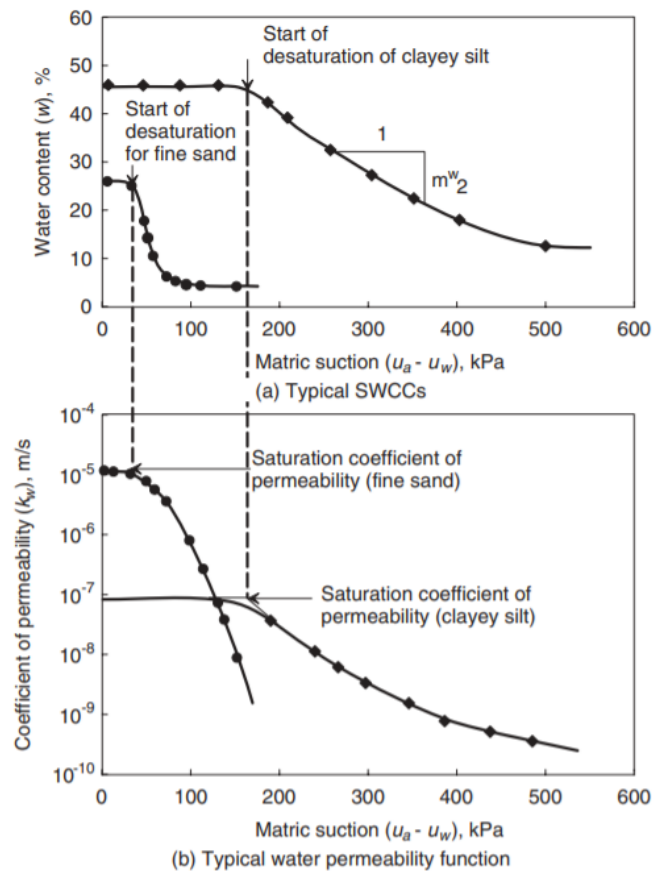


Figure 2-11. Relationship between SWCCs and permeability function for sand and clayey silt (from Fredlund et al. 2012)

2.4.2 Gas Transport Through Waste Rock Piles

Transport of gas (oxygen) within a waste rock pile occurs primarily through two mechanisms, diffusion driven by concentration gradients, and advection driven by pressure gradients (Herasymuik 1996). Previous studies have found that convection of oxygen can account for up to 90% of oxygen transport within a waste rock pile, and diffusion accounts for the remaining 10% (Brown et al. 2014; Pearce et al. 2015). The rate of oxygen ingress into a pile via advection can change dramatically based on the construction of the waste rock pile and will increase the intrinsic oxidation rate within the pile. In the end dumping construction method, a coarse rubble zone is created at the base of the pile that drives most of the oxygen supply into the pile through advection (Wilson 2011; Figure 2-6). End dumped waste rock piles have been found to have internal oxygen concentrations of up to 20%, and the rate limiting factor for generation of ARD is the water within the pile (Pearce et al. 2015). In comparison, waste rock piles constructed via paddock dumping do not have this coarse rubble zone allowing advection of oxygen, and the

rate limiting factor for the generation of ARD is the diffusion of oxygen from the surface down into the waste rock pile.

2.5 Acid Rock Drainage Generation

One of the main environmental concerns with hard rock mines is acid rock drainage; ARD is formed by the natural oxidation (weathering) of sulphide minerals when exposed to oxygen and water. The generation of ARD is a complex process that is impacted by physical, chemical, and biological factors at the mineral scale, waste rock pile scale, and mine scale (INAP 2009). Figure 2-12 is a schematic illustration of the factors that affect the generation and transport of ARD. Further discussion of these factors and their mitigation will be in Section 2.6.

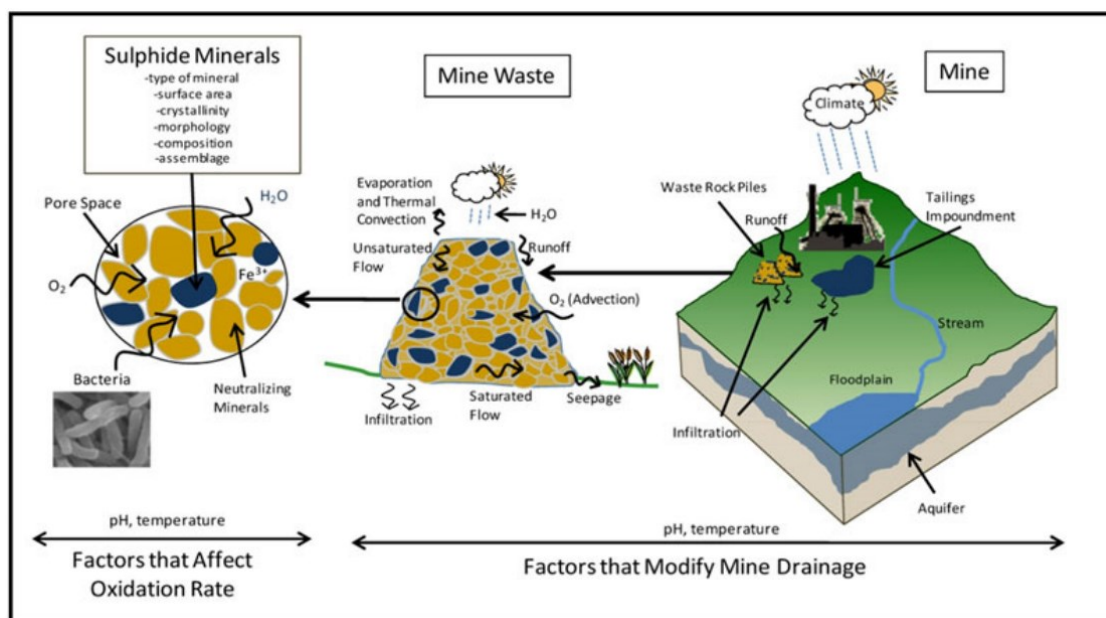
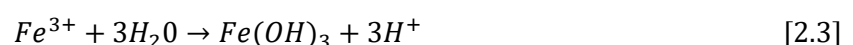
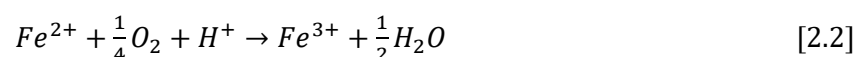
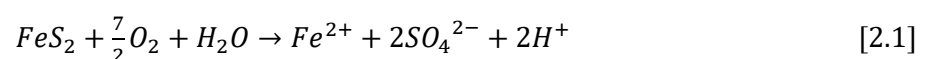
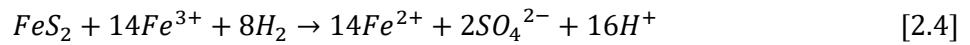


Figure 2-12. Factors that affect sulphide oxidation and transport (from INAP 2009)

The oxidation of pyrite is the most prevalent source of ARD in mining; there are three stages of the reaction. Stage one starts at near neutral pH and progresses slowly at first with pyrite oxidized to ferrous iron and sulphate with 2 moles of acid produced (Equation 2.1). As the reaction continues, the pH decreases, and the process moves to stage two. In stage two, ferrous iron is oxidized to ferric iron (Equation 2.2), if the pH is greater than 3.5, ferric hydroxide precipitates and 3 moles of acid is produced (Equation 2.3). Once the pH is less than 3.5, the ferric iron remains in solution and oxidizes pyrite directly, producing 16 moles of acid (Equation 2.4). At low pH, stage three begins, where the bacteria (*Thiobacillus Ferrooxidans*) oxidize ferrous iron into ferric iron (Equation 2.2). Equation 2.2 and 2.4 combine to create a cyclical reaction and the rate of acid generation increases several orders of magnitude (Stumm and Morgan 1981).





The presence of neutralizing minerals (e.g., carbonates, gibbsite, ferrihydrite, aluminosilicates) can buffer the reaction and create a step-wise development of ARD as the minerals are consumed (INAP 2009). Figure 2-13 illustrates the importance of early intervention to mitigate the impacts of ARD, the reaction kinetics are slow at first in stage one and two, however once stage three is reached the reaction is self sustained and will continue until all pyrite is oxidized.

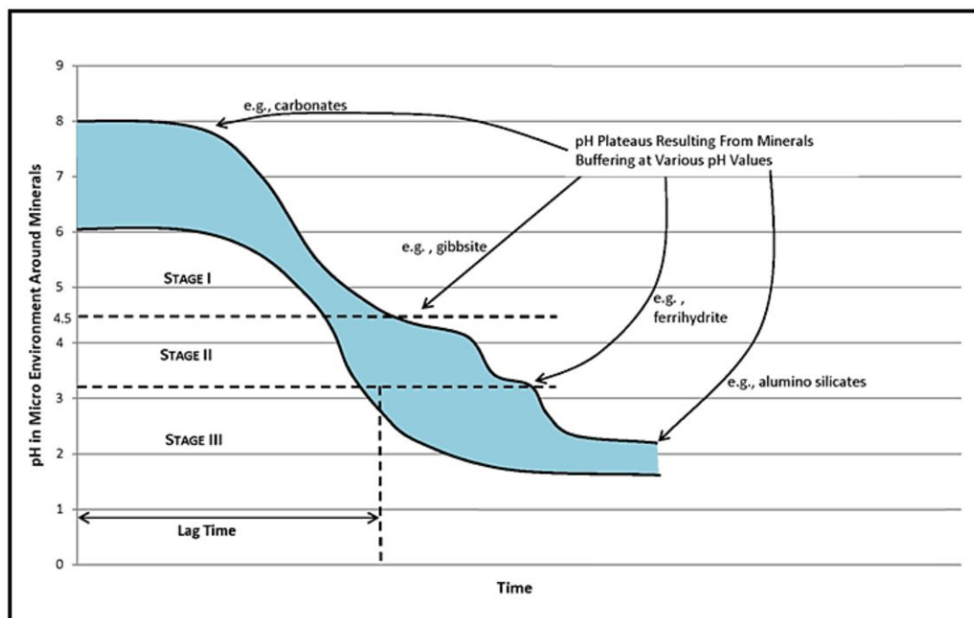


Figure 2-13. Stages in the formation of ARD (Modified from INAP 2009)

2.6 Acid Rock Drainage Prevention and Mitigation Methods

The theory behind prevention and mitigation of ARD is to minimize the supply of reactants in sulphide oxidation (oxygen, water, sulphur, bacteria), and/or maximize the neutralizing potential. This can be in the form of minimizing oxygen supply or water infiltration, reducing or isolating sulphide minerals, use of bactericides, and maximizing availability of acid neutralizing minerals. At the earlier stages of the mine life there will be more options with higher effectiveness and lower cost, as the mine life progresses, the number of options decrease and the cost increases (Figure 2-14). This outlines the need to incorporate ARD prevention into the planning of the mine, as it will ultimately reduce the overall cost of remediation (INAP 2009).

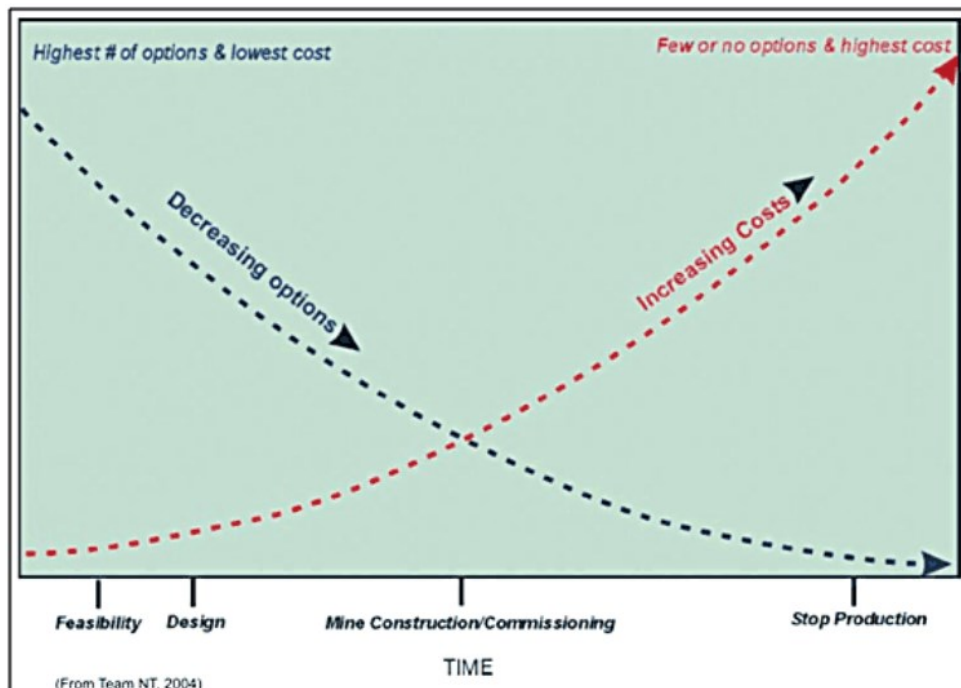


Figure 2-14. ARD mitigation options and effectiveness with time (from INAP 2009)

The focus of the research is on prevention and mitigation methods that use special handling procedures for mine waste. These methods include segregation, encapsulation and layering, blending, co-disposal, and additions and amendments (INAP 2009). Segregation is the selective handling of waste based on its acid producing potential, waste is separated into potentially acid generating (PAG) and non acid generating (NAG) to reduce the volume of problematic material (MEND 2001). Encapsulation and layering involve using the segregated materials to construct the waste rock pile in geometries that will limit the generation of ARD (MEND 1998; 2010). Blending is the mixing of PAG waste rock with neutralizing material to create a neutral discharge that is not deleterious to the environment, this method requires even distribution of both acid producing and neutralizing material and is difficult and costly to implement effectively (MEND 1998; 2001). Co-disposal involves the placement of tailings and waste rock together, the tailings fill the large voids of the waste rock to reduce the hydraulic conductivity of the waste and the waste rock lends stability to the low strength tailings (Bussière 2007). Additions and amendments work to passivate the reactive minerals, neutralize acid production, or impact iron reducing bacteria (INAP 2009).

2.7 Acid Rock Drainage Models

Modelling of acid rock drainage within a waste rock pile is traditionally done with a multi-component multi-phase reactive transport model. There are various geochemical modelling codes that have been created, including the ones described here, TOUGHAMD, MIN3P, SULFIDOX, and THERMOX. A comparison of the main features of each code is summarized in Table 2-1.

TOUGHAMD was created for a PhD thesis by Lefebvre (1994) that was based on the TOUGH2 finite difference model created by Pruess (1991). The model consists of three phases (air, oxygen, and water) in porous or fractured media. Fluid transport mechanisms included in the model are

advective and diffusive gas transport, convective and advective heat transport, unsaturated and saturated flow and the code allows for a constant infiltration flux at surface. The model focuses on the oxidation of pyrite and includes the rates of consumption of oxygen and pyrite and the rates of production for heat and sulphate. A reaction core model is used to simulate a volumetric oxidation rate that accounts for the oxidation of surface pyrite and subsequent oxygen diffusion into the particle to continue to consume pyrite within the core (Lefebvre et al. 2001). TOUGHAMD was used by Lefebvre et al. (2001) to simulate the conditions at two waste rock piles, one at the Doyon Mine and the other at the Nordhalde Mine. The model reproduced observed temperature, oxygen concentration and pyrite fraction behaviour of the waste rock piles. At the Doyon Mine convection was found to be the dominant process in the transport of oxygen within the pile, whereas Nordhalde was found to be a combination of convection and diffusion (Lefebvre et al. 2001).

MIN3P is a finite volume model created by Mayer et al. (2002) that looks at two phases (gaseous and aqueous) within an immobile porous media. Two major simplifications that were made in the creation of this code are the assumptions that diffusion dominates in the transport of gas (oxygen) and the representative volume is isothermal. The boundary condition at the surface includes temporally variable infiltration that allows the model to handle saturated and unsaturated flow. MIN3P uses the reaction core model along with a larger scope of geochemical reactions including speciation and complexation, slow and rapid dissolution, precipitation of secondary minerals, ion exchange, and adsorption. Wilson et al. (2018) used the code to model the field scale results from an active zone lysimeter experiment done at the Diavik Diamond Mine. The isothermal diffusion only assumption required in MIN3P was determined appropriate for the Northern climate and solid walled lysimeters. Wilson et al. (2018) was able to find good agreement between the modelled results and the calculated results of the field scale experiment. However, the model MIN3P may not be appropriate for a scaled-up waste rock pile if convection is present.

SULFIDOX is a finite difference reactive transport code that was developed by Brown et al. (2001) for the Australian Nuclear Science and Technology Organization (ANSTO) based on FIDHELM (Pantelis 1993). This model combines the features of TOUGHAMD and MIN3P to create a more robust model that can incorporate diffusion, advection and convection transport mechanisms while also incorporating a wide range of geochemical reactions. The geochemical reactions that can be included are speciation and complexation, slow and rapid dissolution, and precipitation of secondary minerals. The oxidation of sulphide bearing minerals is based on reaction kinetics and does not incorporate the reaction core methodology. Linklater et al. (2005) demonstrated the use of the code to model the Aitik copper mine in Northern Sweden. The SULFIDOX code was able to model the physical and chemical processes within the Aitik waste rock pile that were consistent with observed behaviour. However, the authors did note that the reactive surface area

of the sulphide minerals was one of the largest areas of uncertainty (Linklater et al. 2005), this could be minimized with the use of the reaction core model used in the other codes.

Hydrus-2D/3D is a finite different model created by Simunek et al. (1998) that simulates water, heat, and solute movement in two- and three-dimensional variably saturated porous media. Boundary conditions of the model includes head and flux, atmospheric, and free drainage. The variably saturated water flow is solved using the Richards equation. The heat transport equation considers transport due to conduction and convection with flowing water. The solute transport equations consider convective-dispersive transport in the liquid phase, as well as diffusion in the gaseous phase. Hydrus-2D has been used by various authors to model fluid transport and acid rock drainage in waste rock piles including Fala et al. (2003, 2005, 2006, 2012), Franklin et al. 2008, Hajizadeh (2015), and Appels et al. (2018).

A reactive transport code, THERMOX, created by da Silva et al. (2009) is similar in capabilities to the SULFIDOX code (Brown et al. 2001). THERMOX is a finite element code that includes all the gas, heat, and water transport mechanisms used in the other models. The main difference between THERMOX and SULFIDOX is the geochemical reactions included. the THERMOX code uses a shrinking core model to simulate the reduction in oxidizable pyrite at the particle surface. The geochemical reactions included are equilibrium precipitation and dissolution reactions and kinetics of pyrite oxidation. The code was verified against the results from Lefebvre et al. (2001) for the Doyon Mine and was able to achieve comparable results.

The focus of modelling acid rock drainage in waste rock piles has been on the geochemistry and reactive transport opposed to the hydrogeology. Although waste rock piles can be highly heterogeneous, the codes discussed focused on the chemistry interactions within the waste rock pile and assumed the porous media was homogeneous. The heterogeneity within the waste rock pile is incorporated by using average soil parameters that effectively creates a typical waste rock pile that can simulate overall pile behaviour (Linklater et al. 2005). Although this is a large simplification, the four models were all able to recreate the observed behaviours in heterogenous waste rock piles (Lefebvre et al. 2001; da Silva et al. 2009; Linklater et al. 2005; Wilson et al. 2018). The simplification of soil properties in reactive transport modelling is justification for the simplifications that will be made in the waste rock sub-model, further discussed in Chapter 3.

Table 2-1. Comparison of multi-component multi-phase reactive transport models

	TOUGHAMD (Lefebvre 1994)	MIN3P (Mayer et al. 2002)	SULFIDOX (Brown et al. 2001)	Hydrus-2D/3D (Simunek et al. 1998)	THERMOX (da Silva 2009)
Based on	TOUGH2	N/A	FIDHELM	N/A	HYDRUS; PHREEQE
Numerical Basis	– Finite Difference	– Finite Volume	– Finite Difference	– Finite Element	– Finite Element
Phases	– Air (not including oxygen) – Oxygen – Water	– Gaseous – Aqueous	– Air – Water	– Air – Water	– Air – Water
Media	– Porous or fractured media	– Immobile porous media	– Rigid porous media	– Rigid porous media	– Porous media
Gas Transport	– Diffusion driven by concentration gradients – Advection driven by pressure or temperature gradients	– Diffusion driven by concentration gradients dominates	– Diffusion driven by oxygen gradients caused by oxygen consumption – Advection driven by pressure or density gradients caused by temperature changes from reactions	– Solute diffusion driven by concentration gradients	– Diffusion driven by oxygen gradients caused by oxygen consumption – Advection driven by pressure or density gradients caused by temperature changes from reactions

	TOUGHAMD (Lefebvre 1994)	MIN3P (Mayer et al. 2002)	SULFIDOX (Brown et al. 2001)	Hydrus-2D/3D (Simunek et al. 1998)	THERMOX (da Silva 2009)
Heat Transport	<ul style="list-style-type: none"> - Convection - Advection by fluid flow - Includes effect of phase change on heat transfer 	<ul style="list-style-type: none"> - Isothermal 	<ul style="list-style-type: none"> - Convection - Advection by fluid flow 	<ul style="list-style-type: none"> - Convection - Advection by fluid flow 	<ul style="list-style-type: none"> - Convection - Latent heat for air and water phases
Water Transport	<ul style="list-style-type: none"> - Constant infiltration at surface - Saturated and unsaturated flow 	<ul style="list-style-type: none"> - Variable infiltration at surface - Saturated and unsaturated flow 	<ul style="list-style-type: none"> - Constant infiltration at surface - Steady state approximation of water content distribution 	<ul style="list-style-type: none"> - Variable infiltration at surface - Saturated and unsaturated flow 	<ul style="list-style-type: none"> - Constant infiltration - Saturated and unsaturated flow
Geochemical Reactions	<ul style="list-style-type: none"> - Reaction core model - Rates of consumption of pyrite and oxygen - Rates of heat and sulphate production 	<ul style="list-style-type: none"> - Reaction core model - Speciation and complexation - Slow and rapid dissolution - Precipitation of secondary minerals - Ion exchange and adsorption 	<ul style="list-style-type: none"> - Speciation and complexation - Slow and rapid dissolution - Precipitation of secondary minerals 	<ul style="list-style-type: none"> - Nonequilibrium transport of solutes involved in sequential first-order decay reactions 	<ul style="list-style-type: none"> - Shrinking core model - Speciation - Only equilibrium reactions - Pyrite oxidation

3 GENERAL MODEL DEVELOPMENT

3.1 Introduction

Many decisions made during the early stages of mine planning can irrevocably affect the options available for mine waste management (INAP 2009). There is a need for the ability to predict long-term behaviour of the entire mine site to aid in the development of mine waste management plans. Typically, each process of a mine is modelled separately with limited coupling or interactions between the models. A tailings management simulation (TMSim) model (Beier 2015; Beier et al. 2020) is a good candidate for a base model that looks at the whole system of mine waste management over the mine lifespan. TMSim is a system dynamics (SD) model created in GoldSim, a dynamic modeling software that provides the ability to evaluate oil sand tailings dewatering technologies on their ability to meet reclamation and closure goals. TMSim, however, does not incorporate ARD and related rock overburden waste management strategies specifically encountered at hard rock mines.

3.1.1 Model Objective

The objectives of this chapter are to (1) create a dynamic systems model that simulates waste rock and overburden management processes that is built with the same approach and can be coupled with the dynamic systems model TMSim (Beier 2015; Beier et al. 2020) and (2) modify the saturated and unsaturated flow sub-model for a tailings cover created by Zheng (Zheng and Beier 2018; Zheng 2019) to apply to waste rock piles.

3.1.2 System Dynamics

System dynamics (SD) is a modelling approach that focuses on overall behavior of a system rather than detailed numerical modelling (Ford 2010; Kossick and Miller 2004). There are three basic building blocks of a SD system; stocks and flows, feedback structures, and delays. Stocks are state variables that track accumulation with the flows representing the increase and decrease in the stock variable. Feedback structures explain the relationship between two variables, and delays can be informational or material in nature (Ford 2010; Zheng and Beier 2018). The modeller organizes the three structures into causal loop diagrams that visually show the connections and

relationships between each component of the model. Model development consists of a qualitative stage and a quantitative stage. The qualitative stage is the construction of causal loop diagrams in the following steps (Ford 2010; Zheng and Beier 2018):

- i. Familiarization with the system
- ii. Construction of specific questions
- iii. Identification of variables, stocks, and flows
- iv. Formulation of causal loop diagrams
- v. Iterative revision of causal loop diagrams

Once the causal loop diagrams have been completed, a computer model can be developed in the quantitative stage in the following steps (Ford 2010; Zheng and Beier 2018):

- i. Conversion of causal loop diagrams to runnable models
- ii. Parameter estimation
- iii. Sensitivity analysis
- iv. Analysis of parameter input and model structures
- v. Continued model maintenance

GoldSim is a Monte Carlo simulation software that uses the system dynamics approach to visually model complex systems. The software allows the construction of large hierarchical, top-down models that are easy to understand, navigate, and explain to many audiences of varying skill levels (Kossik and Miller 2004).

3.1.3 Model Conceptualization

Figure 3-1 depicts a simplified conceptual model of the waste rock pile. The waste rock from excavation of the mine pit will be constructed into a pile that will undergo environmental conditions (e.g., precipitation, evaporation, runoff, and percolation).

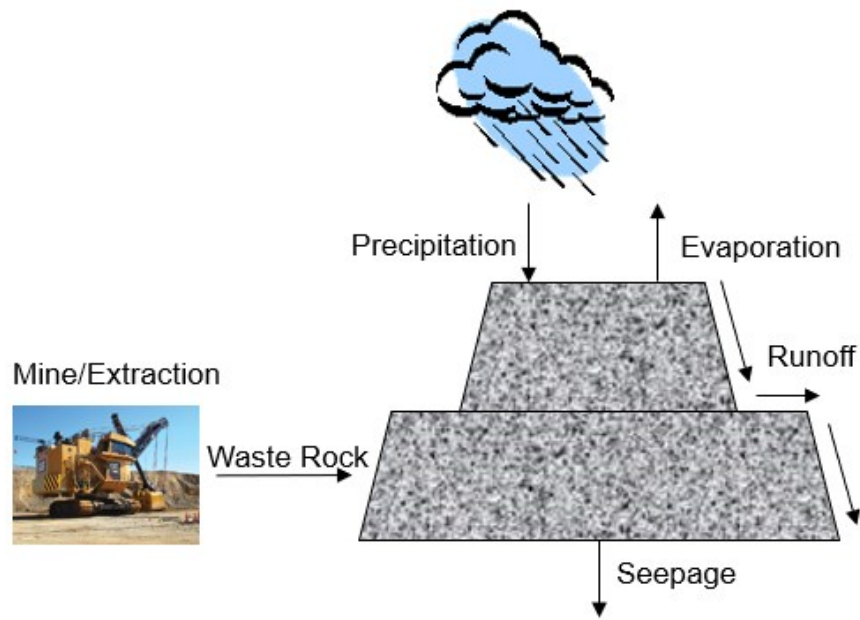


Figure 3-1. Conceptual Model

In the qualitative stage of SD modelling the causal loop diagram is created to understand the relationship between variables and to identify any feedback structures (Ford 2010; Zheng and Beier 2018). The broad scope causal loop diagram, representing unsaturated water flow in a waste rock pile assuming there is only one layer of soil, can be seen in Figure 3-2. The stock variables in the model are the volume of excavated waste rock and water storage within the pile. The flow variables are the mine plan excavation schedule and precipitation, runoff, evaporation, and seepage out of the pile. Two feedback loops are created, one for evaporation and one for water storage. Both feedback loops are negative, meaning they will self-correct and come to equilibrium within the system, whereas a positive feedback loop can become a runaway system. The timestep of the model is one day, and since the flow of waste material and water is an averaged per day value there is no need for an informational or material delay in the causal loop diagram.

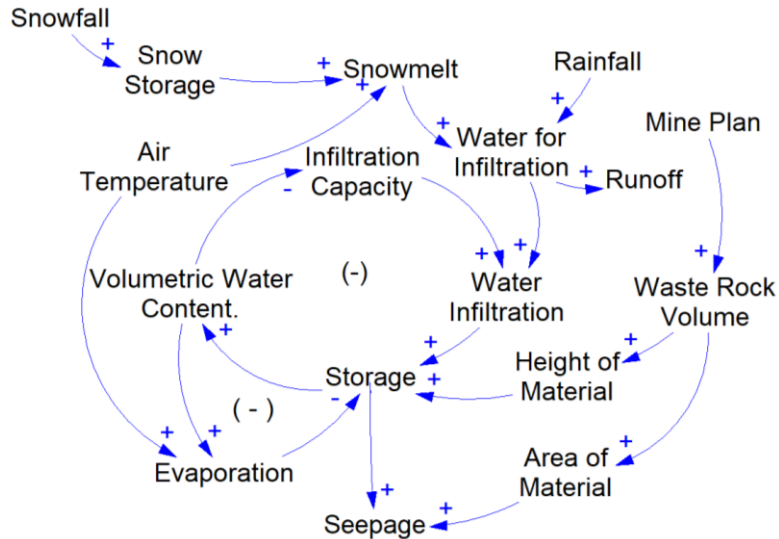


Figure 3-2. Causal Loop Diagram of Unsaturated Water Flow in Waste Rock Pile

3.2 Simulation Model Components

The purpose of this research is to create a simplified model of a hard rock mine system, coupling the mine plan, construction, climate, and unsaturated water flow in a waste rock pile using a whole system probabilistic approach. System dynamics modelling allows the user to model large complex inter-related systems that cannot be modelled with a traditional geoenvironmental modelling software. Therefore, the goal of the model is not to recreate the exact behavior within a waste rock pile, which is difficult in any modelling software due to the inherent heterogeneity within the structure (Herasymuik 1996), but rather to model general pile behaviour trends over the mine lifespan.

The focus of this research is on the placement of waste rock and the transport of fluid (water) through the pile. To fully understand the impact of the various construction methods on the development of ARD, the inclusion of advective and diffusive flow of oxygen and associated geochemical reactions are required, they are however not part of this research.

GoldSim is a powerful tool, however, three-dimensional modelling is not possible with the standard software package. Because of this, the waste rock pile was constructed using a series of one-dimensional columns to simulate a pseudo 3-D structure. The disadvantage of the pseudo 3-D structure approximation is that the lateral flow within the pile is ignored. This is anticipated to

cause little impact to the results of overall pile behaviour as a similar amount of water is entering the pile but is merely distributed in a different way. Coffin (2010) implemented the pseudo 3-D methodology to model the deposition and large strain consolidation of deep tailings deposits and found the 1-D approximation results to be valid when compared to 3-D models (Fredlund et al. 2015). While there will be some error due to the 1-D approximation, the overall pile behaviour should still be representative.

The scope of this research is to create an environmental planning tool with a primary focus on the feasibility stage. This dictates the overall strategy to choose methods that require minimal site or testing data, as there is usually limited data available during the feasibility stage. An overview of model selection and setup and model calibration for the various components are included in the following sections 3.2.1 to 3.2.5. Appendix 1 includes details on GoldSim elements and their uses, Appendix 2 includes the GoldSim Model detail, and Appendix 3 provides a user guide to setting up the inputs for the model.

3.2.1 Waste Rock and Overburden Management

The waste rock and overburden management component accounts for the material flow from the mine plan and the waste rock pile design to “construct” the waste rock pile.

3.2.1.1 Model Selection and Setup

The waste rock and overburden quantities are tracked through time based on the mining sequence provided in the mine plan. Early-stage mine plans will most likely have tonnages in monthly, quarterly, or semi-annually, and this will need to be converted to a daily amount. Daily tonnage values were determined as averages over the period based on the specific number of days in the period. To account for leap days, a matrix of the number of days in each month for the years of construction was created. The rock waste has three streams, PAG, NAG, and overburden. As the overburden would not normally pose an environmental risk, the tonnage is tracked for the user’s information but is not included in the unsaturated flow model of the constructed pile. The daily tonnage of waste rock is converted to a daily volume using a placed

unit weight that accounts for bulking during blasting and excavation and compaction during placement.

Two dumping methods: end-dumping and paddock dumping can be simulated, which requires the user to choose either the WR Model-End Dump or WR Model-Paddock Dump model file. In the end-dumping case, the lift height is assumed to be the total lift height as the tip face would be the entire length of the lift. To simulate the segregation caused during end-dumping, the lift is split up into five vertical sections with increasing hydraulic conductivity with depth and accompanying unsaturated soil parameters. In the paddock dumping case, the lift height within the model is one third of the actual lift. This assumes that the lift is built up in layers that are placed and dozed before the next layer. The hydraulic conductivity and unsaturated soil parameters are assumed to be constant in the vertical direction to simulate no segregation.

The model allows for a four-lift waste rock pile to be simulated. Each lift is represented laterally as a 15x16 matrix, consisting of 240 construction cells. Each lift is stacked to create a system of 240 1-D columns to simulate a pseudo 3-D system, as depicted in Figure 3-3. The lifts are assumed that post pile construction, each lift will maintain one cell width perimeter of a sloped surface (batter), and one cell width perimeter of surface (bench) open to atmosphere (Figure 3-4).

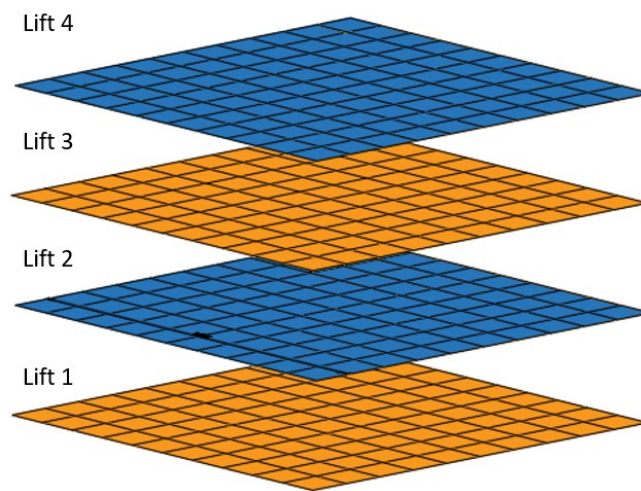


Figure 3-3. Pseudo 3D Structure

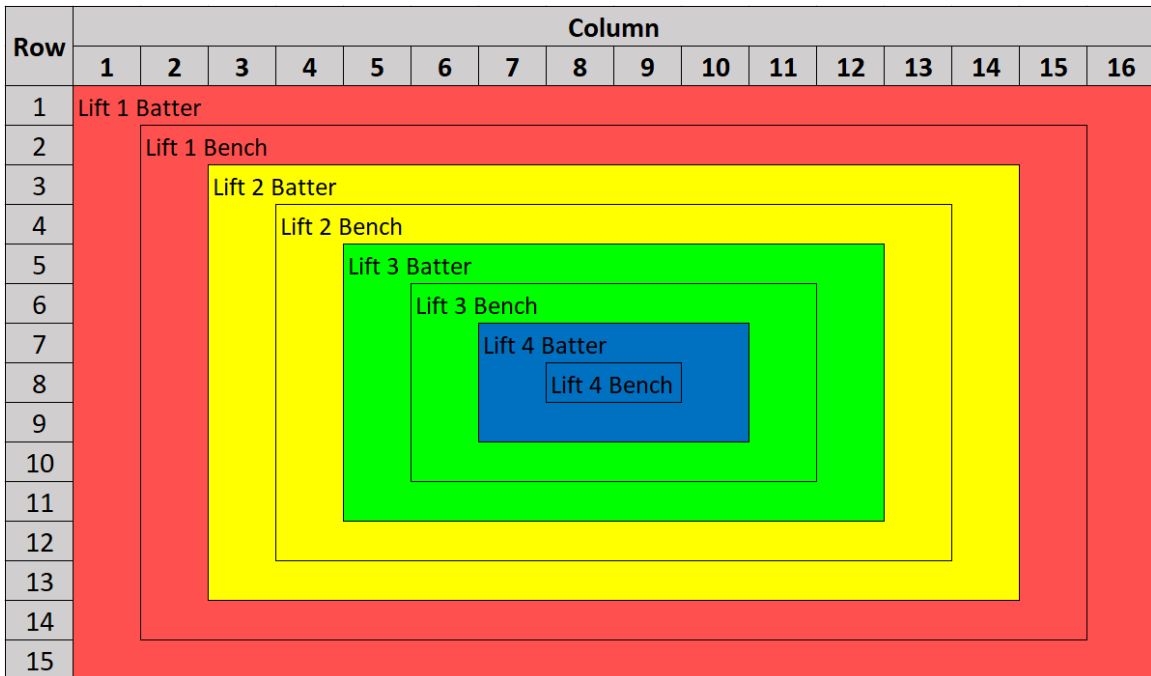


Figure 3-4. Plan Layout of the Model Waste Rock Pile

From the input dashboard within GoldSim, the user selects if the model will simulate PAG separation, layering, or encapsulation; and if there is a compacted surface layer. The compacted surface layer assumes only the first layer is impacted by compaction; this results in a 0.5 m compacted layer for end-dumped lifts and 0.33 m compacted layer for paddock dumped lifts. Figure 3-5 represents a visual representation of the decisions made by the user that impact how the waste rock pile is constructed and configured.

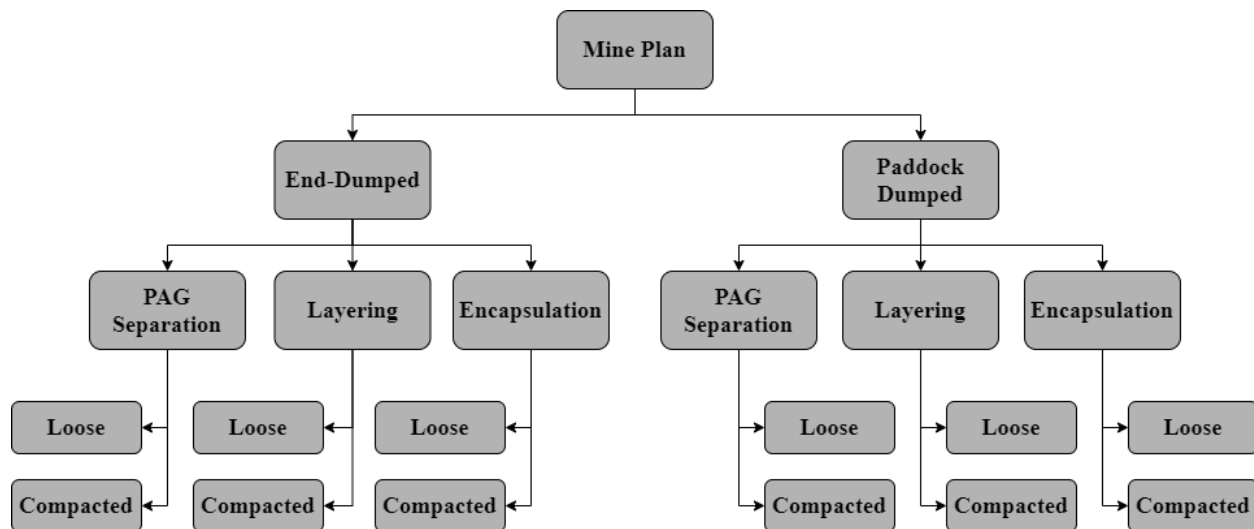


Figure 3-5. Decision tree impacting construction of waste rock pile

Initial Model Approach

Initially, the intention for the deposition of waste rock within the pile was to have the GoldSim model direct the flow of material (waste rock) to each construction cell as it was produced, once a cell was full, it would be “activated”. The daily volume of waste rock produced by the mine plan was directed to a reservoir element (an element that tracks a stock variable) that tracked the daily accumulation of waste rock available for placement in lifts. If there was an available construction area designated for the NAG/PAG waste rock, the rock was directly placed in the lift. If there was a scheduling conflict with the type of waste rock being produced, the material was assumed to be placed in a temporary stockpile and remain in the reservoir element until an active construction cell was available with sufficient haul truck capacity to transport to the pile. As the material would be in the temporary stockpile for a short time, environmental effects were ignored.

The use of a lift status element was used to direct flow to the current lift until the maximum volume was reached, and then directed flow to the next lift. Each construction cell within each lift had an inputted NAG and/or PAG placement quantity and construction sequence. The model determined the active construction cell by completing a matrix walk calculation (Provided by GoldSim Support Team). The script worked by searching the matrix for the cell where construction starts (i.e., 1), when that cell volume reaches the maximum, the script searched the

matrix again for the next cell in the sequence (i.e., 2). A visual representation of the if statements and decisions made in the model is outlined in Figure 3-6 starting with the separation of NAG and PAG and eventual placement in the waste rock pile.

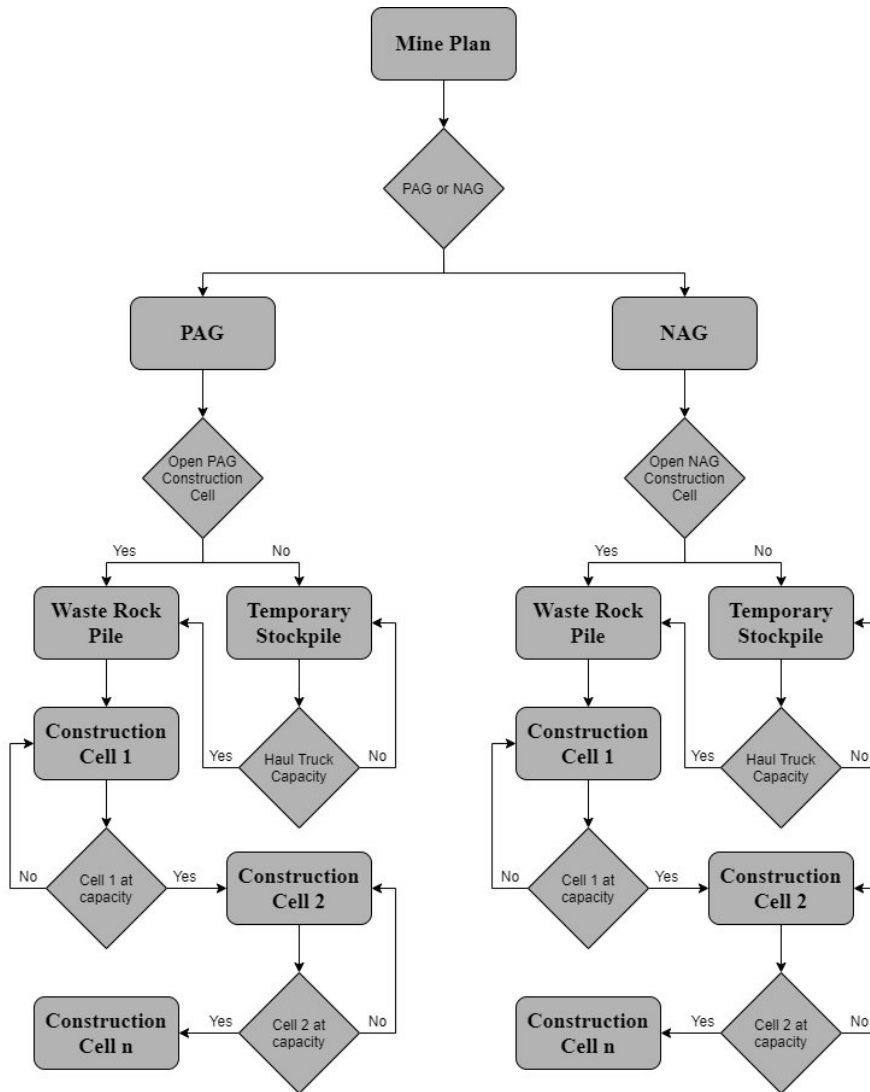


Figure 3-6. Decision tree of PAG and NAG material flow

A multitude of issues were encountered during model development related to the nature of matrix calculations needed for the pseudo 3-D model structure. Two major issues were encountered that required significant time and effort to attempt to resolve.

The first major issue encountered was related to the inability of the GoldSim program to identify divide by zero errors within inserted timesteps. Significant time was spent attempting to debug the model looking for the cause of long runtimes. The model would run normally, until such time that the location of the divide by zero error was occurring and then the program would proceed to simulate time but with significantly reduced speed. During the debugging process, the error was found when the model was run with no inserted timesteps. The error seemed to stem from the fact that for matrices, GoldSim completes the calculation for all cells, and then the if statements are evaluated. In this scenario the if statement removed the divide by zero calculation, but the GoldSim model sequencing did not.

The second major issue encountered was related to the loss of material when cells filled up mid-timestep. The sequence of the model was fill cell n, when cell n reaches capacity, switch active cell to n+1, continue filling cell n+1 at same rate, and repeat. Based on a review of the GoldSim User Manual (2021), the best way to do this was to use the event trigger “at stock test”, which is a conditional expression that compares a reservoir to some value, and GoldSim inserts a timestep when the condition becomes true. Unfortunately, the “at stock test” event trigger cannot be used on matrix elements. An attempt to get around this was to create a representative scalar stock element that simulates the current active cell. When the scalar stock element reaches capacity the “at stock test” triggers an inserted timestep and a discrete event then resets the scalar stock element to zero. However, this method did not work perfectly as the representative scalar stock element would not reset to zero until the next timestep, and therefore material was “lost” in these scenarios. After significant time attempting to solve this issue, it was determined to simplify this section of the model to continue to progress.

Simplified Model Approach

The GoldSim program allows the user to dynamically link a spreadsheet directly into the model, with the spreadsheet element able to import data from specified cells in the spreadsheet. The use of excel spreadsheets were also used in TMSim, therefore ultimately it was decided to simplify this section of the model using excel calculations.

Based on the inputted geometry and construction sequence of the pile, a matrix of the cumulative PAG or NAG waste rock produced by the mine when the cell becomes active is calculated and inputted into GoldSim. The model evaluates the total volume of material (PAG or NAG) produced from the mine and activates each construction cell as its corresponding volume is met. At each time step, if the construction cell is triggered as active, the cell is subject to climatic conditions and unsaturated flow as described in Sections 3.2.2 to 3.2.5.

3.2.1.2 Model Calibration

With the oversimplification of the waste rock deposition calculation, the model calibration became very minimal. Model calibration includes a sum of the volume of material within the four lifts within Goldsim using an integrator element to track the accumulation of material per lift. The volume output from GoldSim was then compared to the volume inputted in excel to confirm no mass loss.

3.2.2 Snowmelt

The snowmelt calculation accounts for the delayed infiltration that occurs from snow accumulation during winter and snowmelt during spring. The snowfall is determined based on any precipitation occurring below a critical temperature (+1°C), occurs as snowfall, otherwise it occurs as rainfall (Martinec et al. 1983).

3.2.2.1 Model Selection and Setup

There are two methodologies to calculate snowmelt rate, energy balance method and degree-day method. The energy balance method is based on the sum of heat fluxes toward and away from the snowpack being equal to the change in heat content of the snowpack (ΔH) for a given time period, as follows:

$$\Delta H = H_{rs} + H_{rt} + H_s + H_l + H_g + H_p \quad [3-1]$$

where H_{rs} is the net solar radiation, H_{rt} is net thermal radiation, H_s is the sensible heat transfer from air, H_l is the latent heat of vaporization from condensation or evaporation/sublimation, H_g is conducted heat from underlying ground, and H_p is advected heat from precipitation. This

is the most accurate method of the two, however, in order to use the method, a large amount of site data is required. Table 3-1 provides a list of required information for the energy balance method.

Table 3-1. Required information to determine heat content of snowpack (NRCS 2004)

Term	Influenced By
H_{rs}, H_{rt}	terrain, season, cloud cover, shading, air temperature, humidity
H_s, H_i	temperature gradients, humidity gradients, and wind speed
H_g	ground temperature, and snowpack temperature
H_p	precipitation temperature and snowpack temperature

At the feasibility stage of a mine, relevant parameters to use the energy balance model successfully would not be available. Therefore, the degree-day method was chosen for its simplicity as the only exogeneous variable is the mean daily air temperature. High resolution data with the time and amount of water released by snowmelt is necessary for short-term flood forecasting and long-term agricultural forecasting (Gray and Landine, 1987). As the main purpose of this model is primarily to understand the total flow leaving the waste rock pile, the simpler model is acceptable. The degree-day method is outlined in Li and Simonovic’s (2002) system dynamics model for predicting floods from snowmelt. The change in snowpack with time is given in the following equation:

$$\frac{dS}{dt} = P_s c - \alpha T \quad [3-2]$$

where S (cm) represents the water in snow storage, P_s (cm day⁻¹) is precipitation as snowfall identified by a critical temperature (T_{crit}), c (cm snow/cm precipitation) is snow-water equivalent coefficient, α (cm °C⁻¹ day⁻¹) is the degree-day factor for snowmelt, and T (°C) is daily mean temperature (Li and Simonovic 2002). When rain falls on snow, the snowpack is able to hold approximately 10% of it’s depth in rain, and runoff does not occur until that is reached (Oreiller et al. 2014). For simplicity in the model, the snowpack ability to hold rainwater was ignored as the runoff amounts would be very small, if any.

3.2.2.2 Model Calibration

Since the degree-day method is a simplification of environmental processes, the model needs to be calibrated using site historical data. The two unknown parameters are the snow-water equivalent (SWE) and the degree-day factor (DDF). The density of settled snow is approximately 200-300 kg/m³ (Paterson 1994) which corresponds to a SWE (snow/rain) of 0.3-0.5. The SWE changes based on the density of the snowpack throughout the year, however, due to the simplicity of the model, a fluctuating SWE breaks the law of conservation of mass. Therefore, for this model, the SWE was assumed to be constant throughout the year. The DDF is a scaling factor for how many centimetres of snowmelt occur per incremental degree above a threshold temperature per day. Based on literature, the DDF ranges from 0.2 for light, fresh snow and 0.8 for dense, wet snow (Anderson 1976; Graveline and Germain 2016; Li and Simonovic 2002; Martinec et al. 1983).

The optimization tool in GoldSim can be utilized to change the SWE and DDF to maximize the coefficient of determination (R^2) between the modelled and measured snowpack depth. The degree-day method does not account for melt that occurs during the warmest hours of the day. To align the spring melt to the measured snowpack melt, the threshold temperature where melt begins for March to May was included as an empirical variable in the optimization.

3.2.3 Evaporation

The evaporation calculation accounts for the evaporation that occurs at surface as a monthly value that is averaged to daily evaporation.

3.2.3.1 Model Selection and Setup

The evaporation model was originally a continuation of the work done by Zheng (2019). Zheng determined the evaporation within a cover system using the work done by Wilson et al. (1997) where the actual evaporation (AE) is a function of the ratio between relative humidity in the soil voids and the relative humidity of the air. However, the Wilson et al. method was created and validated only for sand and silt. This model is focused on the evaporation from a bare waste rock

pile that does not conform to the evaporation mechanics observed by Wilson et al. and therefore the actual evaporation was empirically determined.

In early stages of a project, potential evaporation (PE) rates may not be readily available and therefore, the potential evaporation was determined using the Thornthwaite (1948) method, which only requires the mean daily temperature which can be corrected for latitude and written as follows:

$$PE = K * 16 \left(\frac{10T_a}{I} \right)^\alpha \quad [3-3]$$

$$I = \sum \left(\frac{T_a}{5} \right)^{1.514} \quad [3-4]$$

$$\alpha = 6.75 \times 10^{-7} I^3 - 7.71 \times 10^{-5} I^2 + 1.79 \times 10^{-2} I + 0.49 \quad [3-5]$$

where PE (mm/month) is the monthly potential evaporation, K is the latitude correction factor for total sunlight hours in a month, T_a ($^{\circ}\text{C}$) is the mean monthly air temperature, I is the sum of 12 monthly heat indices (i), and α is a constant. In order to determine the mean monthly air temperature in GoldSim, the “Monthly and Annual Totals” model provided in the GoldSim model library was modified (GoldSim 2021). The Thornthwaite method uses a sum of the 12 monthly heat indices to determine monthly evaporation in a given year. Because future data is required during the calculation, the PE had to be inserted as its own GoldSim sub-model, which allows the contents of the container to be run before the rest of the model. The PE sub-model outputs the monthly evaporation in mm/day to be then used to determine the AE rate.

The AE rate is determined by multiplying the PE rate with the AE/PE ratio. Based on discussions with Dr. G.W. Wilson in 2020 regarding the validity of the Wilson et al. (1997) method of determining the AE/PE ratio a different approach was implemented for this model. Determining the AE rate from a waste rock pile is difficult, and there is some precedent in industry to estimate the PE and to then reduce to AE using a correction factor (Carey et al. 2005). Carey et al. (2005) conducted a study on the AE at the Key Lake Uranium Mine in Saskatchewan, Canada. The study

used an Eddy Covariance device to measure the AE above the waste rock pile for June to August. Carey et al. found that the monthly AE/PE ratio ranged from 0.47 to 0.65 of actual with an average value of 0.58. The user inputted AE/PE ratio should be based on the climate of the mine area, however, in the absence of data, a value between 0.47 to 0.65 would be a suitable starting range.

3.2.3.2 Model Calibration

Model calibration for the AE/PE ratio was completed as part of the Case Study in Section 4.4.3.

3.2.4 Hydrogeology

The hydrogeology model created by Zheng (2019) was a replication in GoldSim of a previous study on system dynamics modelling of infiltration and drainage in layered coarse soil (Huang et al. 2011; 2013). The model was initially created to simulate the change in water storage of a cover system. It was adapted in the current study to model each lift of a waste rock pile.

3.2.4.1 Model Selection and Development

The conceptual set-up of the model seen in Figure 3-7 shows the stock variable of water storage and the various flow variables between soil layers and the boundary inflows and outflows (Zheng 2019).

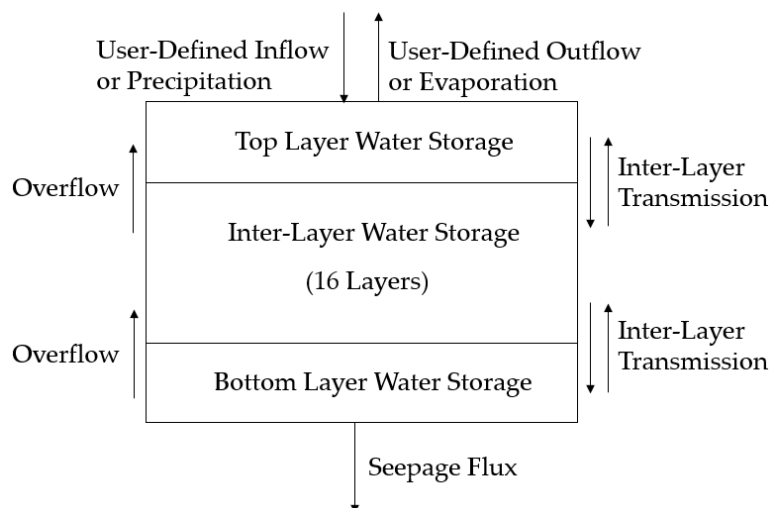


Figure 3-7. Conceptual set-up of the hydrogeology model (modified from Zheng, 2019)

Figure 3-8 displays the geometric set-up of each layer using the finite difference method. The soil parameters are taken from the center of the layer as the average across the layer (Zheng 2019).

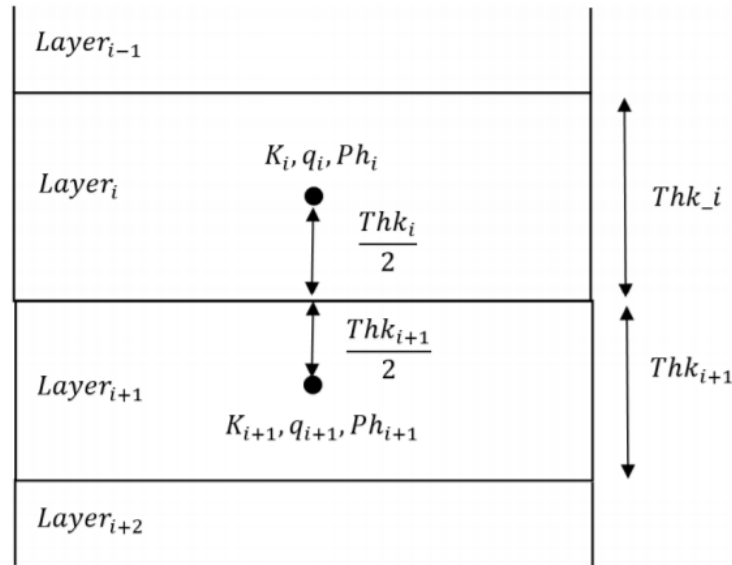


Figure 3-8. Geometric setup of the GoldSim model (modified from Zheng, 2019)

Using the set-up in Figure 3-8, the transmission rate (f) between two layers can be calculated using a modified version of the Darcy's equation, where the inter-layer hydraulic conductivity is assumed to be the average of the two layers, as follows:

$$f_i = \frac{K_{i-1} + K_i}{2} \left(\frac{Ph_i - Ph_{i-1}}{\frac{1}{2}(Thk_i + Thk_{i-1})} + 1 \right) \quad [3-6]$$

where, K (m/s) is the unsaturated hydraulic conductivity of the soil layer, Ph (m) is the pressure head within the soil layer, as a positive number for model simplicity, Thk (m) is the thickness of the soil layer and subscript i varies from 2 to n and n is the total number of soil layers (Romano et al. 1998). The unsaturated hydraulic conductivity can be calculated using the van Genuchten parameters that are estimated using the soil water characteristic curve (van Genuchten 1980 and Maulem 1976). The van Genuchten equations were re-arranged in GoldSim by Zheng (2019) as follows:

$$K = K_{sat} S_e^{\frac{1}{2}} \left[1 - \left(1 - S_e^{\frac{1}{m}} \right)^m \right]^2 \quad [3-7]$$

$$Ph = \frac{\left[\left(\frac{1}{S_e} \right)^{\frac{1}{m} - 1} \right]^{\frac{1}{n}}}{a} \quad [3-8]$$

$$S_e = \frac{q - Q_r}{Q_s - Q_r} \quad [3-9]$$

$$m = 1 - \frac{1}{n} \quad [3-10]$$

$$q = \frac{S_i}{Thk_i} \quad [3-11]$$

where, K_{sat} (m/s) is the saturated hydraulic conductivity, S_e is the normalized effective volumetric water content, a (1/m), n and m are van Genuchten model fitting parameters, q is the volumetric water content of the layer, Q_r and Q_s are the residual and saturated volumetric water content and S_i (m) is the amount of water stored in the soil layer. Zheng (2019) expanded the model to include overflow if the soil layer becomes fully saturated, allowing for the following equation for change in water storage:

$$\frac{dS_i}{dt} = f_i + Overflow_{i+1} - f_{i-1} \quad [3-12]$$

where the Overflow (cm/min) is the overflow from layer $i+1$ to layer i and the subscript i varies from 2 to $n-1$ as there is no overflow into the bottom layer. The total water storage (S_T) within all the soil layers is determined as the sum of the water storage in each layer.

$$S_T = \sum S_i \quad [3-13]$$

This model ignored the effect of hysteresis on the SWCC and only the drying curve parameters are used. This is anticipated to be minimal as the model aims to model overall pile behaviour.

3.2.4.2 Model Calibration

The model was validated for infiltration and drainage separately by Zheng (2019) using the SV60 scenario modelled by Huang et al. (2011; 2013). The GoldSim model was able to successfully replicate the conditions observed in the field and in the Huang et al. (2011; 2013) SD model.

Zheng (2019) used 18 soil layers for the model in order to replicate the work done by Huang et al. (2011; 2013). The depths used by Zheng (2019) were for covers and were on the order of 1 to 5 m. In order to ensure the model continued to behave correctly with increasing the depth to 10 m, an array of soil layers was tested for model changes. The cumulative seepage out of a 1-D column over a 1-year period was modelled using 5, 10, 20, 30, and 40 soil layers, or “containers”. As Zheng (2019) used 18 layers, the 20-layer model was used as the base case, 20 was opted over 18 in order to simplify the discretization over 10 metres. Figure 3-9 depicts the seepage results of models with 5, 10, 30, and 40 soil layers compared to the base case. The models with 5 and 10 soil layers retained more water within the column and did not align with the behaviour of the base case. Once the discretization was less than 0.5 m (20 layers) the results of the models did not vary significantly.

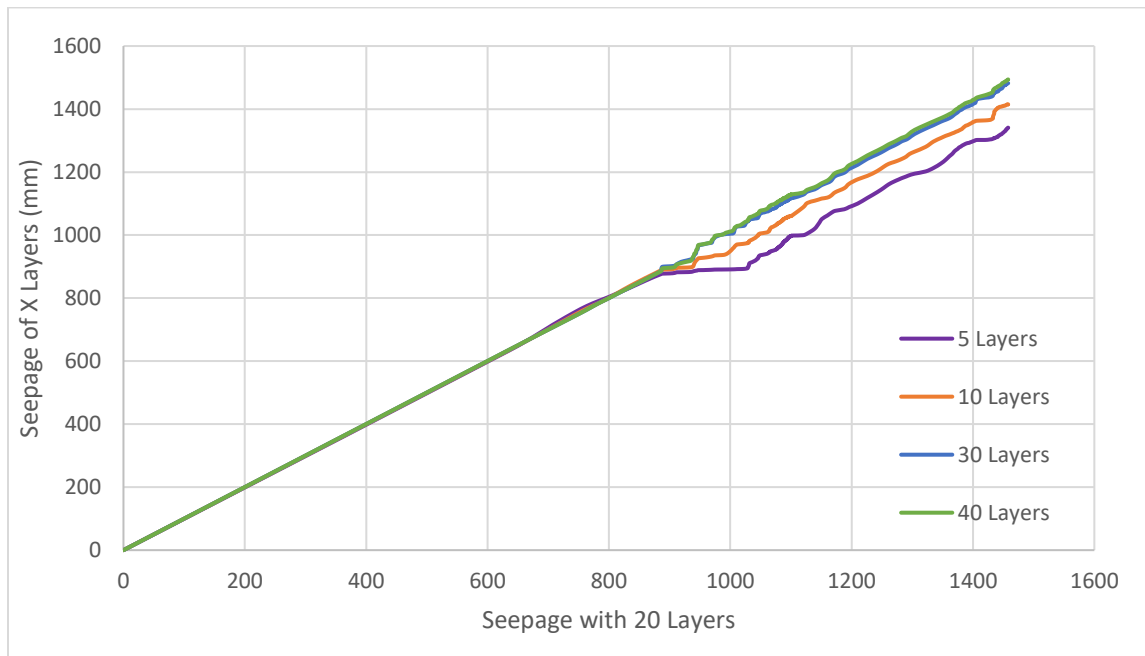


Figure 3-9. Comparison of Cumulative 1D Seepage to Base Case

To better understand the variations in the models, the R^2 was determined for the four cases. Table 3-2 summarizes the results of the statistical analysis, which align with the above interpretation that 5 and 10 soil layers is unsuitable, but there is limited difference between 20, 30 and 40 soil layers. In the interest of reducing model size and run times, 20 soil layers was chosen as the final discretization for each lift.

Table 3-2. Coefficient of Determination

# of Layers	R^2
5 Layers	0.7290
10 Layers	0.9598
30 Layers	0.9947
40 Layers	0.9849

3.2.5 Runoff

The runoff calculation was a continuation of the work completed by Zheng (2019) and accounts for the runoff that occurs on the batter (slope) of the waste rock pile.

3.2.5.1 Model Selection and Development

The runoff model developed by Zheng (2019) is calculated based on the assumption that “the surficial soil layer becomes immediately saturated during precipitation events (Smith et al. 2002) and that the overland flow is negligible for high permeable soils subject to low-intensity rainfall (Dunne and Black 1920, Dingman 2002)”. Additional field data and descriptions on the calibration of this approximation are included in Jubinville (2013). The runoff prediction model is based on the concept that the infiltration capacity of the soil is equal to the hydraulic conductivity, up to the saturated hydraulic conductivity. When a soil is fully saturated the infiltration capacity will be equal to the saturated hydraulic conductivity and any additional precipitation rate will become surface runoff as depicted in Figure 3-10.

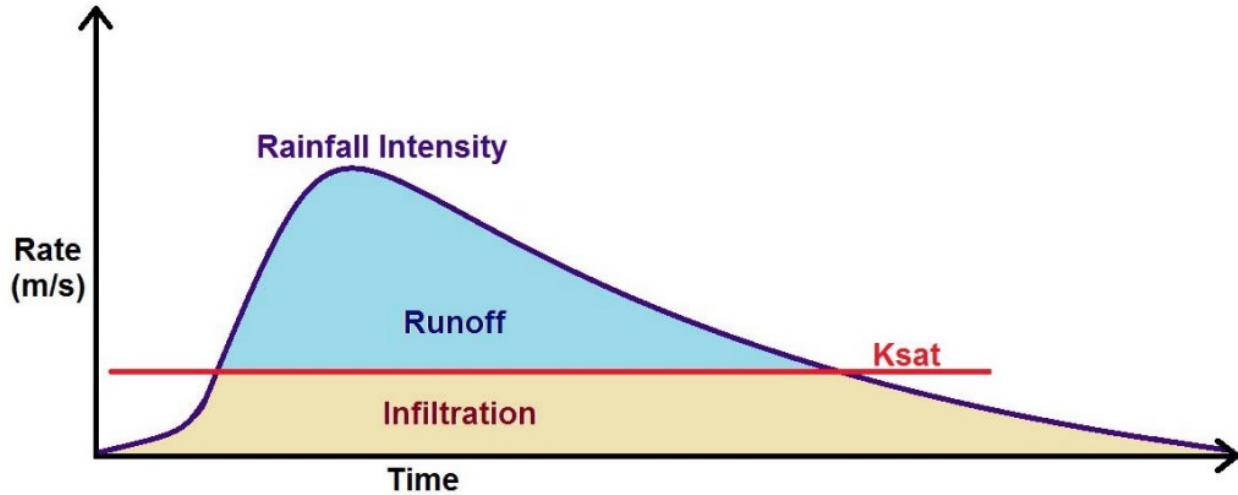


Figure 3-10. Runoff prediction for a typical rainfall event
(from Jubinville 2013, after Wilson 2006)

In GoldSim, the infiltration capacity is calculated using the following if statements:

If the precipitation rate is less than the hydraulic conductivity, the infiltration capacity is equal to the precipitation rate and the surface runoff is from overflow from Layer 1 as follows:

$$\text{Infiltration Capacity} = \text{Precipitation Rate} \quad [3-14]$$

$$\text{Surface Runoff} = \text{Overflow}_1 \quad [3-15]$$

If the precipitation rate is greater than the hydraulic conductivity, the infiltration capacity is equal to the saturated hydraulic conductivity and the additional precipitation becomes surface runoff as follows:

$$\text{Infiltration Capacity} = K_{sat} \quad [3-16]$$

$$\text{Surface Runoff} = \text{Precipitation Rate} - K_{sat} + \text{Overflow}_1 \quad [3-17]$$

The inclusion of lateral runoff into the model was difficult as the model is a system of 1-D columns to create a pseudo 3-D system and runoff requires lateral movement of water. An attempt to

include lateral runoff from the benches (surface) was initially included to simulate the benefits of lateral inclined layers as investigated by Broda et al. 2014, Dawood and Aubertin 2014, Maknoon 2016, and Martin et al. 2017. The inclusion of lateral runoff was ultimately removed from consideration in the model due to erroneous water balance issues and significant effort was required to hard code the movement of water to each cell. In order to simplify the model, any runoff that occurs on the surface was assumed to be removed from the system water balance rather than move laterally. As the material is coarse waste rock, the runoff was assumed to be minimal, and the total runoff (or water removed from the system) is tracked to verify the runoff was negligible.

As more runoff occurs from a steep slope than a shallow slope, the inclusion of runoff from the batter (slope) was included as an empirical user inputted ratio. The runoff from the cell flows outward into the lower lift, in the case of the corner cell, the runoff is split into the three surrounding cells in the below lift as seen in Figure 3-11.

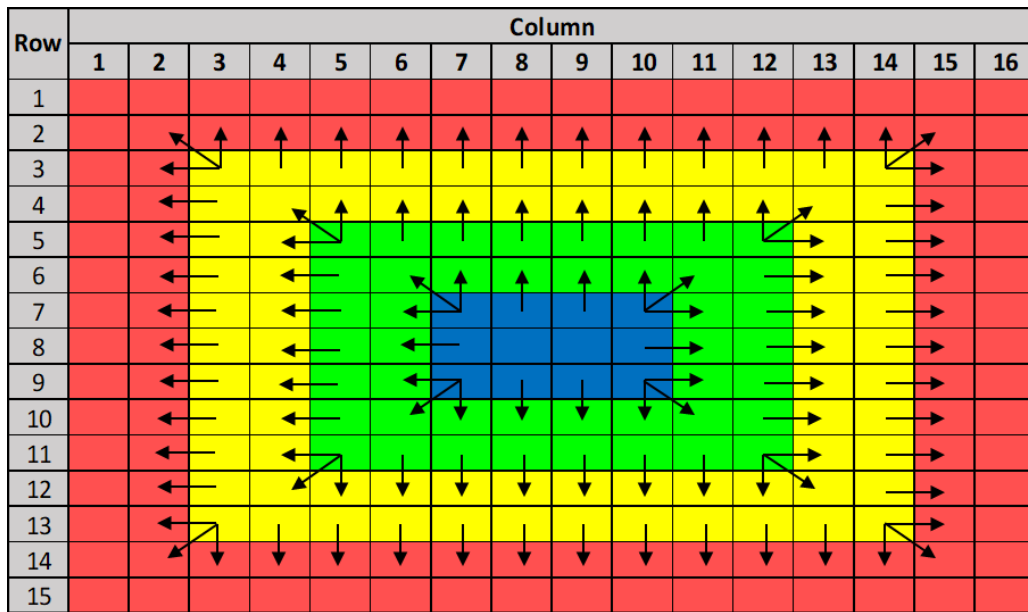


Figure 3-11. Direction of Runoff from Batter (Slope)

3.2.5.2 Model Calibration

Model calibration for the runoff calculation was confirmed as part of the water balance for the Case Study in Section 4.6.1.

4 DEMONSTRATION OF MODEL APPLICATION

4.1 Introduction

The focus of the model outlined in Section 3 was to develop a simplified model of a hard rock mine system that could be implemented during the feasibility stage of a mine. The intention of this was to allow for special handling mitigation methods to be simulated, in order to accommodate changes at the early stages of a mine based on modelling results. A case study for a mine site at the feasibility stage was used to demonstrate the application of the model. Inclusion of details from the Case Study in the model are further defined in the following sections.

4.2 Mining Inputs

4.2.1 Mine Plan

A mine plan for the Case Study project was obtained in 2018. The mine plan provided the tonnages of overburden, NAG, PAG, and ore over a five-year period. Year 1 and 2 were provided in monthly quantities, and Years 3 to 5 were provided in quarter and bi-annual quantities that were adjusted to monthly. The monthly quantities were then inputted into the GoldSim input dashboard, and the model then reduces to daily quantities as outlined in Section 3.2.1.1.

4.2.2 Stockpile Design

The 2015 design of the PAG stockpile for the Case Study was used for the model pile. The heaped fill waste rock pile was recreated in AutoCAD (Figure 4-1) and the surface area of each of the four lifts was determined. As the pile will contain both NAG and PAG, a uniform bulk density of 1.9 tonne/m³ was determined using the total weight of NAG and PAG to be produced, and the total volume of the NAG and PAG waste rock piles. The new bulk density ended up with insufficient PAG material to complete the pile, therefore the surface areas were proportionally reduced to a final pile volume of 1,631,000 m³. A summary of the lifts and pile geometry can be found in Table 4-1.

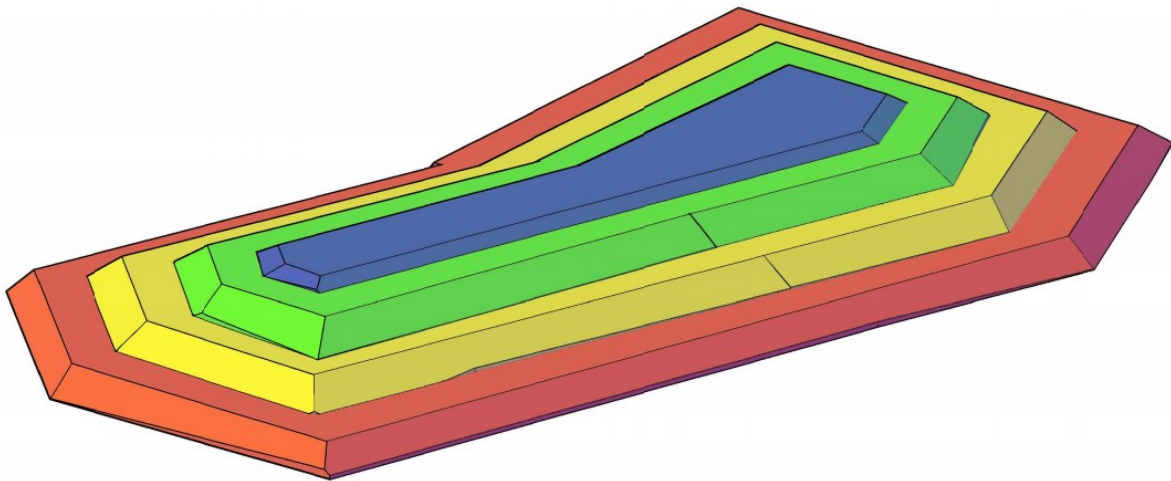


Figure 4-1. Waste Rock Pile Design

Table 4-1. Geometry of Modelled Pile

Lift	Surface Area (m²)	Height (m)	Volume (m³)
Lift 4	12,685	4	43,869
Lift 3	32,279	10	275,717
Lift 2	57,021	10	511,992
Lift 1	86,612	10	799,423
Total	86,612	34	1,631,000

As discussed in Section 3.2.1.1, the area of each 1-D column must remain constant throughout the four lifts. To account for this, the area of the cells was calculated in a stepwise way:

1. The area of the lift 4 cells was determined based on the number of cells assigned to Lift 4 and the total area of lift 4.
2. The area of lift 4 was subtracted from the lift 3 area, and the additional surface area was then accounted for by the remaining lift 3 cells that do not have lift 4 cells above them.
3. The area of lift 3 was subtracted from the lift 2 area, and the additional surface area was then accounted for by the remaining lift 2 cells that do not have lift 3 cells above them.
4. The area of lift 2 was subtracted from the lift 1 area, and the additional surface area was then accounted for by the remaining lift 1 cells that do not have lift 2 cells above them.

The total area of each 1-D column (cell) for the pile is detailed in Figure 4-2. Due to an error in the initial estimation of surface area, the lift 4 cells ended up with larger surface areas than the rest of the pile. In order to increase the pile size, the GoldSim array size would need to be updated and some of the connections would require substantial updates, particularly the runoff discussed in Section 3.2.5. As the surface of lift 4 is essentially the same, it was determined that a larger area is acceptable as the behaviour will remain the same; however, if additional discretization in the top lift was wanted, the model could be updated as required in future.

Row	Column															
	1	2	3	4	5	6	7	8	9	10	11	12	13	14	15	16
1	230	230	230	230	230	230	230	230	230	230	230	230	230	230	230	230
2	230	325	325	325	325	325	325	325	325	325	325	325	325	325	325	230
3	230	325	277	277	277	277	277	277	277	277	277	277	277	277	325	230
4	230	325	277	386	386	386	386	386	386	386	386	386	386	277	325	230
5	230	325	277	386	362	362	362	362	362	362	362	362	386	277	325	230
6	230	325	277	386	362	565	565	565	565	565	565	362	386	277	325	230
7	230	325	277	386	362	565	344	344	344	344	565	362	386	277	325	230
8	230	325	277	386	362	565	344	4624	4624	344	565	362	386	277	325	230
9	230	325	277	386	362	565	344	344	344	344	565	362	386	277	325	230
10	230	325	277	386	362	565	565	565	565	565	565	362	386	277	325	230
11	230	325	277	386	362	362	362	362	362	362	362	362	386	277	325	230
12	230	325	277	386	386	386	386	386	386	386	386	386	386	277	325	230
13	230	325	277	277	277	277	277	277	277	277	277	277	277	277	325	230
14	230	325	325	325	325	325	325	325	325	325	325	325	325	325	325	230
15	230	230	230	230	230	230	230	230	230	230	230	230	230	230	230	230

Figure 4-2. Area (m²) of each cell of waste rock pile

The model includes three acid rock drainage mitigation methods that modify the placement of NAG and PAG waste rock. The mitigation strategies are implemented in the following ways: PAG separation assumes the entire pile is PAG; layering assumes each lift is 50% PAG covered with a 50% layer of NAG; and encapsulation assumes the pile has NAG cells beside and above to surround the PAG cells. Figure 4-3 was created in AutoCAD to illustrate the placement of NAG and PAG for the three mitigation options.

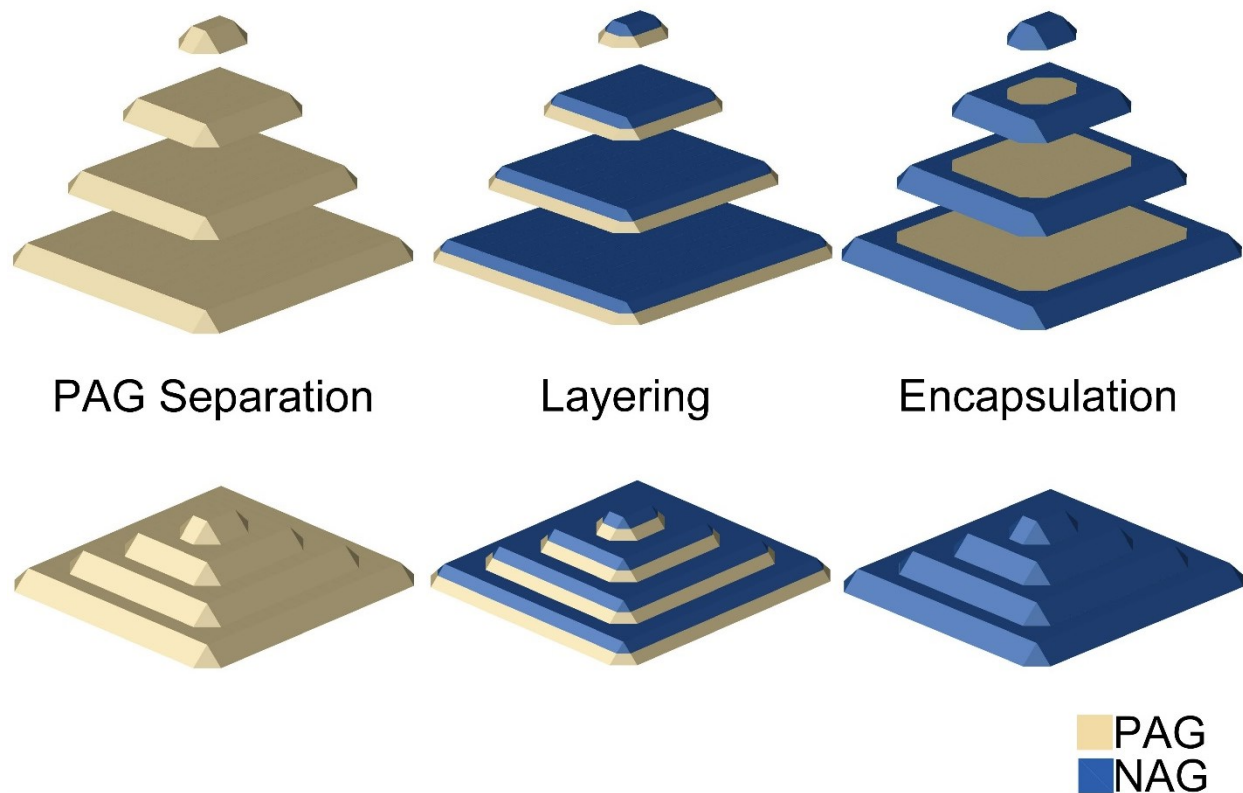


Figure 4-3. Waste Rock Pile ARD Mitigation Options Design

4.3 Waste Rock Inputs

4.3.1 Unsaturated Soil Parameters

Physical characteristics of the waste rock at the mine were unavailable at the time of model development, therefore waste rock parameters from a nearby gold mine in the Abitibi-Témiscamingue region was used for the research. The parameters of the waste rock were taken from the work completed on waste rock from Doyon Mine by Larochelle (2018) and are summarized in Table 4-2.

Table 4-2. Waste Rock Soil Parameters

Parameter	Value
Θ_{RESIDUAL}	0.078
$\Theta_{\text{SATURATED}}$	0.38
Van Genuchten α	0.42 cm ⁻¹
Van Genuchten n	1.82
$K_{\text{SATURATED}}$	0.0004 m/s

To simulate an end-dumped waste rock pile, the lift is created with increasing particle size with depth. With increasing particle size, the soil water characteristics and saturated hydraulic conductivity would change. Therefore, multiple sets of soil parameters are needed to model the end-dumped scenario. Herasymuik (1996) discussed the distinction of waste rock into categories based on the percentage of material passing the 4.75 mm (#4) sieve. He proposed six classifications, less than 10%, 10-19%, 20-29%, 30-39%, 40-49%, and more than 50% passing. Barsi (2017; 2019) followed this classification system on the Diavik waste rock and soil parameters for each of the classifications, excluding less than 10% category due to lack of samples. Due to the lack of availability of various soil water characteristic curves for a comparative waste rock, the five sets of soil parameters Barsi found were used as a correction factor. The soil water characteristic curves created by Barsi were determined using the Fredlund and Wilson method (Fredlund et al. 1997). In order to compare to van Genuchten parameters, the curves were back analyzed using the program RETC. The soil parameters of the Diavik waste rock can be seen in Table 4-3. The saturated volumetric water content was kept constant at 0.25 to follow the methodology used by Barsi (2017; 2019). The soil parameters were then normalized to the values of Soil D (Table 4-4).

Table 4-3. Soil parameters for Diavik waste rock (modified from Barsi, 2017)

	B (10-19%)	C (20-29%)	D (30-39%)	E (40-49%)	F (>50%)
Q_R	0.060	0.047	0.034	0.044	0.030
Q_S	0.25	0.25	0.25	0.25	0.25
α	80.15	45.26	21.85	15.29	4.61
n	1.48	1.54	1.70	1.81	2.76
K_{sat}	1.0E-03	5.4E-04	3.2E-04	1.8E-04	9.0E-05

Table 4-4. Correlations of soil parameters normalized to soil D

	B (10-19%)	C (20-29%)	D (30-39%)	E (40-49%)	F (>50%)
Q_R	1.77	1.40	1	1.31	0.88
Q_S	1	1	1	1	1
α	3.67	2.07	1	0.70	0.21
n	0.87	0.90	1	1.06	1.62
K_{sat}	3.13	1.69	1	0.56	0.28

Only five soil groups were used in order to align with the work done by Barsi (2017) as well as for symmetry of two soil groups finer and two soil groups coarser than the reference group. Using the soil parameters of the Doyon waste rock as the intermediate soil type, the other four sets of parameters were corrected using the normalized correlations from Table 4-4. The five sets of soil parameters used in the model can be seen in Table 4-5 and the SWCC are in Figure 4-4, the labelling was reset to A to reduce confusion within the model.

Table 4-5. Unsaturated soil parameters for five waste rock soil types used in model

	A (10-19%)	B (20-29%)	C (30-39%)	D (40-49%)	E (>50%)
Q_R	0.138	0.109	0.078	0.102	0.069
Q_s	0.38	0.38	0.38	0.38	0.38
α	154.04	86.99	42.00	29.38	8.86
n	1.58	1.65	1.82	1.94	2.95
K_{sat}	1.3E-03	6.8E-04	4.0E-04	2.3E-04	1.1E-04

Using the unsaturated soil parameters calculated in Table 4-5, the following equation for soil water content, as a function of pressure head was used to determine the soil water characteristic curves found in Figure 4-4.

$$\theta = \theta_R + \frac{(\theta_S - \theta_R)}{[1 + (ah)^n]^m} \quad [4-1]$$

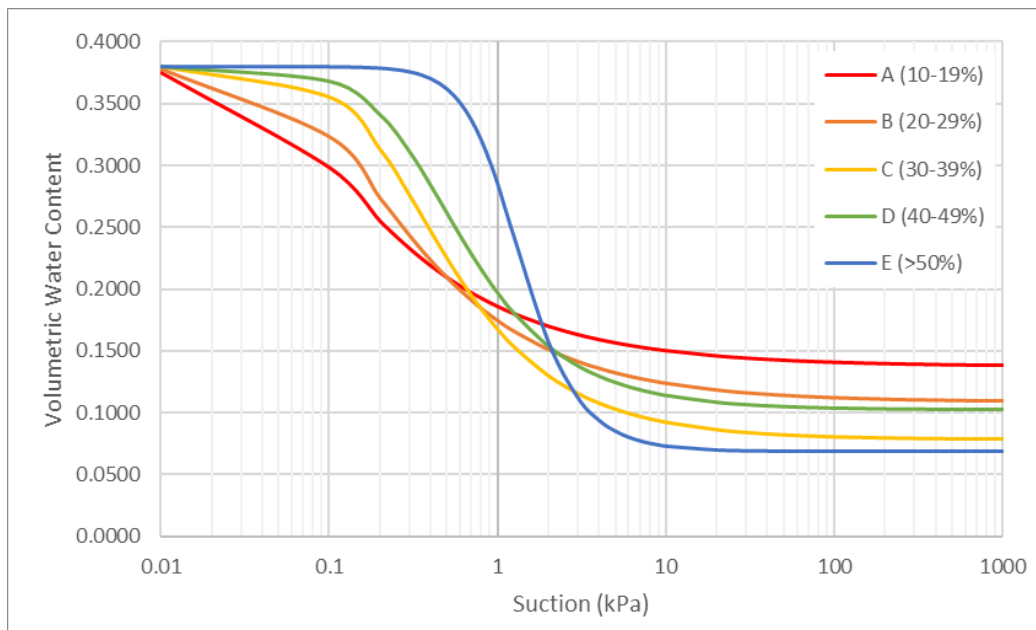


Figure 4-4. Soil water characteristic curves for five waste rock soil types used in model

4.3.2 Unsaturated Soil Parameters for Compacted Surface Layer

Unsaturated soil properties after compaction were not known for the surrogate waste rock. In lieu of this, an approximation was made based on discussions with Dr. G.W. Wilson in 2020. The approximation assumed that a compacted soil would have bulk density 10% larger than the uncompacted soil, which would result in a lower void ratio and saturated volumetric water content. Once the new void ratio was determined based on the new bulk density, a version of the Kozeny-Carmen equation (Equation 4-2) was used to determine saturated hydraulic conductivity; this form of the equation was evaluated by Chapuis and Aubertin (2003), who concluded the form may be used for any soil, either plastic or non-plastic.

$$\text{Log}(K_{sat}) = 0.5 + \log\left(\frac{e^3}{G_s^2 S_s^2 (1+e)}\right) \quad [4-2]$$

Where e is the void ratio, G_s is the specific weight of solids, and S_s is the specific surface of solids (m^2/kg). The soil water characteristic curve of the compacted soil was created using the following assumptions:

1. The compacted curve would be offset from 0.38 to 0.24 volumetric water content.
2. The compacted curve would be parallel to the uncompacted curve until they intersected, which would be the compacted air entry value.
3. The compacted curve would then follow the uncompacted curve to residual volumetric water content.

Two compaction curves were required, as soil type E is the surface material for the end dumping case, and soil type C is the only material used for the paddock dumping case. The RETC program was run using the approximated compacted curve data points, with forced residual volumetric water content, saturated water content, and saturated hydraulic conductivity to determine the fitted α and n Van Genuchten parameters. The SWCC were then recreated using Equation 4-1, as shown in Figure 4-5. The R^2 was determined for the two curves, and found to be 0.986 for soil type C, and 0.997 for soil type E.

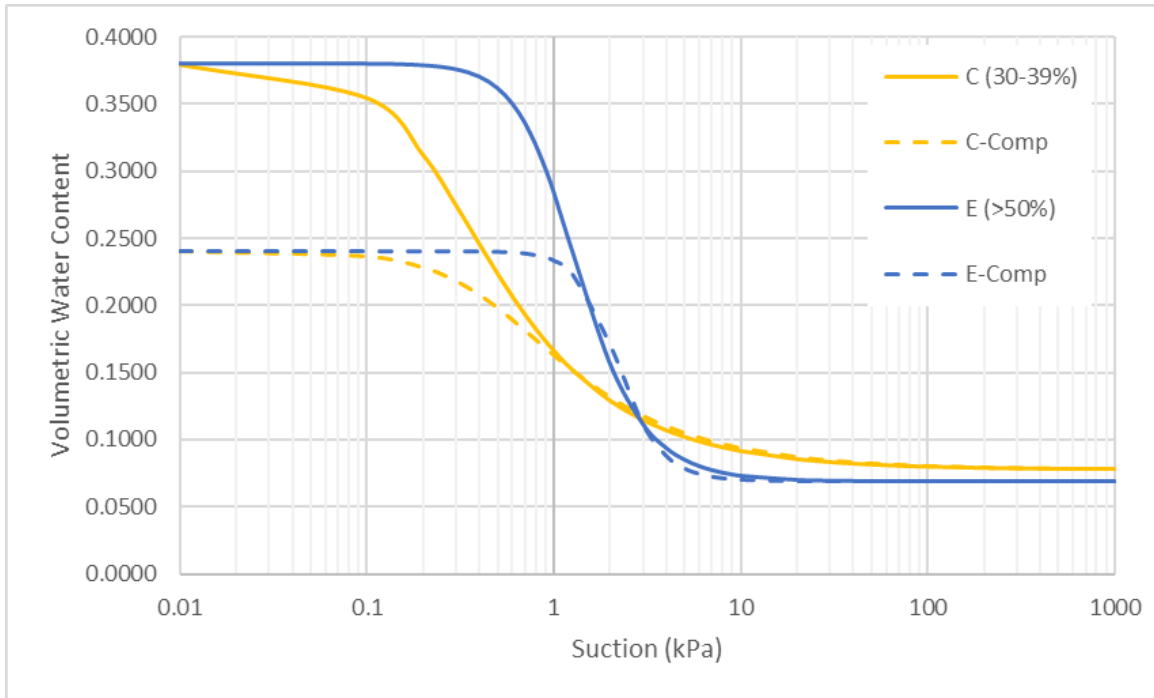


Figure 4-5. Soil water characteristic curves for compacted soil types used in model

4.4 Climate Inputs

4.4.1 Weather Data

Historical data for Val D'Or was collected using the Environment Climate Change Canada website. For Val D'Or, there was four weather stations near the airport that had collected data at various intervals (hourly, daily, monthly) and periods of time from 1955 to 2018. All four station data sets were combined in order to create a data set with daily average values for minimum and maximum temperature, precipitation, relative humidity, and snowpack depth. Where daily values were missing, the 24-hour hourly data was used to get the minimum and maximum temperature and averaged daily values. Any other data gaps were inputted as an average of the previous and subsequent data values.

4.4.2 Evaporation

A simulated scenario using the waste rock parameters outlined in Section 4.3 was modelled for a 10 m 1-D column in GoldSim and Hydrus 1-D. Table 4-6 summarizes the climate input from a weather station in the Abitibi-Témiscamingue region of Quebec in the format of daily average values for each month.

Table 4-6. Daily average precipitation and potential evaporation

Month	Daily Average Precipitation (mm)	Daily Average Potential Evaporation (mm)
January	1.35	0
February	0.78	0
March	1.62	0
April	0.50	0.52
May	0.80	1.23
June	2.37	2.27
July	1.75	2.4
August	3.42	2.12
September	2.60	1.33
October	4.01	0.78
November	2.99	0
December	3.32	0

The simulations were run for a period of one year from January to December. The GoldSim model was run multiple times, changing only the AE/PE ratio until alignment with the Hydrus 1-D model was reached. The actual evaporation correction factor was determined based on a combination of the alignment of cumulative evaporation and cumulative seepage out of the pile and the total evaporation. The AE/PE ratio for the simulation was found to be 0.485, which aligns with the expected range of 0.47-0.65 discussed in Section 3.2.3. The cumulative evaporation over the year for the two simulations can be seen in Figure 4-6, with the direct comparison in Figure 4-7. The GoldSim model followed a smooth parabolic shape, with evaporation slightly underestimated in May and June and overestimated July to October, this direct comparison is also observed in Figure 4-7.

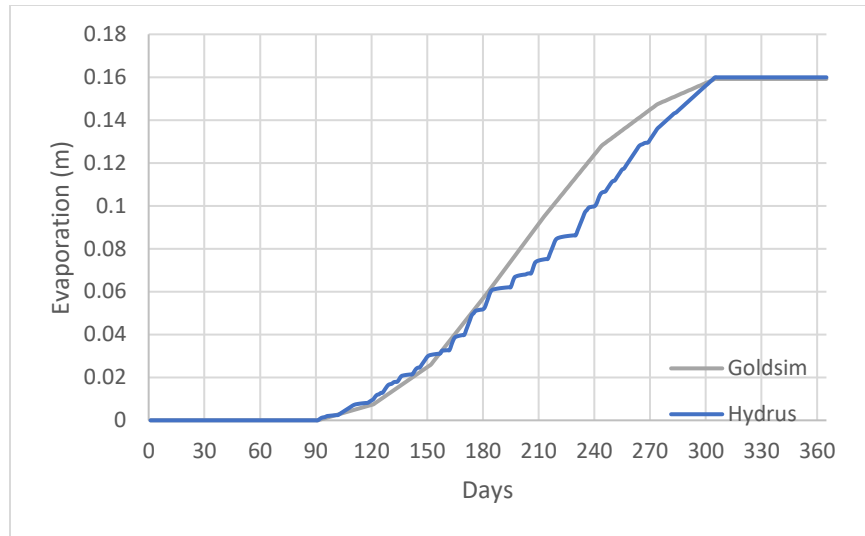


Figure 4-6. Cumulative evaporation over one year of scenario modelled

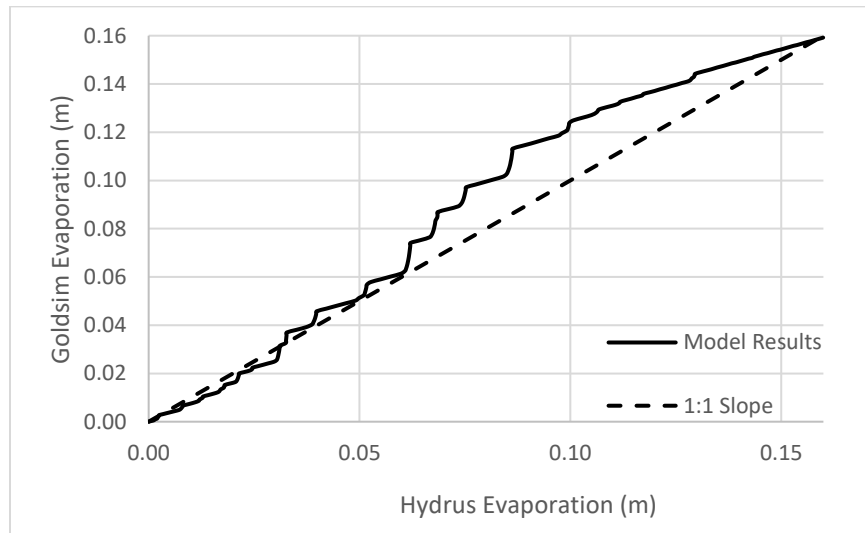


Figure 4-7. Comparison of the cumulative evaporation modelled using GoldSim and Hydrus

The Hydrus 1-D model determines the AE based on current soil conditions, which allows for a more varied evaporation, with small periods of higher and lower evaporation. Despite the differences in the two models, there is still fair agreement between the two with an R^2 value of 0.9787 for the cumulative evaporation over the period of one year. The cumulative one-dimensional seepage out of the pile for the two models was also modelled (Figure 4-8). The direct comparison of model results can be seen in Figure 4-9 along with the 1:1 slope for reference.

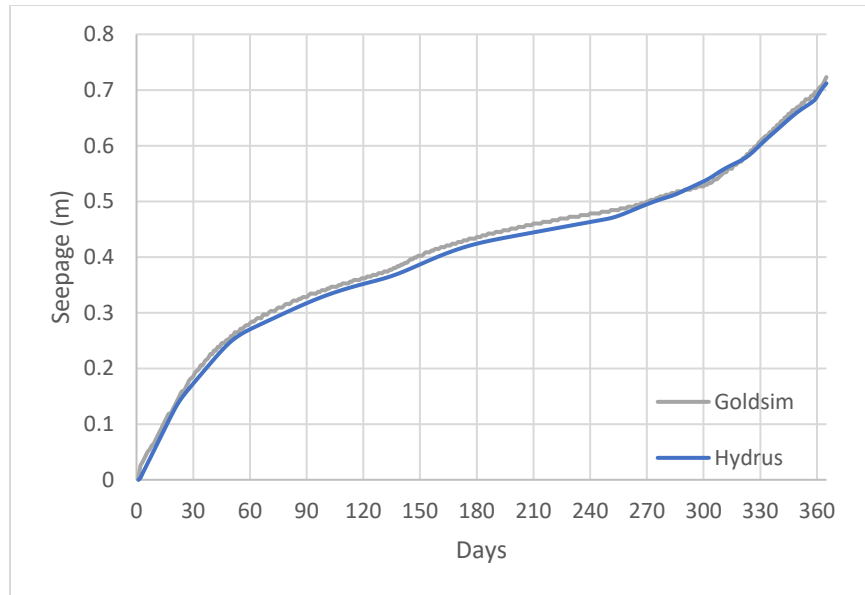


Figure 4-8. Cumulative 1-D seepage over one year of scenario modelled

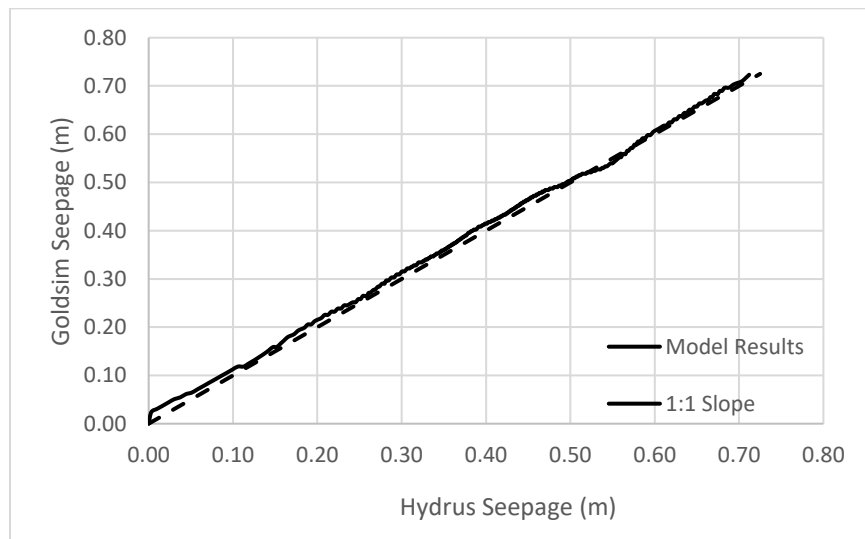


Figure 4-9. Comparison of the cumulative 1-D seepage modelled using Goldsim and Hydrus

The cumulative 1-D seepage out of the piles followed similar behaviour trends with an R^2 of 0.9941. As well, the percentage error of the total cumulative evaporation and total cumulative 1-D seepage for the two models was found to be 0.46% and 1.58% respectively. The constant AE/PE ratio method utilized in GoldSim seems to be suitable for the needs of the model based on the simulated evaporation and seepage.

4.4.3 Snowmelt

Since the degree-day method is a simplification of environmental processes, the model needs to be calibrated using site historical data from the Val D'Or climate station for the years 1955-1991.

The optimization tool in GoldSim was utilized to change the SWE and DDF to maximize the R² value between the modelled and measured snowpack depth. The degree-day method does not account for melt that occurs during the warmest hours of the day. To align the spring melt to the measured snowpack melt, the threshold temperature where melt begins for March to May was included as a variable in the optimization. The optimization provides a R² of 0.8548, Table 4-7 displays the optimized calibration parameters.

Table 4-7. Calibration parameters after model optimization

Parameter	Snow-water Equivalent (cm snow/cm rain)	Degree-day Factor (cm/°C/day)	Melt Threshold Temperature (°C)
Value	0.2844	0.6	-7.2

When the model is run for the 36 years of snowpack data available, the modelled and measured mean snowpack depth can be plotted together (Figure 4-10). There is a fair correlation between the two curves, however, the modelled snowpack depth is smaller than measured in the early winter months. This is due to the model having a constant SWE that is closer to dense, settled snow, that is not as accurate for less dense, fresh snow.

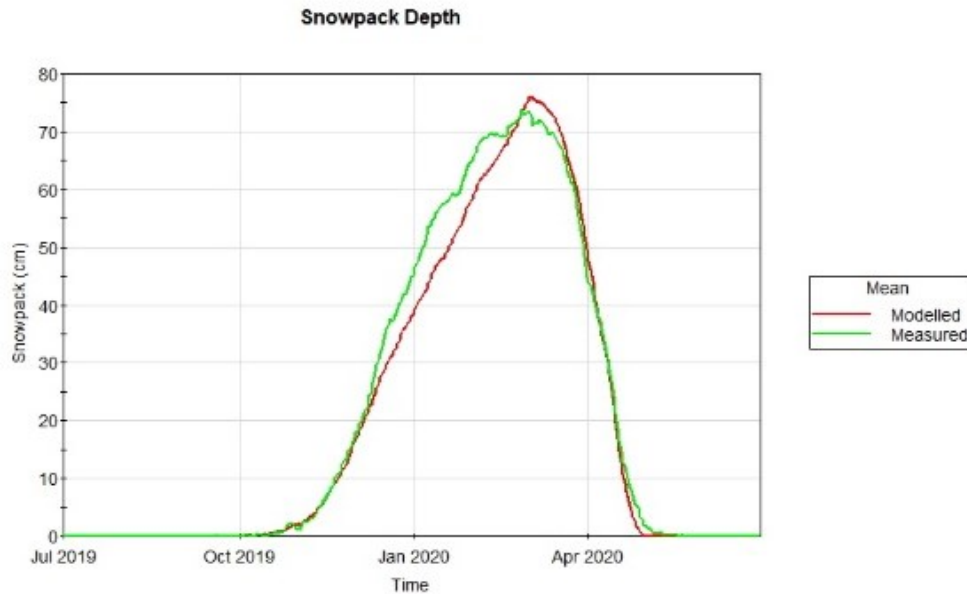


Figure 4-10. 36-year mean modelled and measured snowpack depth in GoldSim

4.5 Modelling Results

The GoldSim Model was run for a period of 50 years, the first five years are simulated during pile construction, and the additional 45 years are to illustrate short-term and long-term behaviour of the waste rock pile. The GoldSim model was run eight times, with the following scenarios:

1. End Dump – PAG Separation
2. End Dump – Layering
3. End Dump – Encapsulation
4. End Dump – Compaction with Layering
5. Paddock Dump – PAG Separation
6. Paddock Dump – Layering
7. Paddock Dump – Encapsulation
8. Paddock Dump – Compaction with Layering

A summary of the modelling results is detailed in the following sections to highlight the model capabilities and comparison of construction scenarios. All model results for the eight scenarios can be found within Appendix 4.

4.5.1 General Model Behaviour

Scenario 1 (End Dump – PAG Separation) was chosen as an example model to illustrate the GoldSim model behaves as expected. Figure 4-11 includes the water balance results for the 50 year simulation for a 3-D column in the centre of the pile that contains all four lifts. Long-term behaviour of the pile stabilizes, and the overall cumulative behaviour is linear with a cyclical pattern for each year. As the model is run for 50 years, the initial behaviour during construction of the pile is difficult to view, therefore Figure 4-12 is truncated to only include the first 6 years of the model to better highlight the changes during pile construction.

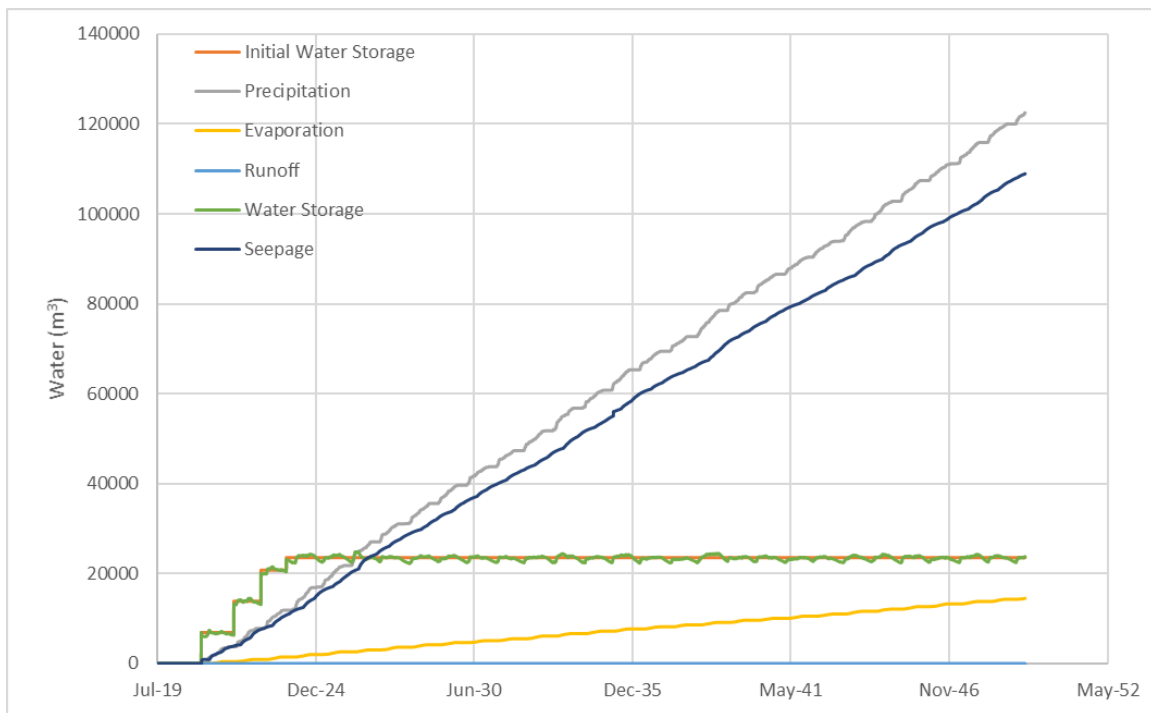


Figure 4-11. 50 Year Water Balance for Scenario 1: End Dumping with PAG Separation

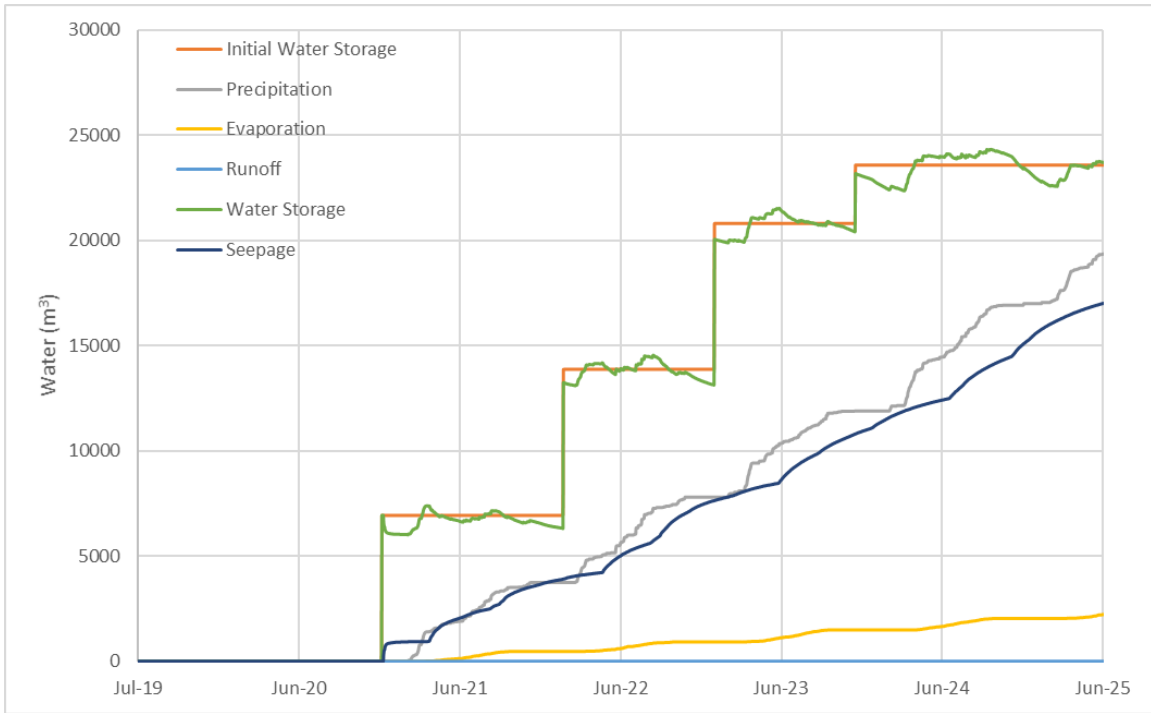


Figure 4-12. 6 Year Water Balance for Scenario 1: End Dumping with PAG Separation

4.5.2 Dumping Method Comparison

The mitigation option PAG Separation was chosen as an example scenario to illustrate the impacts of the waste rock dumping method on the model. Select information was included for a 1-D column in the centre of the pile that contains all four lifts to highlight the differences between the two methods. Figure 4-13 and Figure 4-14 include the normalized water storage and cumulative seepage for the 50-year model simulation.

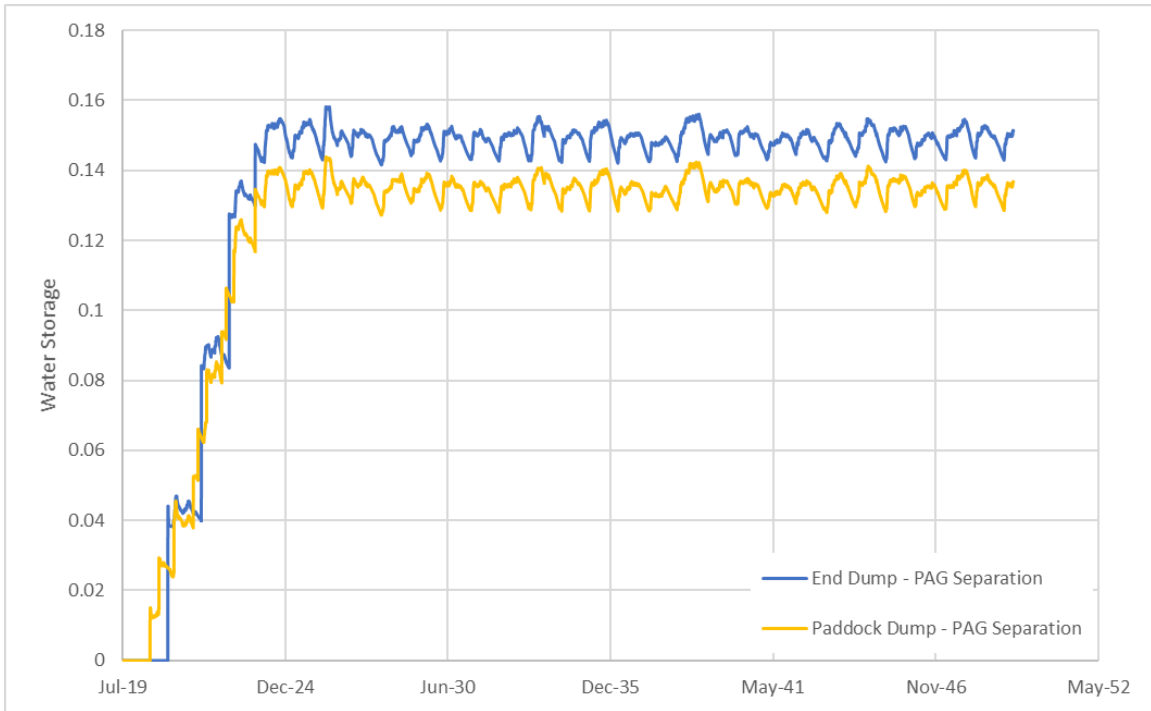


Figure 4-13. Comparison of normalized 1D water storage for each dumping method

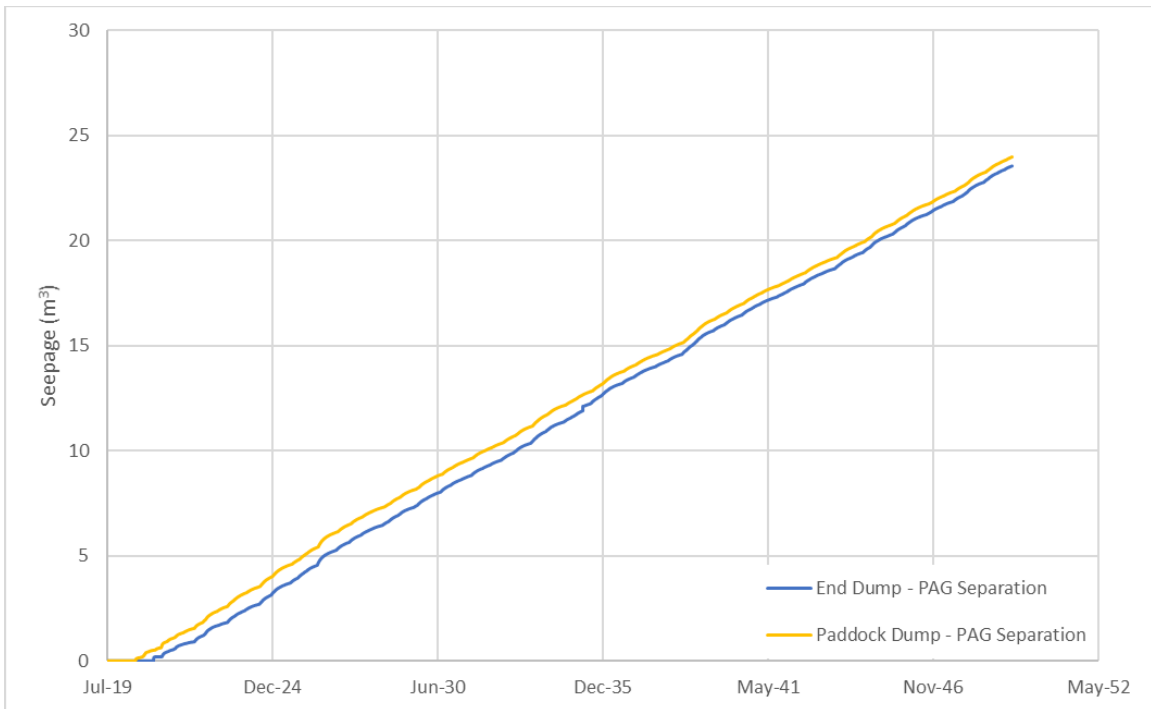


Figure 4-14. Comparison of seepage for each dumping method

4.5.3 Mitigation Method Comparison

The end dumping scenarios were chosen to illustrate the impacts of the ARD mitigation methods on the model. Select information was included for a 1-D column in the centre of the pile that contains all four lifts to highlight the differences between the two methods. Figure 4-15 and Figure 4-16 include the normalized water storage and cumulative seepage for the 6-year model simulation.

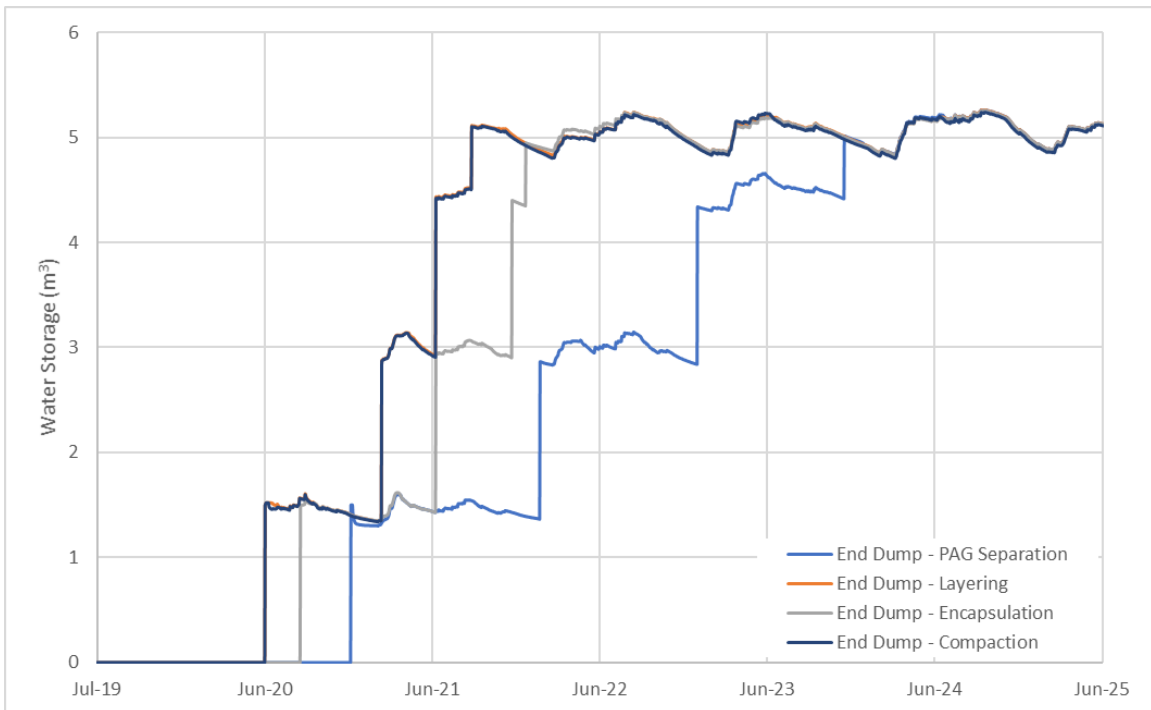


Figure 4-15. 1-D Water Storage for ARD mitigation methods with End Dumping

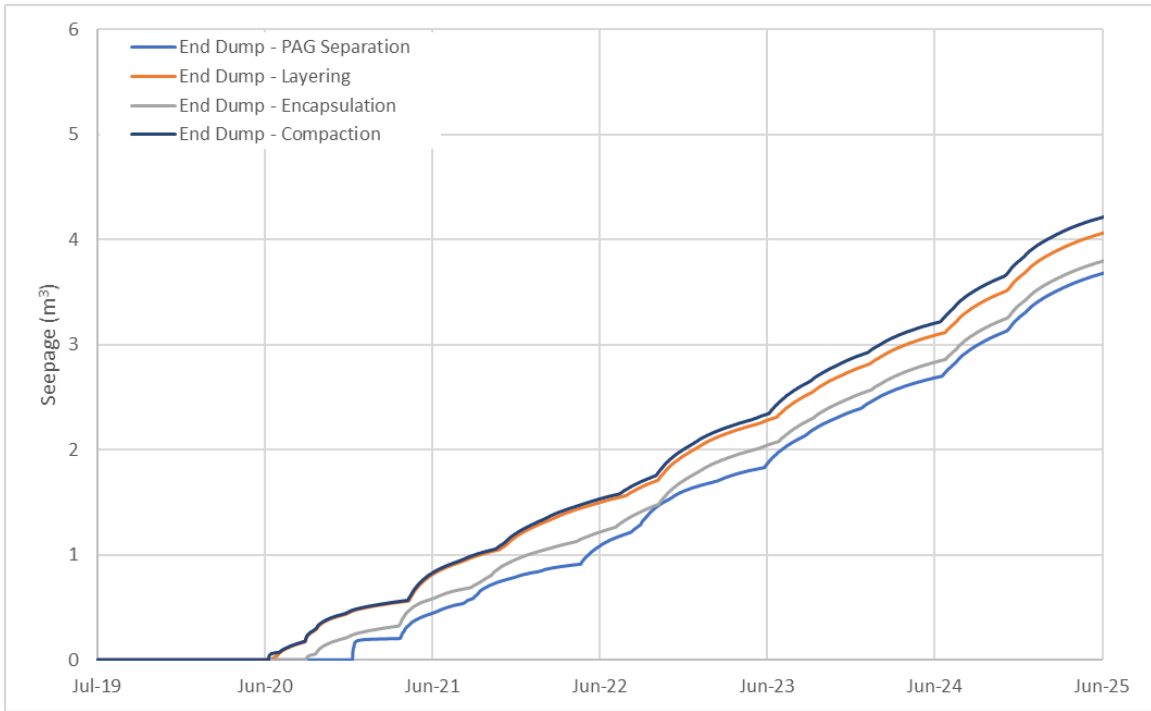


Figure 4-16. 1-D Seepage for PAG mitigation methods with End Dumping

4.5.4 All Scenarios Comparison

The long-term overall pile behaviour for all scenarios, including cumulative precipitation, cumulative evaporation, cumulative runoff from the lift 1 batter (slope), runoff from surface, water storage, and cumulative seepage is outlined in Figure 4-17 to Figure 4-22.

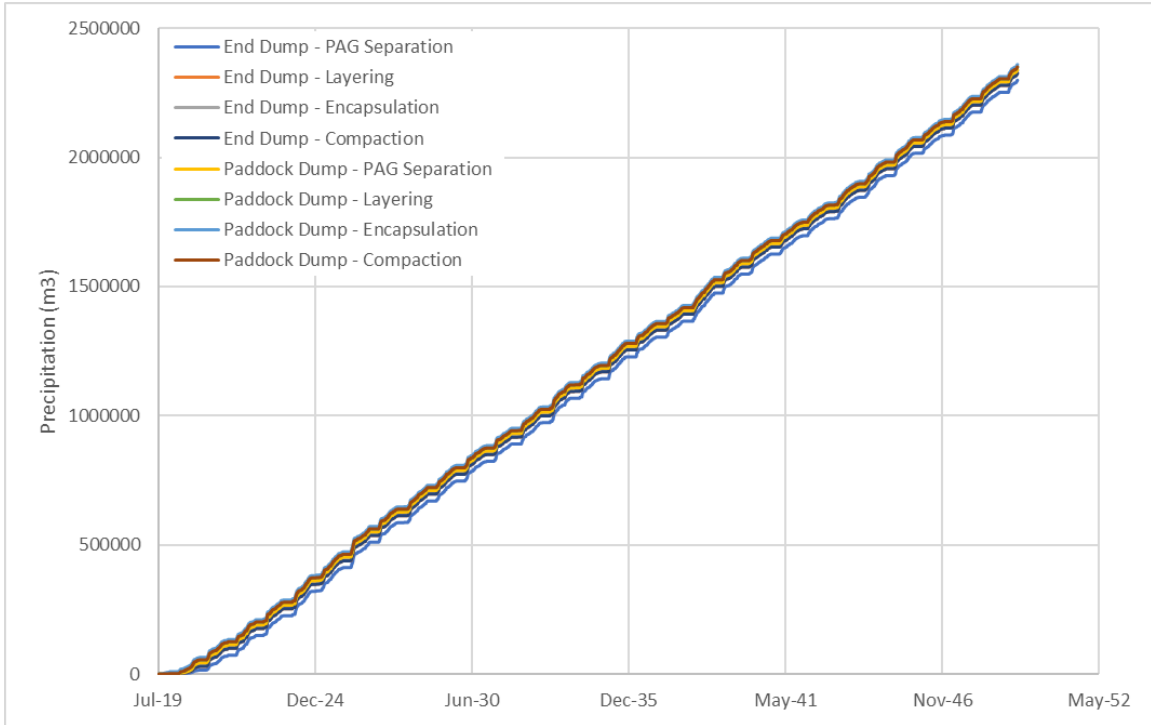


Figure 4-17. Long-term Global Pile Precipitation

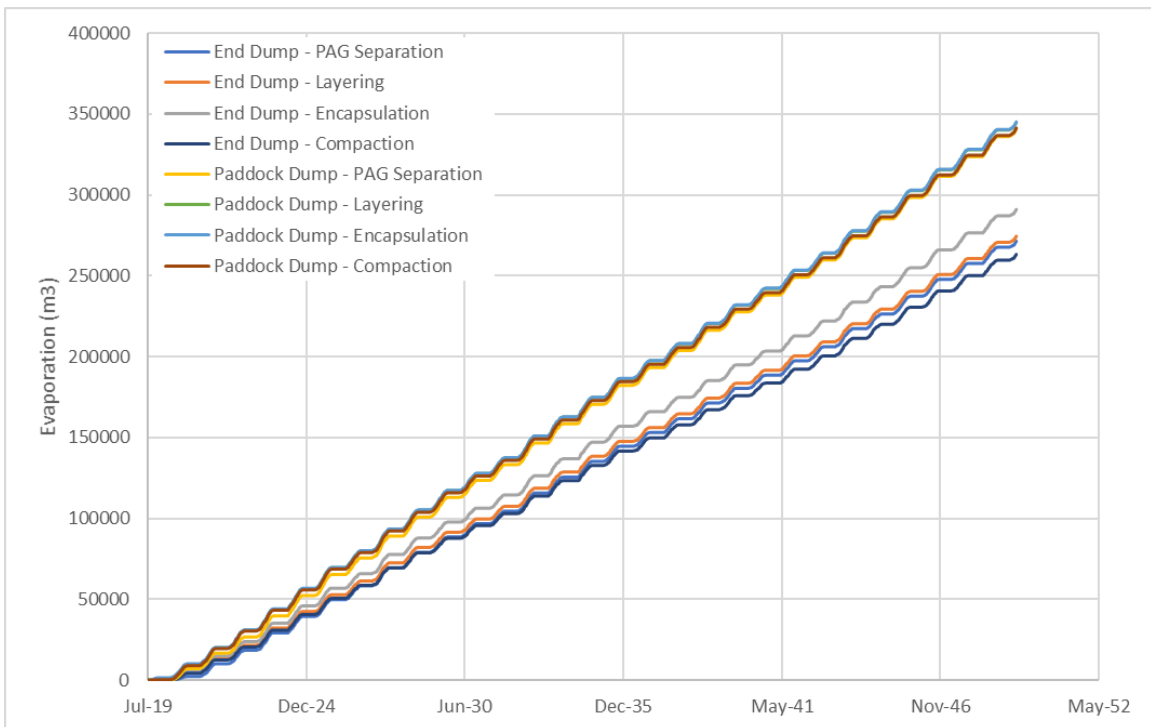


Figure 4-18. Long-term Global Pile Evaporation

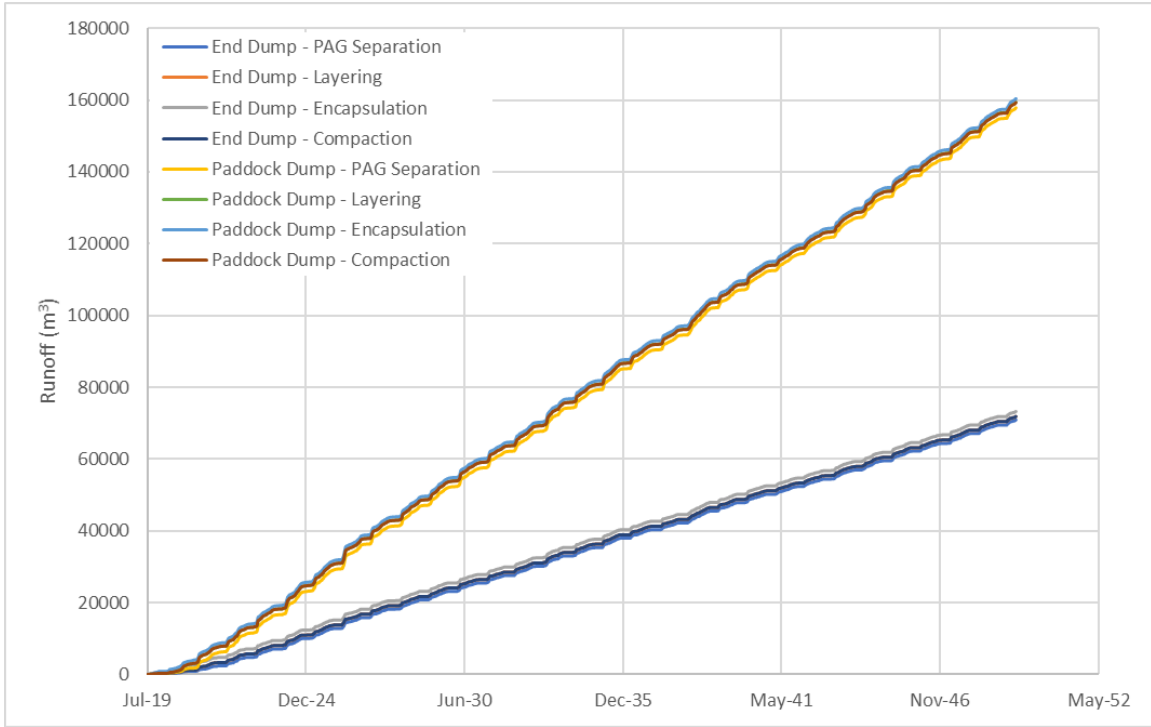


Figure 4-19. Long-term Global Pile Runoff from Lift 1 Batter

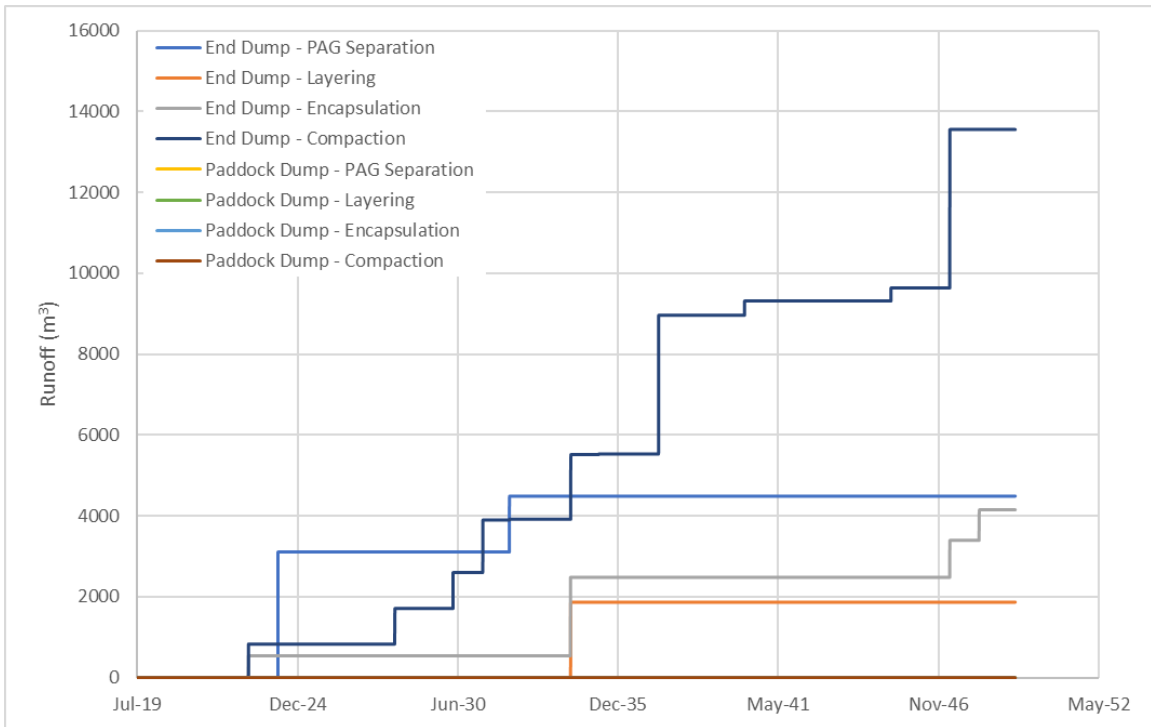


Figure 4-20. Long-term Global Pile Runoff from Surface

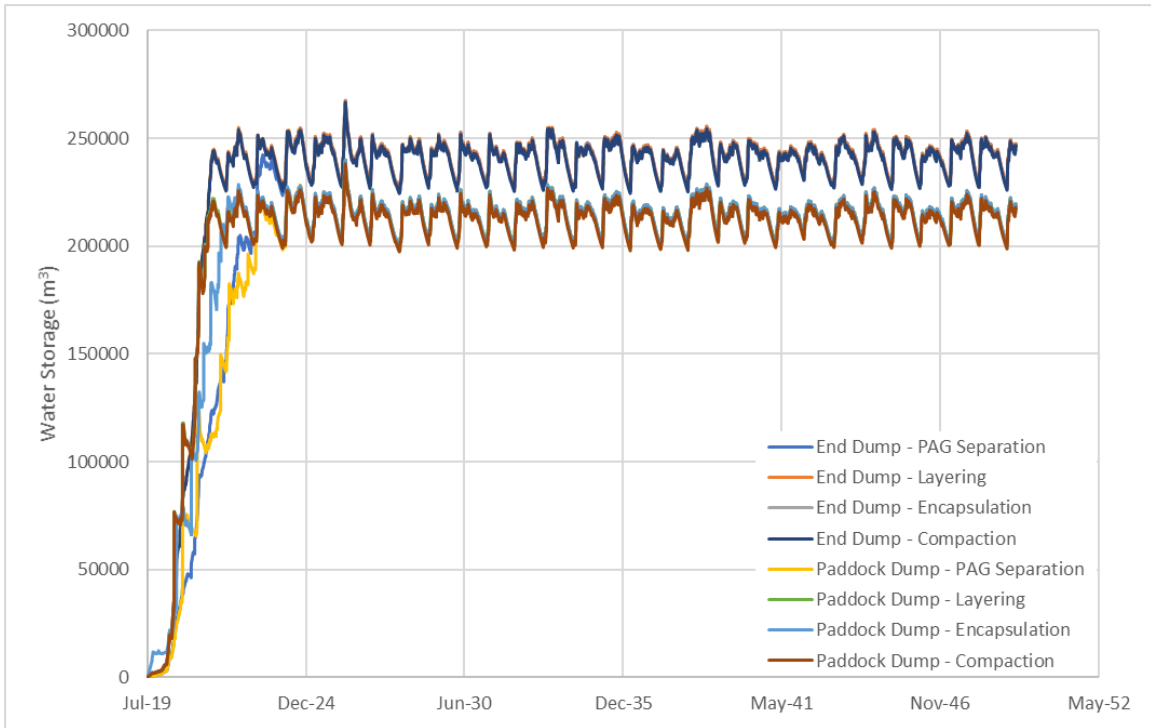


Figure 4-21. Long-term Global Pile Water Storage

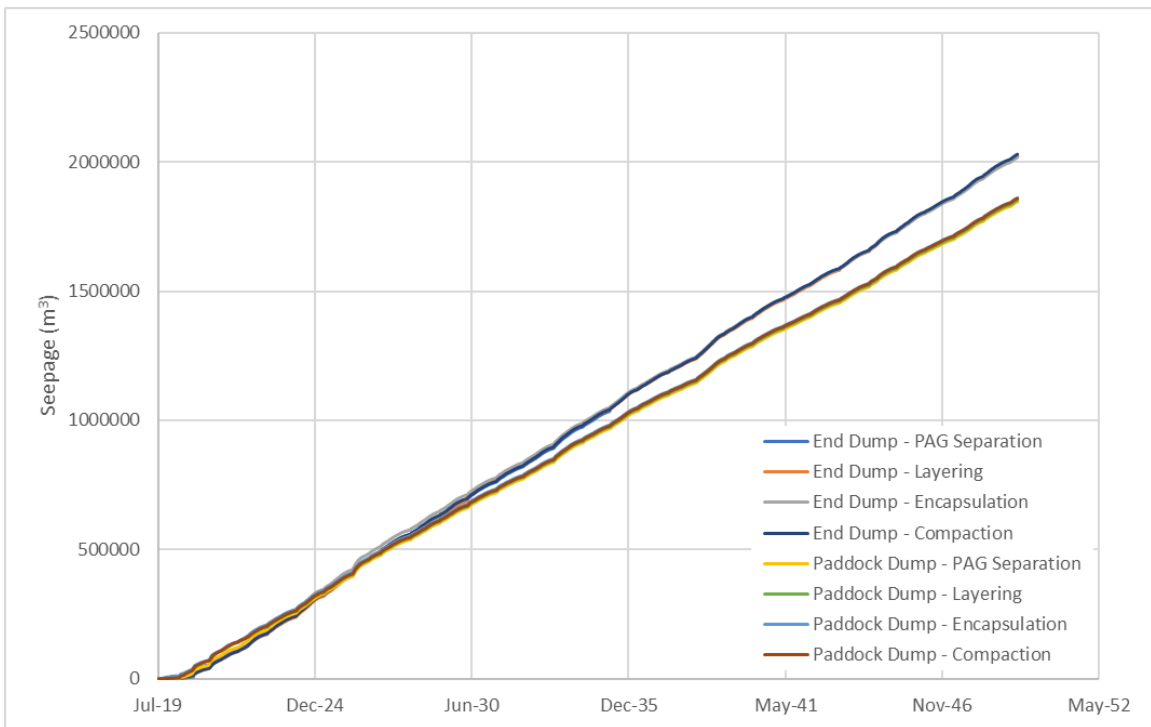


Figure 4-22. Long-term Global Pile Seepage

4.6 Discussion

4.6.1 General Model Behaviour

Figure 4-11 and Figure 4-12 demonstrate that the column behaves as expected, the seepage and evaporation are a function of the precipitation, and the water storage follows a yearly cyclical pattern which seems to be highly dependent on the inputted initial water content (water storage) of the waste rock. The focus of this research has been to develop a system dynamics model that could be used at the feasibility stage of mine development. Due to this, model setup focused on using theories that required minimal field data requirements (degree-day method for snowmelt, Thornthwaite method for potential evaporation, reduction factor for actual evaporation, ignoring hysteresis in unsaturated flow, and empirical runoff coefficient). Despite these simplifications, individual aspects of the model were validated and the model is expected to generate satisfactory results to predict general waste rock pile behaviour that can provide insight at the feasibility stage.

The water balance of the 3-D column was calculated by summing the inputs (initial water storage, precipitation) and outputs (evaporation, runoff, seepage, and water storage). The water balance for the 3-D column for Scenario 1 (End Dump – PAG Separation) is -1152 m^3 , where water output is larger than the water input. As a percentage of input water, the water balance has an error of -0.79% and generally an error less than 5% is acceptable.

4.6.2 Dumping Method Comparison

Figure 4-13 and Figure 4-14 demonstrate the impact each dumping method has on the pile behaviour. The end dumping scenario has a higher water storage than the paddock dumping scenario, as the material retains more moisture, and due to this, the water seepage is lower. Whereas in the paddock dumping scenario, the pile retains less moisture and has a higher water seepage. The difference in behaviour of the two dumping methods will be further discussed in Section 4.6.4 in the broader context of all hydrological parameters.

4.6.3 Mitigation Method Comparison

Figure 4-15 and Figure 4-16 display the pile behaviour for each mitigation method for the end dumping scenarios. As can be seen in the figures, the mitigation method scenarios were most impacted by sequencing and availability of the material. As discussed in Section 3.2.1.1, the waste rock material management model component was unable to be completed within GoldSim. Therefore, the model does not have the ability to optimize waste rock generation schedule for PAG and NAG with material required for pile construction. The model assumes PAG and NAG cells are constructed independent of each other, for example, depending on material production, the PAG cells may be filled on two lifts, as material requirements for NAG in the bottom lift lags. This discrepancy causes construction schedules, when each lift “turns” on, for each mitigation method scenario to be offset. However, post construction behaviour of the pile for all mitigation method scenarios converges, highlighting that the physical characteristics of the waste rock determine pile “steady state”.

The comparison between various PAG and NAG configurations could not be demonstrated as the models contained essentially the same material type as the density of NAG and PAG was assumed to be the same. The true value of different geometries of material types are apparent when modelling the geochemistry of the material, which was not the scope of this thesis.

4.6.4 All Scenarios Comparison

Global pile behaviour was impacted by the same construction sequencing issues for each mitigation method discussed above in Section 4.6.3. Initial behaviour during construction for each mitigation method did have some impact due to sequencing, however pile behaviour generally converged to similar behaviour for End Dump and Paddock Dump scenarios. The End Dump scenarios have a higher water storage and cumulative seepage, but lower cumulative evaporation and cumulative runoff from lift 1 batter (slope). In contrast, Paddock Dump scenarios have a lower water storage and seepage, with higher cumulative evaporation and cumulative runoff from lift 1 batter (slope).

As part of the Case Study, a confirmation of the runoff assumption was required as part of the validation for the runoff calculation discussed in Section 3.2.5. The modelled scenario with the highest runoff was Scenario 4 End Dump – Compaction with Layering. This is expected as the surface layers for the end dumping case have a lower hydraulic conductivity than the paddock dumped cases and the surface compaction scenario would further reduce the hydraulic conductivity. For the scenario with the highest runoff, over the 50 year period of the simulation, the runoff from surface was 0.55% of the inputted water. This number is small enough to validate the assumption that all surface runoff would be removed from the pile.

5 CONCLUSIONS AND RECOMMENDATIONS

5.1 Conclusions

The goal of the research was to develop a model using a systems dynamics approach to be coupled with TMSim that could account for the deposition of waste rock at hard rock mines that could be used at the feasibility stage of mine planning. The GoldSim software was used to develop the model, with two aspects, i) the deposition of waste rock based on mine processes to create the “pile”, and ii) the environmental conditions and associated variably saturated flow of water within the waste rock pile.

The conceptualization of the waste rock in the pile was constructed in four lifts, with the first three lifts taller than the final lift. These four lifts were divided laterally into 15 rows and 16 columns to create a pseudo 3-D structure of 240 1-D columns. For increased accuracy, each lift needed to be discretized into smaller layers to simulate the flow of water. Based on a sensitivity analysis of an early version of the model, the number of layers chosen was 20 and 10 for the taller (10m) and shorter (4m) lifts, respectively. This created a “pile” that was 240 1-D columns, with 70 individual layers. Understandably, this created a large number of calculations that were required for each time step. Final model run-times to simulate 50 years required up to a week to complete. Review of this method, and use of the GoldSim software is further discussed in Section 5.2.

Due to the size of the GoldSim model, it was chosen to create two separate models for each waste rock deposition method, ending with two GoldSim models: WR Model – End Dumped and WR Model – Paddock Dumped. The modelling of the waste rock pile being constructed encountered many errors during development previously discussed in Chapter 3 and ultimately had to be simplified to simple excel calculations in order to run the model. Using excel tables, the user is able to define the height, area, and volume of each lift which then auto calculates the dimensions of cells within each lift. Using similar tables, the user is able to designate the geometry of the waste rock pile that is PAG and NAG in configurations such as PAG segregation, encapsulation, and layering; with surface compaction as an additional option.

As the waste rock pile was “constructed” each complete cell would become active to environmental conditions such as precipitation, evaporation, runoff, and infiltration. The variably saturated system was modelled using a modified version of the variably saturated flow sub-model for a tailings cover created by Zheng to apply to larger scale layers. Modifications of the model included potential evaporation calculation and snow accumulation and meltwater calculation. The model was run, and the results were compared to the same model in Hydrus-1D with similar results.

The model was run using a case study for a mine site at the feasibility stage to demonstrate the application of the model. Overall, the model behaved as expected with general pile water balance behaviour observed over the course of the run-time with 5 years construction and 45 years long term behaviour. The models clearly show the benefits of paddock dumping versus end dumping with reduced water storage volumes within the pile. However, the comparison between various PAG and NAG configurations could not be demonstrated as the models contained essentially the same material type as the density of NAG and PAG was assumed to be the same. The true value of different geometries of material types are apparent when modelling the geochemistry of the material. The coupling of geochemistry with this model is anticipated to be completed under a different research scope.

5.2 Recommendations for Future Work

This research focused on the development of a waste rock deposition sub-model that could then later be coupled with TMSim. Due to the matrix issues described in the previous sections, significant work is likely needed before this sub-model can be adequately coupled with TMSim. There are two routes to improving the waste rock deposition component, 1) GoldSim software is further developed to allow the use of event triggers with matrix elements and 2) GoldSim software is coupled with additional software such as MATLAB, Excel VBA, or a volumetric planning software. Additional recommendations for future work on this sub-model include:

- The potential evaporation is determined using the mean air temperature of the site, if additional information is known for a site, there may be motivation to update the model

with a potential evaporation method that requires inputs such as wind speed, solar radiation, and relative humidity.

- The infiltration from snowmelt calculation assumes only the mean air temperature of the site is known, if additional information is known for a site, there may be motivation to update the model to use the energy balance method for a more accurate snowpack and snowmelt infiltration.
- For simplicity, the model currently only uses one-dimensional water flow. The model could be improved by adding a lateral flow component. A lateral flow component would be useful for any mitigation strategy that relies on increased runoff and lateral flow within NAG layers to minimize PAG moisture content (Aubertin et al. 2009; Broda et al. 2014; Dawood and Aubertin 2014).
- Due to time constraints, an empirical runoff coefficient was chosen to simulate runoff from a slope. With additional effort, a runoff sub-model using exterior software such as Slope/W could be used to improve the runoff coefficient.
- Inclusion of the advective and diffusive transport of oxygen within the pile based on the construction techniques to simulate the effect of oxygen availability on the intrinsic oxidation rate within the pile discussed in Section 2.4.2.

Following the additional efforts to improve this model as future work, the model would then need to be coupled with geochemistry reactions and eventually TMSim in order to model the whole mine waste system as a whole.

REFERENCES

- Akindunni, F.F., Gillham, R.W., and Nicholson, R.V. 1991. Numerical simulations to investigate moisture-retention characteristics in the design of oxygen-limiting covers for reactive mine tailings. *Canadian Geotechnical Journal*, **28**(3), 446-451.
- Amos, R.T., Blowes, D.W., Bailey, B.L., Segó, D.C., Smith, L., and Ritchie, A.I.M. 2015. Waste-rock hydrogeology and geochemistry, *Applied Geochemistry*, **57**: 140-156.
- Anderson, E.A. 1976. A point energy and mass balance model of a snow cover. NOAA Technical Report NWS 19, US Department of Commerce, National Oceanic and Atmospheric Administration, National Weather Service, Office of Hydrology, Washington, D.C.
- Appels, W.M., Ireson, A.M., and Barbour, S.L. 2018. Impact of bimodal textural heterogeneity and connectivity on flow and transport through unsaturated mine waste rock. *Advances in water resources*, **112**: 254-265.
- Aubertin, M., Cifuentes, E., Apithy, S.A., Bussière, B., Molson, J., and Chapuis, R.P. 2009. Analyses of water diversion along inclined covers with capillary barrier effects, *Canadian Geotechnical Journal*, **46**(10): 1146-1164.
- Azam, S., Wilson, G.W., Fredlund, D.G., and Van Zyl, D. 2009. Geotechnical characterization of mine waste rock. In *Proceedings of the Seventh International Conference Soil Mechanics and Geotechnical Engineering*. Alexandria, Egypt, 5-9 October. International Society for Soil Mechanics and Geotechnical Engineering, 3421 – 3425.
- Azam, S., Wilson, G.W., Herasymuk, G., Nichol, C., and Barbour, L.S. 2007. Hydrogeological behaviour of an unsaturated waste rock pile: A case study at the Golden Sunlight Mine, Montana, USA, *Bulletin of Engineering Geology and the Environment*, **66**(3): 259-268.
- Barsi, D. 2017. Spatial variability of particles in waste rock piles. M.Sc. thesis, Department of Civil and Environmental Engineering, The University of Alberta, Edmonton, AB.

- Barsi, D. 2019. Classifying variability of material properties in mine waste rock, *CIM Journal*, **10**(2): 77-93.
- Beier, N.A. 2015. Development of a Tailings Management Simulation and Technology Evaluation Tool. Ph.D. thesis, Department of Civil and Environmental Engineering, The University of Alberta, Edmonton, AB.
- Beier, N., Zheng, X., and Segó, D. 2020. Development of an oil sands tailing management simulation model, *Environmental Geotechnics*, **8**(7): 452-466.
- Broda, S., Aubertin, M., Blessent, D., Hirthe, E., and Graf, T. 2014. Improving control of contamination from waste rock piles, *Environmental Geotechnics*, **4**(4): 274-283.
- Brown, P.L., Crawford, J., Irannejad, P., Miskelly, P.C., Noël, M.M., Pantelis, G., Plotnikoff, W.W., Sinclair, D.J., and Stepanyants, Y.A. 2001. SULFIDOX: Version 1.1. A tool for modelling the temporal and spatial behaviour of heaps containing sulfidic minerals, ANSTO Technical Report.
- Brown, P.L., Logsdon, M.J., Vinton, B., Schofield, I., Payne, K. 2014. Detailed characterisation of the waste rock dumps at the Kennecott Utah Copper Bingham Canyon Mine – Optionality for Closure. Proceedings of the Eighth Australian Workshop on Acid and Metalliferous Drainage (Eds. H Miller and L. Preuss), Adelaide, Australia, 1-12.
- Bussière, B., Aubertin, M., and Chapuis, R.P., 2003. The behavior of inclined covers used as oxygen barriers. *Canadian Geotechnical Journal*, **40**(3): 512-535.
- Bussière, B., 2007. Colloquium 2004: Hydrogeotechnical properties of hard rock tailings from metal mines and emerging geoenvironmental disposal approaches. *Canadian Geotechnical Journal*, **44**(9): 1019-1052.

- Carey, S.K., Barbour, S.L., and Hendry, M.J., 2005. Evaporation from a waste-rock surface, Key Lake, Saskatchewan. *Canadian Geotechnical Journal*, **42**(4): 1189-1199.
- Cash, A.E. 2014. Structural and hydrologic characterization of two historic waste rock piles. M.Sc. thesis, Department of Civil and Environmental Engineering, The University of Alberta, Edmonton, AB.
- Chapuis, R.P. and Aubertin, M., 2003. On the use of the Kozeny Carman equation to predict the hydraulic conductivity of soils. *Canadian Geotechnical Journal*, **40**(3): 616-628.
- Coffin, J.G. 2010. A three-dimensional model for slurry storage facilities. Ph.D. thesis, Department of Civil Engineering, The University of Colorado, Boulder, CO.
- da Silva, J.C., do Amaral Vargas, E., and Sracek, O. 2009. Modeling multiphase reactive transport in a waste rock pile with convective oxygen supply, *Vadose Zone Journal*, **8**(4): 1038-1050.
- Darling, P. 2011. *SME mining engineering handbook*. Society for Mining, Metallurgy, and Exploration, Englewood, CO.
- Dawood, I. and Aubertin, M. 2014. Effect of dense material layers on unsaturated water flow inside a large waste rock pile: A numerical investigation, *Mine Water and the Environment*, **33**(1): 24-38.
- Dawson, R.F., Morgenstern, N.R., and Stokes, A.W. 1998. Liquefaction flowslides in Rocky Mountain coal mine waste dumps, *Canadian Geotechnical Journal*, **35**(2): 328-343.
- Dingman, S.L. 2002. *Physical hydrology*. 2nd Edition, Prentice Hall, New Jersey, USA.
- Dunne, T. and Black, R.D., 1970. An experimental investigation of runoff production in permeable soils. *Water Resources Research*, **6**(2): 478-490.

- Fala, O., Aubertin, M., Molson, J.W., Bussière, B., Wilson, G.W., Chapuis, R., and Martin, V. 2003. Numerical modelling of unsaturated flow in uniform and heterogeneous waste rock piles. In Proceedings of the 6th International Conference on Acid Rock Drainage (ICARD), Australasian Institute of Mining and Metallurgy, Cairns, Australia, Publication Series, Vol. 3, 895-902.
- Fala, O. and Molson, J., 2005. Numerical modelling of flow and capillary barrier effects in unsaturated waste rock piles. *Mine Water and the Environment*, **24**(4): 172-185.
- Fala, O., Molson, J., Aubertin, M., Bussière, B., and Chapuis, R.P. 2006. Numerical simulations of long term unsaturated flow and acid mine drainage at waste rock piles. In Proceedings of the 7th International Conference on Acid Rock Drainage (ICARD), Australasian Institute of Mining and Metallurgy, Cairns, Australia, Publication Series. 26-30.
- Fala, O., Molson, J., Aubertin, M., Dawood, I., Bussière, B. and Chapuis, R.P., 2013. A numerical modelling approach to assess long-term unsaturated flow and geochemical transport in a waste rock pile. *International Journal of Mining, Reclamation and Environment*, **27**(1): 38-55.
- Fines, P.E. 2006. Hydrologic characterization of two full-scale waste rock piles. M.A.Sc. thesis, The Department of Mining Engineering, The University of British Columbia, Vancouver, B.C.
- Ford, A. 2010. *Modeling the environment*. Island Press, Washington, DC.
- Franklin, M., Fernandes, H.M. and Genuchten, M.T., 2008. Modeling the water flow in unsaturated waste rock pile: an important step in the overall closure planning of the first uranium mining site in Brazil. In *Uranium, Mining and Hydrogeology*, 177-186.
- Fredlund, D.G., Rahardjo, H., and Fredlund, M.D. 2012. *Unsaturated soil mechanics in engineering practice*. John Wiley & Sons, Hoboken, N.J.

- Fredlund, D.G. and Xing, A. 1994. Equations for the soil-water characteristic curve, *Canadian geotechnical journal*, **31**(4): 521-532.
- Fredlund, M.D., Tran, D., and Fredlund, D.G. 2015. The calculation of actual evaporation from an unsaturated soil surface. In *Proceedings of the 10th International Conference on Acid Rock Drainage*, Santiago, Chile, 21-24 April 2015. Society for Mining, Metallurgy, and Exploration, 20-24.
- Fredlund, M.D., Fredlund, D.G., and Wilson, G.W. 1997. Prediction of the soil-water characteristic curve from grain-size distribution and volume-mass properties. In *Proceedings of the 3rd Brazilian Symposium on Unsaturated Soils*, Rio de Janeiro, Brazil, 21-25 April 1997, 13-23.
- Golder Associates Ltd. 1987. *Regional Study of Coal Mine Waste Dumps in British Columbia, Stage II*. Canadian British Columbia Mineral Development Agreement, 862–1231.
- GoldSim. 2021. Monthly and Annual Totals. <https://support.goldsim.com/hc/en-us/articles/115015577348-Monthly-and-Annual-Totals>, accessed 2019.
- Graveline, M. and Germain, D. 2016. Ice-block fall and snow avalanche hazards in Northern Gaspésie (Eastern Canada): Triggering weather scenarios and process interactions, *Cold Regions Science and Technology*, **123**: 81-90.
- Gray, D.M. and Landine, P.G. 1987. Albedo model for shallow prairie snow covers, *Canadian Journal of Earth Sciences*, **24**(9): 1760-1768.
- Hajizadeh Namaghi, H., Li, S., and Jiang, L. 2015. Numerical simulation of water flow in a large waste rock pile, Haizhou coal mine, China. *Modeling Earth Systems and Environment*, **1**(1): 1-10.
- Hawley, P.M. and Cunning, J. 2017. *Guidelines for mine waste dump and stockpile design*. CSIRO Publishing, Clayton, Vic.

- Herasymuik, G.M. 1996. Hydrogeology of a sulphide waste rock dump. M.Sc. thesis, Department of Civil Engineering, The University of Saskatchewan, Saskatoon, SK.
- Hillel, D. 1980. Applications of soil physics. Academic Press, New York, NY.
- Huang, M., Bruch, P.G., and Barbour, S.L. 2013. Evaporation and water redistribution in layered unsaturated soil profiles, *Vadose Zone Journal*, **12**(1): 1-14.
- Huang, M., Elshorbagy, A., Lee Barbour, S., Zettl, J., and Cheng Si, B. 2011. System dynamics modeling of infiltration and drainage in layered coarse soil, *Canadian Journal of Soil Science*, **91**(2): 185-197.
- The International Network for Acid Prevention (INAP), 2009. Global Acid Rock Drainage Guide (GARD Guide).<http://www.gardguide.com/>.
- Jubinvile, S.K. 2013, Prediction of rainfall runoff for soil cover modelling. M.Sc. thesis, Department of Civil and Environmental Engineer, The University of Alberta, Edmonton, AB.
- Johnson, D.B. and Hallberg, K.B., 2005. Acid mine drainage remediation options: a review. *Science of the total environment*, **338**(1-2): 3-14.
- Kossik, R. and Miller, I. 2004. A probabilistic total system approach to the simulation of complex environmental systems. 2004 Winter Simulation Conference, Washington, DC, 1757-1761.
- Larochelle, CG, 2018. Use of acid-generating tailings as a capillary breakage layer in a blanket with capillary barrier effects. M.Sc. thesis, Department of Civil, Geological, and Mining Engineering, Polytechnique Montréal, Montréal, QC (in French).
- Lefebvre, R. 1994. Characterization and numerical simulation of acid mine drainage in waste rocks. PhD. thesis, Laval University, Quebec City, QC (in French).

- Lefebvre, R., Hockley, D., Smolensky, J., and Gélinas, P. 2001. Multiphase transfer processes in waste rock piles producing acid mine drainage: 1: Conceptual model and system characterization, *Journal of contaminant hydrology*, **52**(1-4): 137-164.
- Li, L. and Simonovic, S.P. 2002. System dynamics model for predicting floods from snowmelt in North American Prairie watersheds, *Hydrological Processes*, **16**(13): 2645-2666.
- Linero, S., Palma, C., and Apablaza, R. 2007. Geotechnical characterization of waste material in very high dumps with large scale triaxial testing. In *Proceedings of International Symposium on Rock Slope Stability in Open Pit Mining and Civil Engineering*, Perth, Australia, 12-14 September 2007, Australian Centre for Geomechanics, 59-75.
- Linklater, C.M., Sinclair, D.J., and Brown, P.L. 2005. Coupled chemistry and transport modelling of sulphidic waste rock dumps at the Aitik Mine Site, Sweden, *Applied Geochemistry*, **20**(2): 275-293.
- Lottermoser, B. 2010. *Mine wastes: Characterization, treatment and environmental impacts*. 3rd Edition. Springer Berlin Heidelberg, Berlin, Heidelberg.
- Maknoon, M. 2016. Slope stability analyses of waste rock piles under unsaturated conditions following large precipitations. Ph.D. thesis, Department of Civil, Geological, and Mining Engineering, Polytechnique Montréal, Montréal, QC (in French).
- Maknoon, M. and Aubertin, M. 2013. An investigation of the slope stability of unsaturated waste rock piles. *GeoMontreal 2013, 66th CGS Conference*, Montreal, QC, Canada.
- Martin, V., Bussière, B., Plante, B., Pabst, T., Aubertin, M., Medina, F., Bréard-Lanoix, M.L., Dimech, A., Dubuc, J., Poaty, B., and Wu, R. 2017. Controlling water infiltration in waste rock piles: Design, construction, and monitoring of a large-scale in-situ pilot test pile. In *Proceedings of the 70th Canadian Geotechnical Society Conference*.

- Martinec, J., Rango, A., and Major, E. 1983. The snowmelt-runoff model (SRM) user's manual. National Aeronautics and Space Administration, Washington, D.C.
- Mayer, K.U., Frind, E.O., and Blowes, D.W. 2002. Multicomponent reactive transport modeling in variably saturated porous media using a generalized formulation for kinetically controlled reactions, *Water Resources Research*, **38**(9): 13-21.
- Mine Environment Neutral Drainage Program (MEND). 1998. Blending and Layering Waste Rock to Delay, Mitigate or Prevent Acid Rock Drainage and Metal Leaching: A Case Study Review. MEND 2.37.1, National Resources Canada, Ottawa, ON.
- Mine Environment Neutral Drainage Program (MEND). 2001. Volume 4 - Prevention and Control. MEND 5.4.2d. *Edited by* G.A. Tremblay and C.M. Hogan, National Resources Canada, Ottawa, ON.
- Mine Environment Neutral Drainage Program (MEND). 2010. Evaluation of the Water Quality Benefits from Encapsulation of Acid-Generating Tailings by Acid-Consuming Tailings. MEND 2.46.1. National Resources Canada, Ottawa, ON.
- Mualem, Y. 1976. A new model for predicting the hydraulic conductivity of unsaturated porous media, *Water Resources Research*, **12**(3): 513-522.
- National Resources Conservation Services (NRCS). 2004. National Engineering Handbook, Part 4 - Hydrology. United States Department of Agriculture, Washington, D.C.
- Neuner, M., Smith, L., Blowes, D.W., Segó, D.C., Smith, L.J., Fretz, N., and Gupton, M. 2013. The Diavik Waste Rock Project: Water flow through mine waste rock in a permafrost terrain, *Applied Geochemistry*, **36**: 222-233.

- Nicholson, R.V., Gillham, R.W., Cherry, J.A., and Reardon, E.J., 1989. Reduction of acid generation in mine tailings through the use of moisture-retaining cover layers as oxygen barriers. *Canadian geotechnical journal*, **26**(1): 1-8.
- O'kane, M., Wilson, G.W., and Barbour, S.L., 1998. Instrumentation and monitoring of an engineered soil cover system for mine waste rock. *Canadian Geotechnical Journal*, **35**(5): 828-846.
- Oreiller, M., Nadeau, D.F., Minville, M., and Rousseau, A.N. 2014. Modelling snow water equivalent and spring runoff in a boreal watershed, James Bay, Canada, *Hydrological Processes*, **28**(25): 5991-6005.
- Pantelis, G. 1993. FIDHELM: Description of model and users guide, ANSTO Report M123. Australian Nuclear Science and Technology Organisation.
- Paterson, W.S.B. 1994. *The physics of glaciers*. Pergamon, Tarrytown, NY.
- Pearce, S., Lehane, S., and Pearce, J. 2016. Waste material placement options during construction and closure risk reduction – quantifying the how, the why and the how much. *In Proceedings of Mine Closure 2016, Perth, Western Australia, 15-17 March 2016*. Australian Centre for Geomechanics, 691-706.
- Pearce, S., Scott, P., and Weber, P. 2015. Waste rock dump geochemical evolution: matching lab data, models and predictions with reality. *In Proceedings of the 10th International Conference on Acid Rock Drainage and IMWA Annual Conference*.
- Peterson, H.E. 2014. Unsaturated hydrology, evaporation, and geochemistry of neutral and acid rock drainage in highly heterogeneous mine waste rock at the Antamina Mine, Peru. Ph.D. thesis, Department of Geological Sciences, The University of British Columbia, Vancouver, B.C.

- Pruess, K. 1991. TOUGH2-A general-purpose numerical simulator for multiphase fluid and heat flow. U.S. Department of Energy. Washington, D.C.
- Romano, N., Brunone, B., and Santini, A. 1998. Numerical analysis of one-dimensional unsaturated flow in layered soils, *Advances in Water Resources*, **21**(4): 315-324.
- Simunek, J., Sejna, M., and Van Genuchten, M.T. 1999. The HYDRUS-2D software package. International Ground Water Modeling Center, Colorado School of Mines, Golden, CO.
- Smith, R.E., Smettem, K.R. and Broadbridge, P., 2002. Infiltration theory for hydrologic applications. American Geophysical Union.
- Smith, L., Marcoline, J., Wagner, K., Nichol, C., and Beckie, R. 2004. Hydrologic and geochemical transport processes in mine waste rock. *In Environmental Aspects of Mine Wastes. Edited by J.L. Jabor, D.W. Blowes, and A.I.M Ritchie.* Mineralogical Association of Canada, Ottawa, ON.
- Stumm, W. and Morgan, J.J. 1981. Aquatic chemistry: An introduction emphasizing chemical equilibria in natural waters. Wiley, New York.
- Thorntwaite, C.W. 1948. An approach toward a rational classification of climate, *Geographical Review*, **38**(1): 55-94.
- Valenzuela, L., Bard, E., Campaña, J., and Anabalón, M.E. 2008. High waste rock dumps—challenges and developments. In *Proceedings of the First International Seminar on the Management of Rock Dumps, Stockpiles and Heap Leach Pads*, 5-6 March 2008. Australian Centre for Geomechanics, 65-78.
- van Genuchten, M.T. 1980. A closed-form equation for predicting the hydraulic conductivity of unsaturated soils, *Soil Science Society of America Journal*, **44**(5): 892-898.

- Wilson, D., Amos, R.T., Blowes, D.W., Langman, J.B., Smith, L. and Segó, D.C., 2018. Diavik Waste Rock Project: Scale-up of a reactive transport model for temperature and sulfide-content dependent geochemical evolution of waste rock. *Applied geochemistry*, **96**: 177-190.
- Wilson, G.W. 2011. Rock dump hydrology: An overview of full-scale excavations and scale-up experiments conducted during the last two decades. In *Proceedings of the Seventh Australian Workshop on Acid and Metalliferous Drainage*, Darwin, Northern Territory, 21-24 June 2011. JKTech Pty Ltd., 307-322.
- Wilson, G.W., Fredlund, D.G., and Barbour, S.L. 1997. The effect of soil suction on evaporative fluxes from soil surfaces, *Canadian Geotechnical Journal*, **34**(1): 145-155.
- Yazdani, J., Barbour, L., and Wilson, W. 2000. Soil water characteristic curve for mine waste rock containing coarse material. In *Proceedings of the CSCE Annual Conference*, London, ON, 7-10 June 2000. Canadian Society for Civil Engineering, 198-202.
- Zheng, T. and Beier, N. 2018. System dynamics approach to tailings management simulation. *In Tailings and Mine Waste*, Keystone, CO.
- Zheng, X. 2019. Development of a tailings simulation model using system dynamics. M.Sc. thesis, Department of Civil and Environmental Engineering, The University of Alberta, Edmonton, AB.

APPENDIX 1 – GOLDSIM ELEMENTS AND FUNCTIONS

Tables below describe commonly used GoldSim elements and functions from GoldSim’s user manual (GoldSim, 2021).

Table A1 - 1: Input Elements in GoldSim











Element	Default Symbol	Browser Icon	Function
Data			Defines scalar, vector or matrix data.
Stochastic			Defines uncertain data as probability distributions.
Time Series			Accepts time histories of data and converts them to an appropriate form for use in the model.
Lookup Table			Defines a one, two or three dimensional lookup table (response surface).
History Generator			Generates stochastic time histories based on specified statistics.

Table A1 - 2: Stock Elements in GoldSim







Element	Default Symbol	Browser Icon	Function
Integrator			Integrates values. Also can compute moving average of a specified input.
Reservoir			Integrates (and conserves) flows of materials, allowing for upper and lower bounds to be specified.
Pool			More complex version of Reservoir, making it easier to model multiple inflows and outflows.

Table A1 - 3: Function Elements in GoldSim














Element	Default Symbol	Browser Icon	Function
Expression		f_x	Defines mathematical or logical expressions.
Script		<code></></code>	Allows you to create your own custom element using a simple procedural language.
Previous Value		t	Returns the value of its input from the previous model update.
Extrema		\sqrt{w}	Computes the highest (peak) or lowest (valley) value achieved by its input.
Selector			Defines expressions with nested if...then logic.
Splitter			Splits an incoming signal into multiple outputs based on specified fractions.
Allocator			Allocates an incoming signal into multiple outputs given specified demands and priorities.
Sum		Σ	Facilities the addition of multiple values.
Convolution			Solves a convolution integral.

Table A1 - 4: Sub-Category of Function Elements in GoldSim







Element	Default Symbol	Browser Icon	Function
External (DLL)			Dynamically links to a user-specified external function (compiled as a DLL).
Spreadsheet			Dynamically links to an Excel spreadsheet.
File			Dynamically copies a file to a specified directory (for use by External elements).

Table A1 - 5: Event Elements in GoldSim

















Element	Default Symbol	Browser Icon	Function
Timed Event			Generates discrete event signals based on a specified rate of occurrence, regularly or according to a specified distribution (i.e., randomly).
Triggered Event			Generates discrete event signals based on one or more specified conditions.
Decision			Generates one of up to three defined discrete event signals based on specified conditions.
Random Choice			Generates a user defined discrete event signal based on specified probabilities.
Milestone			Records the time at which a particular event or specified condition(s) occurs.
Status			Generates a condition (True/False) in response to particular events or specified conditions.
Discrete Change			Generates a discrete change signal (a value) that can subsequently discretely modify the values of other elements (e.g., Integrators and Reservoirs).
Interrupt			Interrupts a simulation when a specified event or condition occurs and displays a user-defined message and/or writes a message to the run log.

Table A1 - 6: Delay Elements in GoldSim



















Element	Default Symbol	Browser Icon	Function
Material Delay			Delays (and optionally disperses) material flows.
Information Delay			Delays (and optionally disperses) a signal.
Event Delay			Delays a discrete event signal. Can also be used to simulate queues.
Discrete Change Delay			Delays a discrete change signal. Can also be used to simulate queues.

Table A1 - 7: Results Elements in GoldSim

Element	Default Symbol	Browser Icon	Function
Time History Result			Displays time history results.
Distribution Result			Displays probability distributions.
Final Value Result			Displays bar, column and pie charts (and tables) of final values.
Multi-Variate Result			Displays multi-variate results (scatter plots, correlation tables, raw data).
Array Result			Displays result vectors and matrices.

APPENDIX 2 – GOLDSIM MODEL DETAIL

Model Overview

The WR-End Dump GoldSim Model was selected as the example to illustrate the model setup. Differences between the End Dump and Paddock Dump models are described within the text in Section 3.2.1.

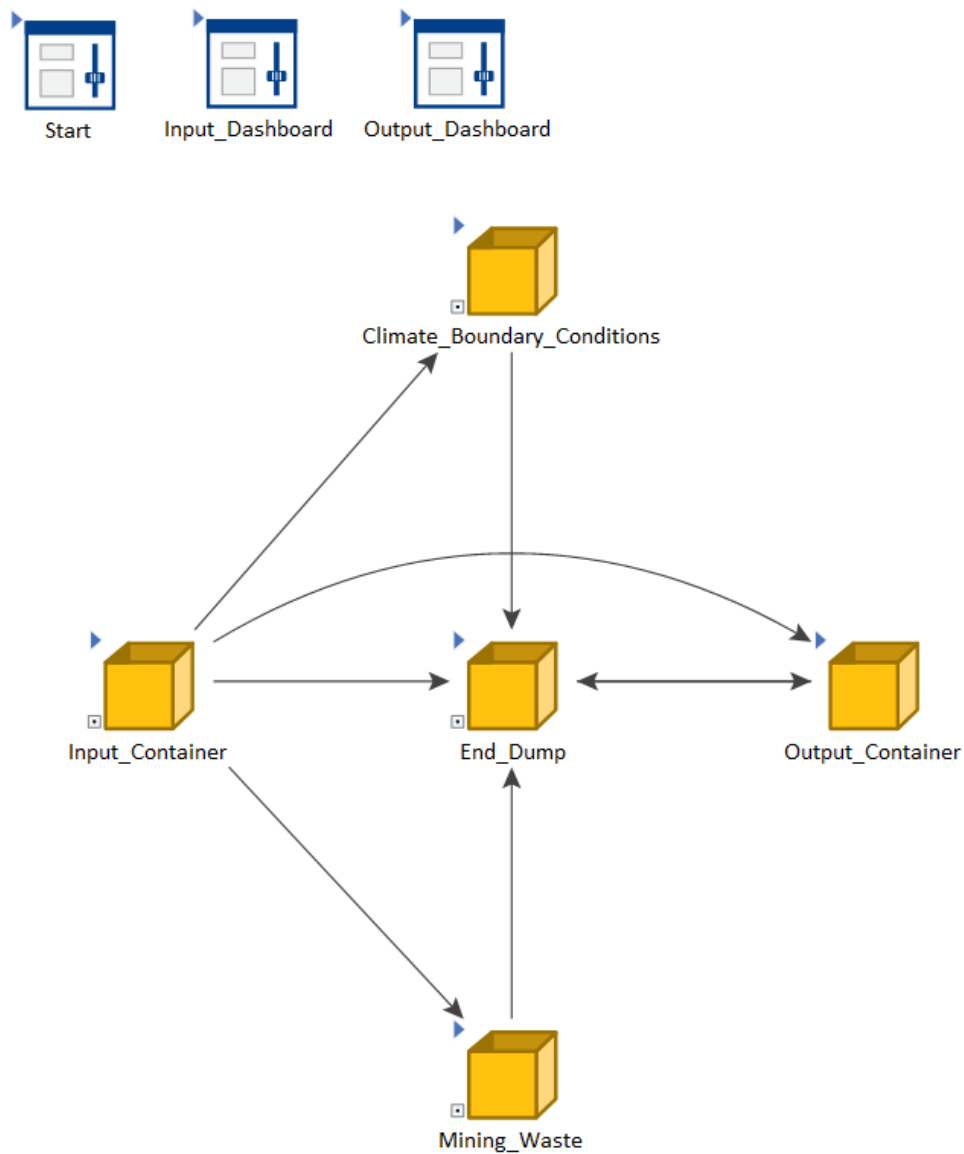


Figure A2 - 1: Overview of model

WR-End Dump Goldsim Model

This model incorporates waste rock deposition within a hydrogeology model to simulate various pile construction methods to mitigate acid rock drainage.

Click "Go to Inputs" to view inputs and run model, "Explore Model" to view the model, and "Go to Outputs" to view outputs if the model has been run.

Please refer to "WR-Paddock Dump" player file to simulate a waste rock pile constructed using paddock dumping.

Go to Inputs

Explore Model

Go to Outputs

Figure A2 - 2: Dashboard - Start

Model Inputs

Additional inputs can be found:

- in "End_Dump_Inputs" Excel file for pile design
- within model input container for constants and inputs that would require model updates if changed

[Go to Model Input Container](#)

Mitigation Method: PAG Separation Layering Encapsulation

Compacted Surface?

Year historical weather starts:

Latitude:

Model Run Start Month: July

Placement of PAG and NAG for Layering: (0=NAG, 1=PAG)

	Lift 1&2&3	Lift 4
1	0	0
2	0	0
3	0	0
4	0	0
5	0	0
6	0	1
7	0	1
8	0	1
9	0	1
10	0	1
11	1	0
12	1	0
13	1	0
14	1	0
15	1	0
16	1	0
17	1	0
18	1	0
19	1	0
20	1	0

[Back to Start](#)

Unsaturated Soil						
	Soil E	Compacted	Soil D	Soil C	Soil B	Soil A
Van Genuchten - alpha [1/cm]	0.0886	0.0487	0.2938	0.42	0.8699	1.5404
Van Genuchten - n	2.95	4.14	1.94	1.82	1.65	1.58
Initial Volumetric Water Content	0.15	0.15	0.15	0.15	0.15	0.15
Residual Volumetric Water Content	0.069	0.069	0.102	0.078	0.109	0.138
Saturated Volumetric Water Content	0.38	0.24	0.38	0.38	0.38	0.38
Saturated Hydraulic Conductivity [m/s]	0.00013	0.0000415	0.00023	0.0004	0.00068	0.0013

Monthly Tonnage (PAG)												
[tonne]	January	February	March	April	May	June	July	August	September	October	November	December
2019	0	0	0	0	0	0	7983	6861	0	3996	1898	5631
2020	17152	7425	67458	18592	110602	111316	61552	55596	59570	56812	58706	54920
2021	120171	120171	112420	100135	96905	96909	63729	63729	63729	91702	91702	91702
2022	90993	90993	90993	90023	90023	90023	53892	53892	53892	53892	53892	53892
2023	54480	54480	54480	54480	54480	54480	8032	8032	8032	8032	8032	8032
2024	6595	6595	6595	6595	6595	6595	0	0	0	0	0	0

Monthly Tonnage (NAG)												
[tonne]	January	February	March	April	May	June	July	August	September	October	November	December
2019	0	0	0	0	0	0	46704	64851	160799	104272	120594	26715
2020	29690	27910	46118	44492	79884	66237	103990	93926	100636	102879	106308	99451
2021	110277	110277	103163	123828	119833	119833	159891	159891	159891	110160	110160	110160
2022	90336	90336	90336	89368	89368	89368	61285	61285	61285	61285	61285	61285
2023	61955	61955	61955	61955	61955	61955	7607	7607	7607	7607	7607	7607
2024	7757	7757	7757	7757	7757	7757	0	0	0	0	0	0

Monthly Tonnage (Overburden)												
[tonne]	January	February	March	April	May	June	July	August	September	October	November	December
2019	0	0	0	0	0	0	7983	6861	0	3996	1898	5631
2020	17152	7425	67458	18592	110602	111316	61552	55596	59570	56812	58706	54920
2021	120171	120171	112420	100135	96905	96909	63729	63729	63729	91702	91702	91702
2022	90993	90993	90993	90023	90023	90023	53892	53892	53892	53892	53892	53892
2023	54480	54480	54480	54480	54480	54480	8032	8032	8032	8032	8032	8032
2024	6595	6595	6595	6595	6595	6595	0	0	0	0	0	0

Coefficient of Runoff from: Thickness of Top Layer:

Unit Weight of Waste Rock: Thickness of Bottom Layer:

[Outputs](#)

Figure A2 - 3: Dashboard – Model Inputs

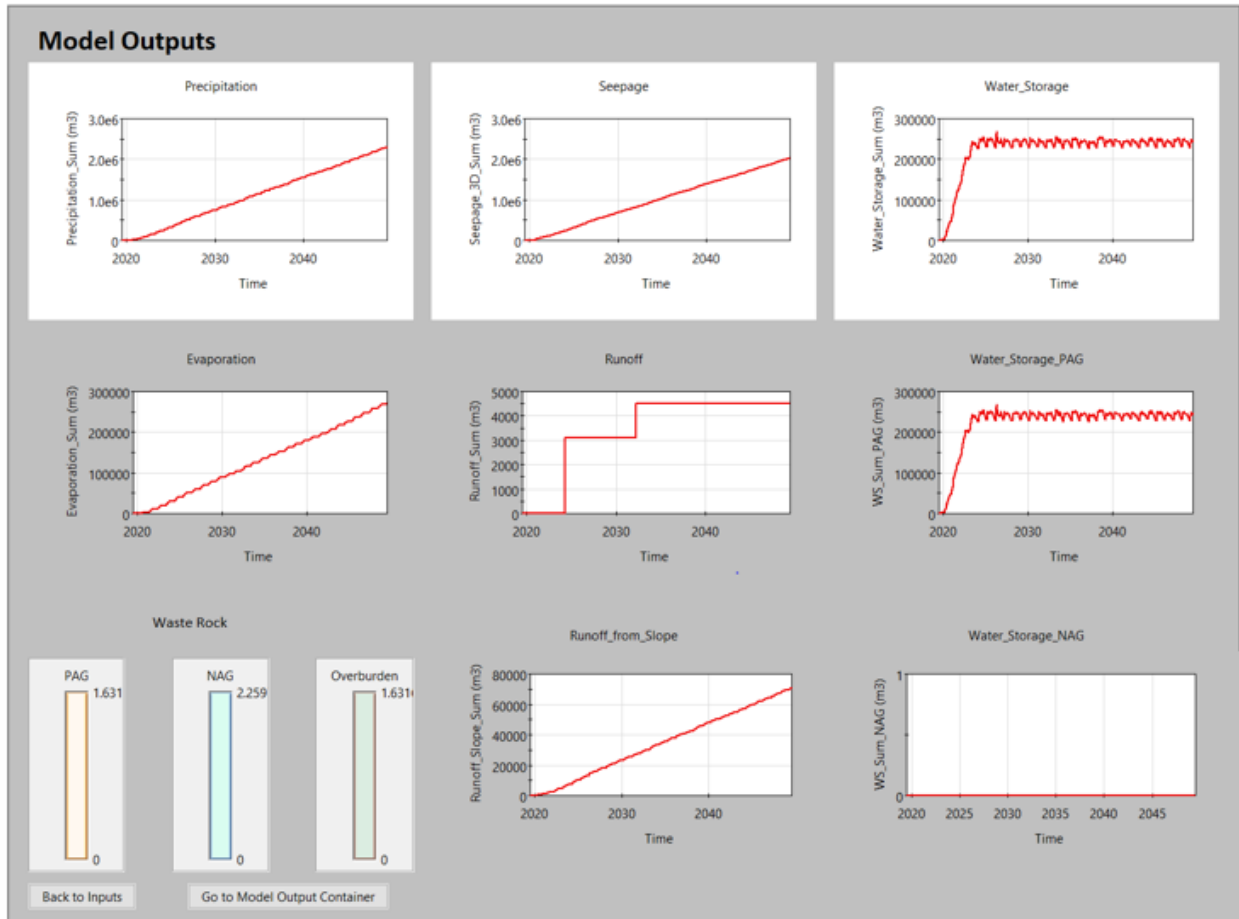


Figure A2 - 4: Dashboard – Model Outputs

Input Container

The input container contains the main inputs provided for the GoldSim model. Additional input elements can be found within the other areas of the model, however these inputs are unlikely to be changed frequently and are directly related to assumptions made during model development.

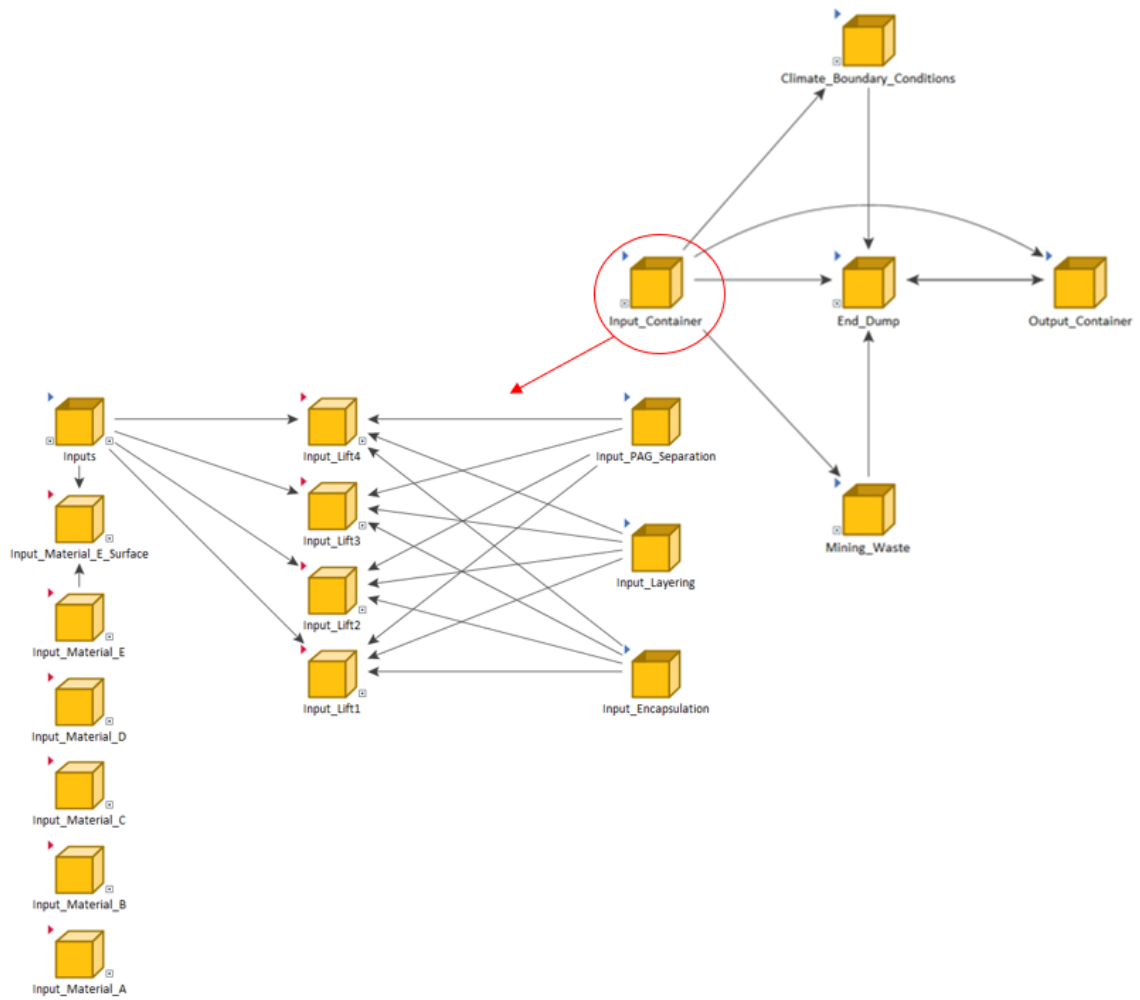


Figure A2 - 5: Input_Container

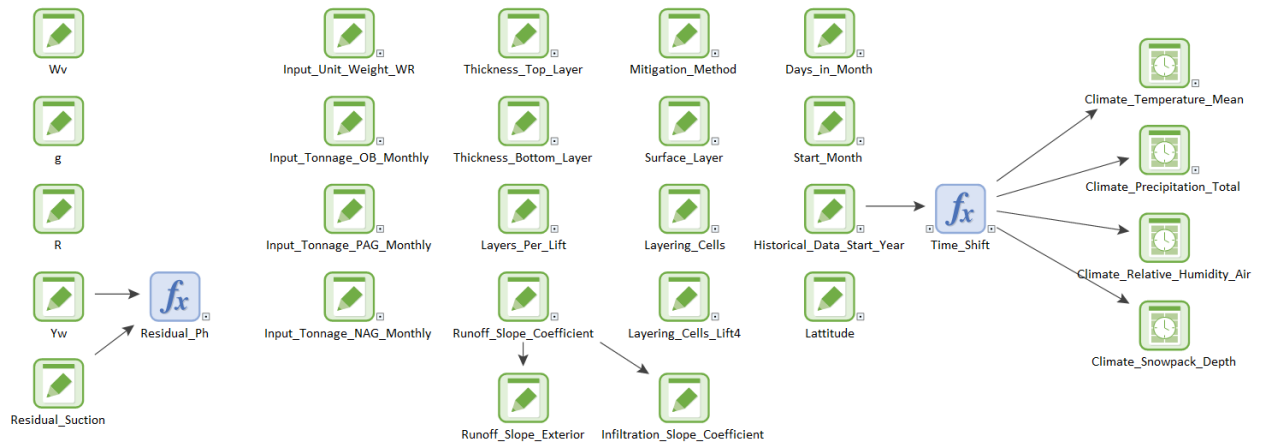


Figure A2 - 6: Inputs

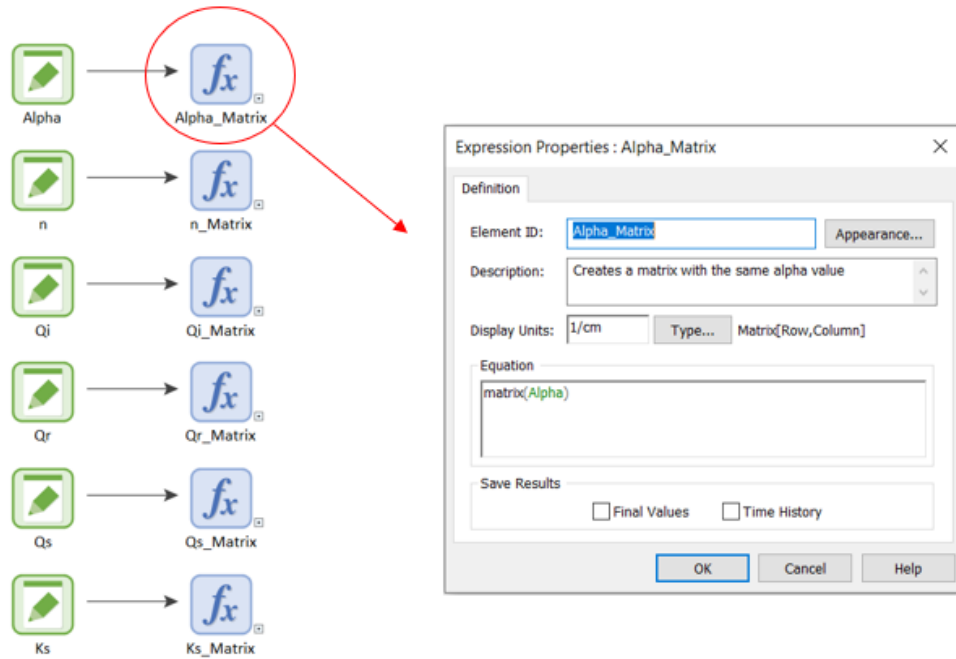


Figure A2 - 7: Input_Material_A

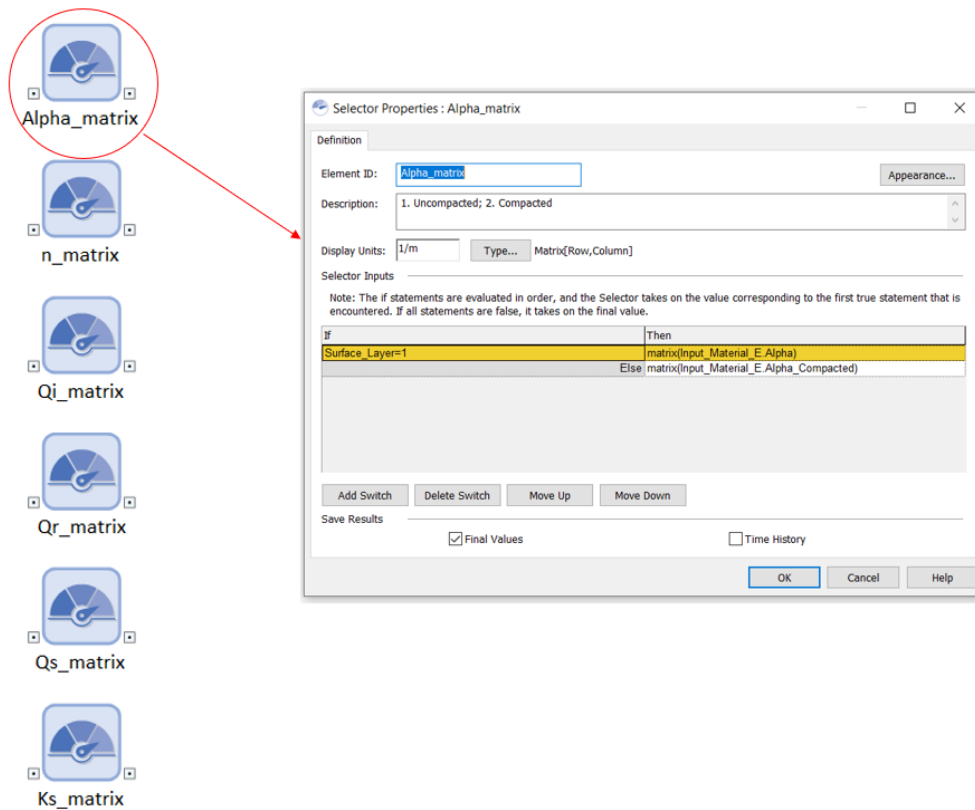


Figure A2 - 8: Input_Material_E_Surface

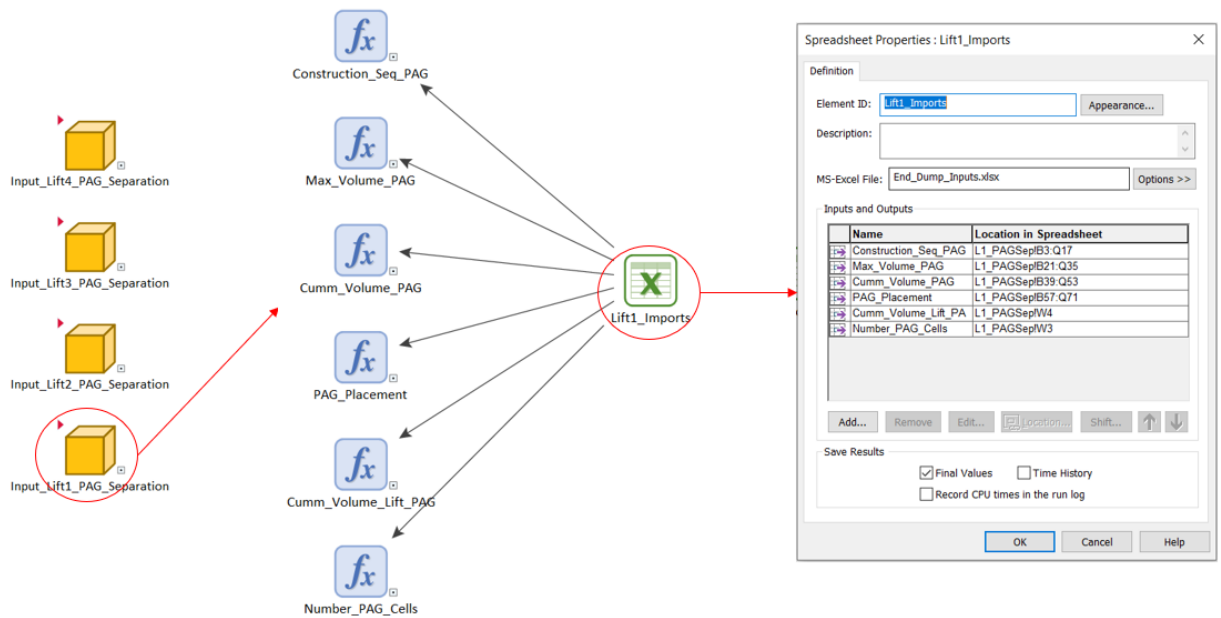


Figure A2 - 9: Example - Input_PAG_Separation

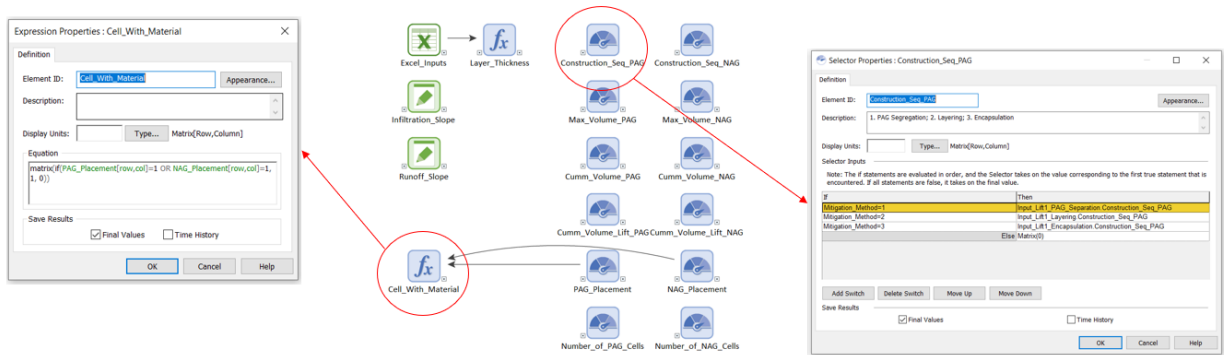


Figure A2 - 10: Example – Input_Lift_1

Climate Container

The climate container contains relevant calculations required or climate inputs into the saturated/unsaturated flow model including precipitation, snowpack melt water, and evaporation. Model selection, setup, and calibration for snowmelt and evaporation are described within the text in Section 3.2.2. and 3.2.3.

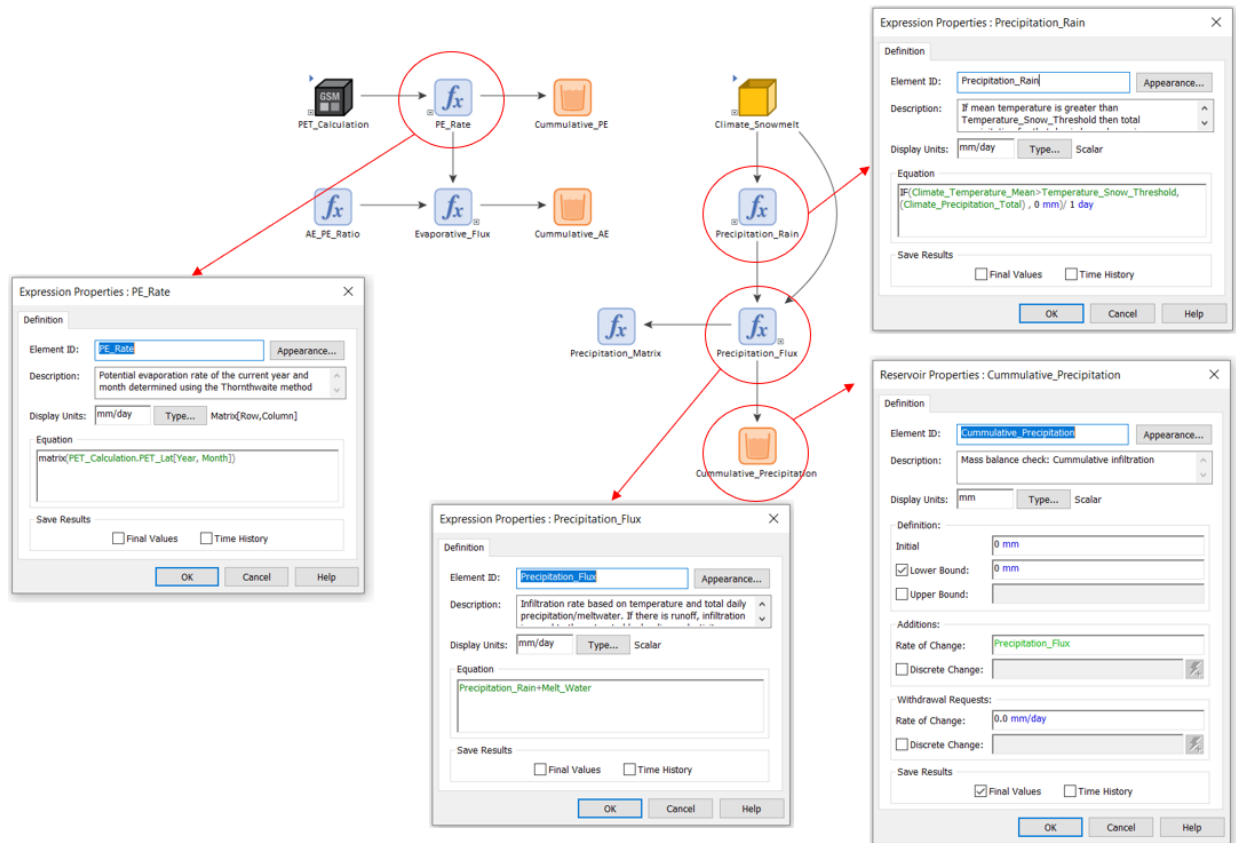


Figure A2 - 11: Climate_Boundary_Conditions

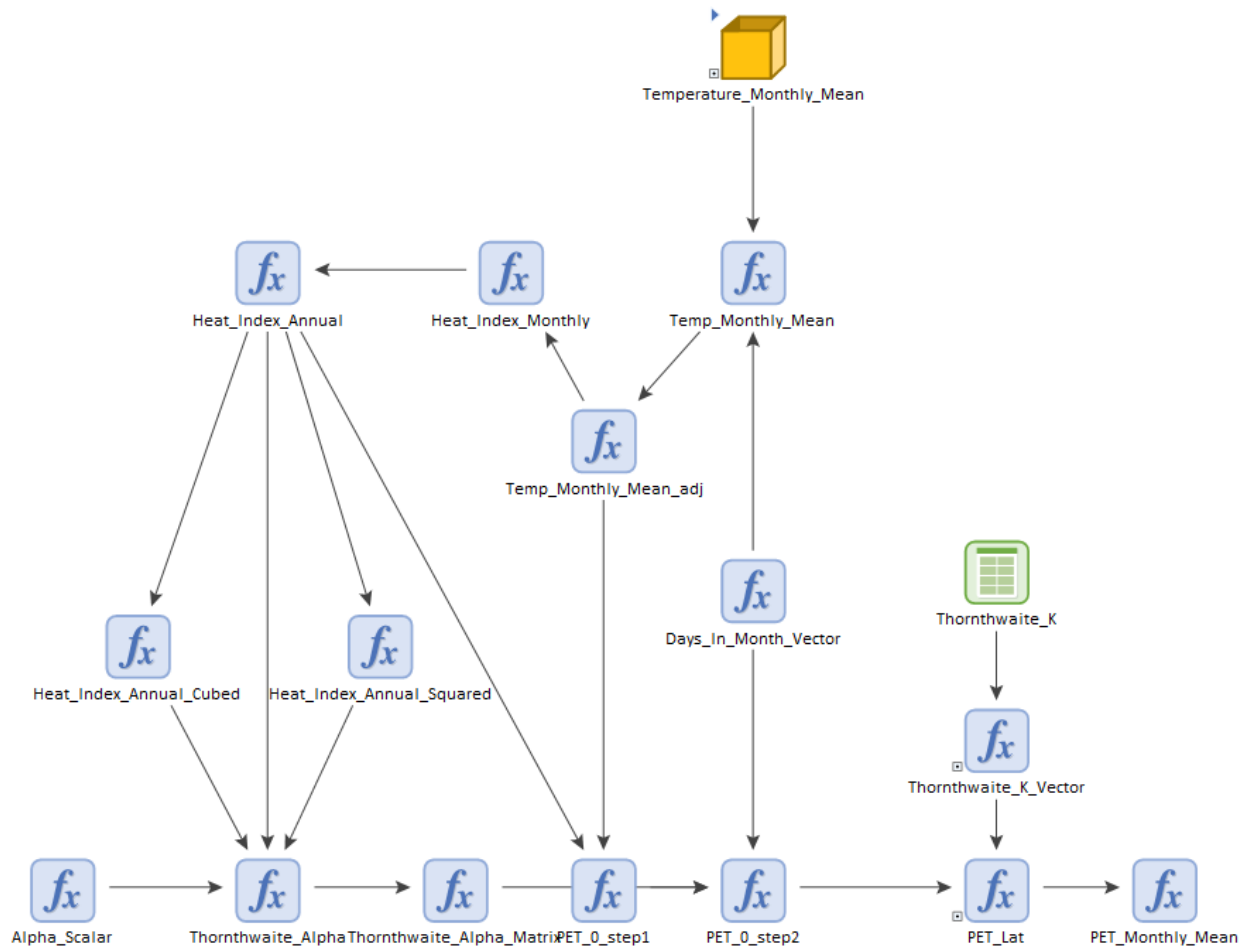


Figure A2 - 12: PET_Calculation

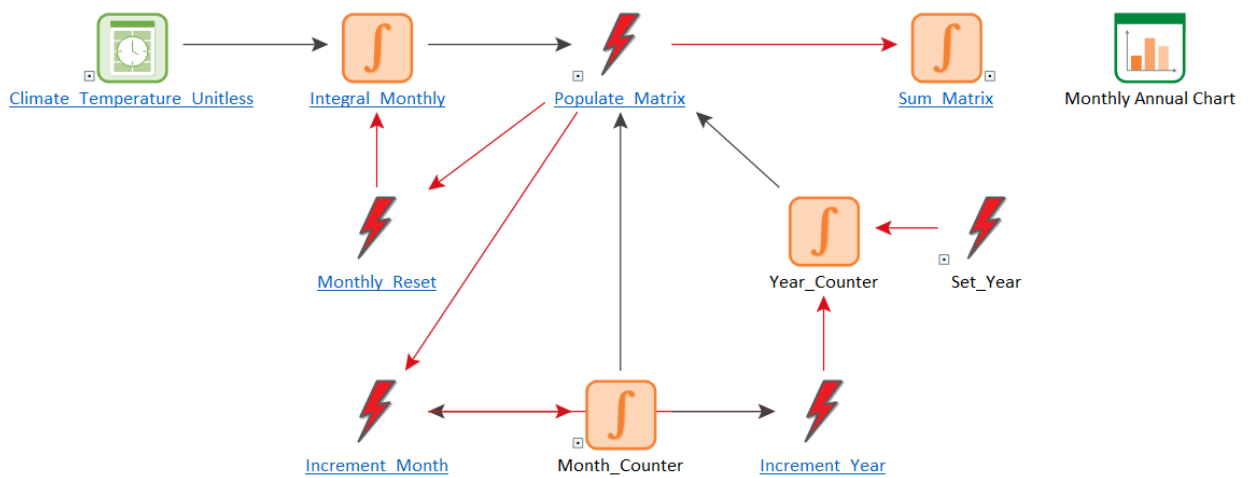


Figure A2 - 13: Temperature_Monthly_Mean (Taken from Goldsim Model Library - Monthly and Annual Totals)

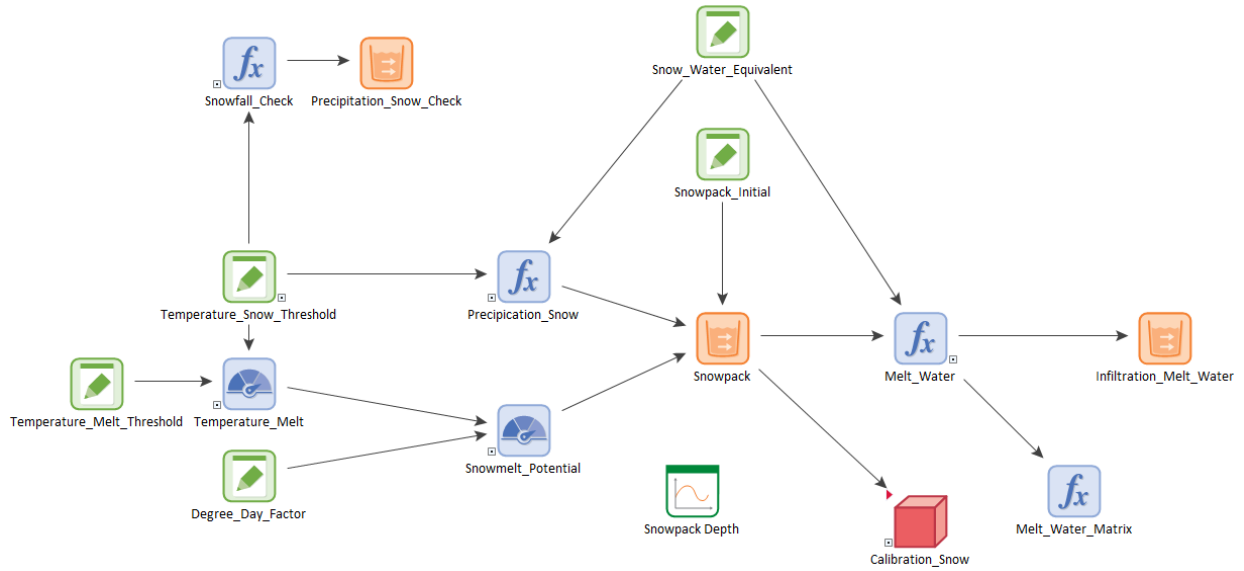


Figure A2 - 14: Climate_Snowmelt

Expression Properties : Precipitation_Snow

Definition

Element ID: Appearance...

Description: If mean temperature is less than Temperature_Snow_Threshold then total

Display Units: Type... Scalar

Equation

```
IF(Climate_Temperature_Mean < Temperature_Snow_Threshold,
(Climate_Precipitation_Total / Snow_Water_Equivalent), 0 cm) / 1 day
```

Save Results

Final Values Time History

OK Cancel Help

Figure A2 - 15: Precipitation_Snow

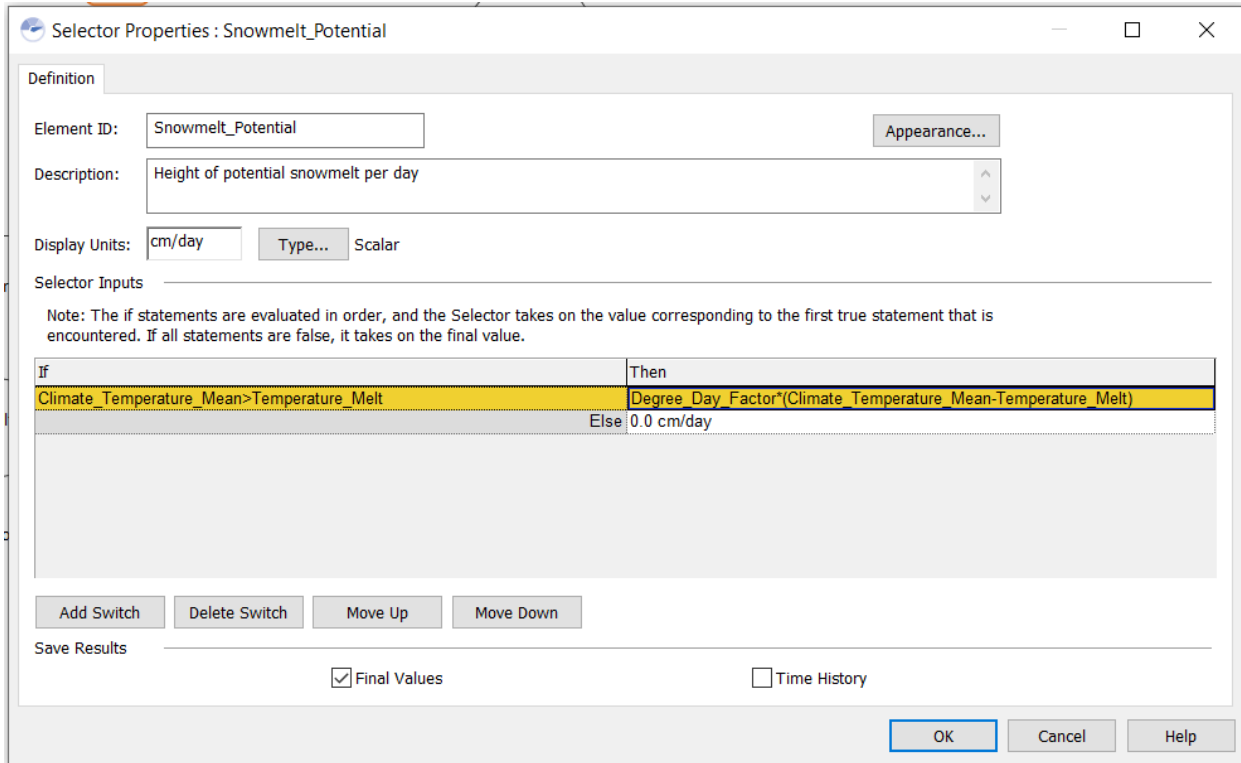


Figure A2 - 16: Snowmelt_Potential

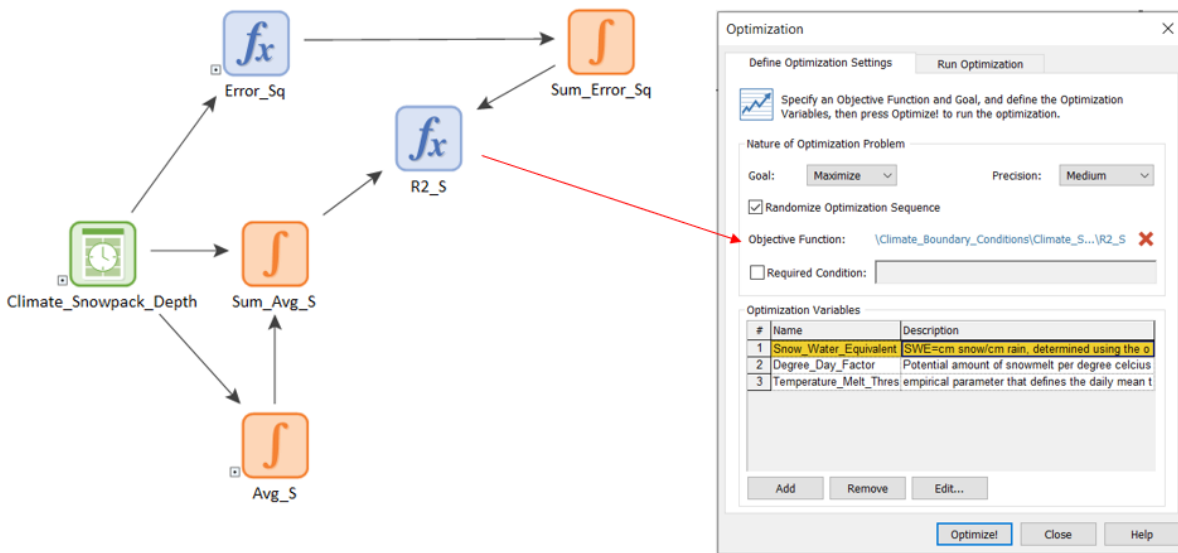


Figure A2 - 17: Optimization to determine empirical factors to match historical snowpack depth

Mining Waste Container

The mining waste container pulls information from the mine plan into GoldSim and converts to the required daily volume input required to “build” the waste rock pile. Model selection, setup, and calibration for waste rock and overburden management are described within the text in Section 3.2.1.

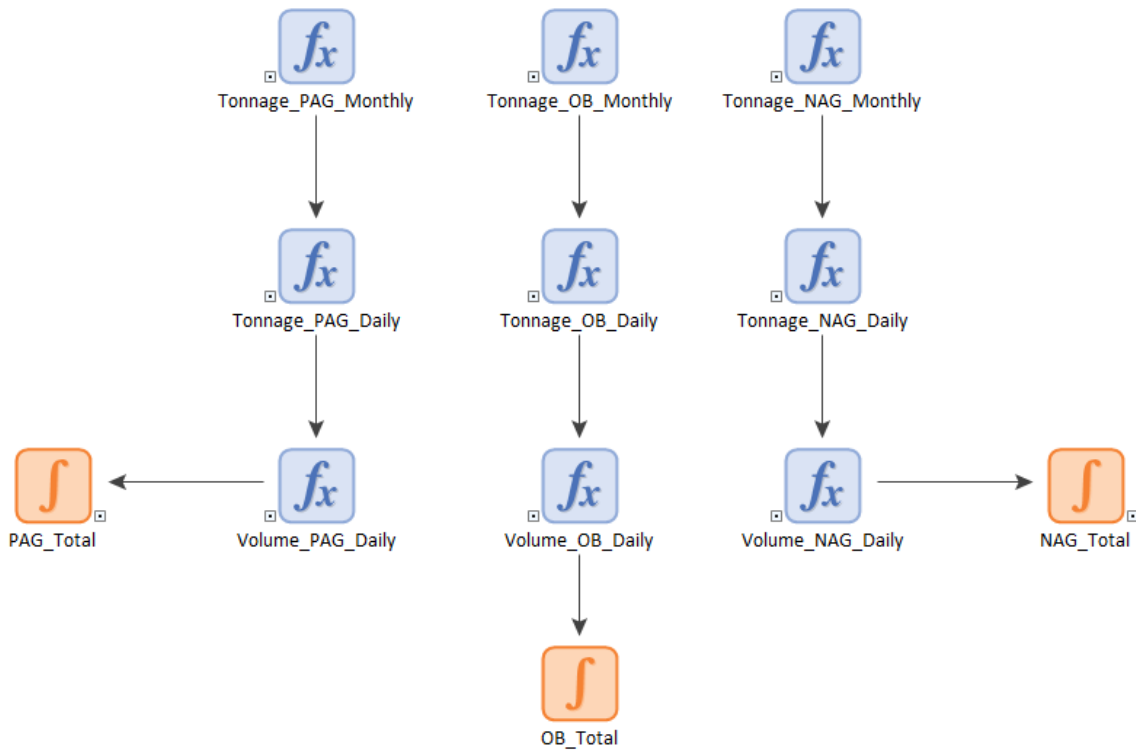


Figure A2 - 18: Mining_Waste

Saturated/Unsaturated Flow (End_Dump Container)

The saturated/unsaturated container calculates the infiltration, percolation, seepage, and water storage through each lift, and each simulated layer within the lifts. Model selection, setup, and calibration for hydrogeology and runoff are described within the text in Section 3.2.4. and 3.2.5.

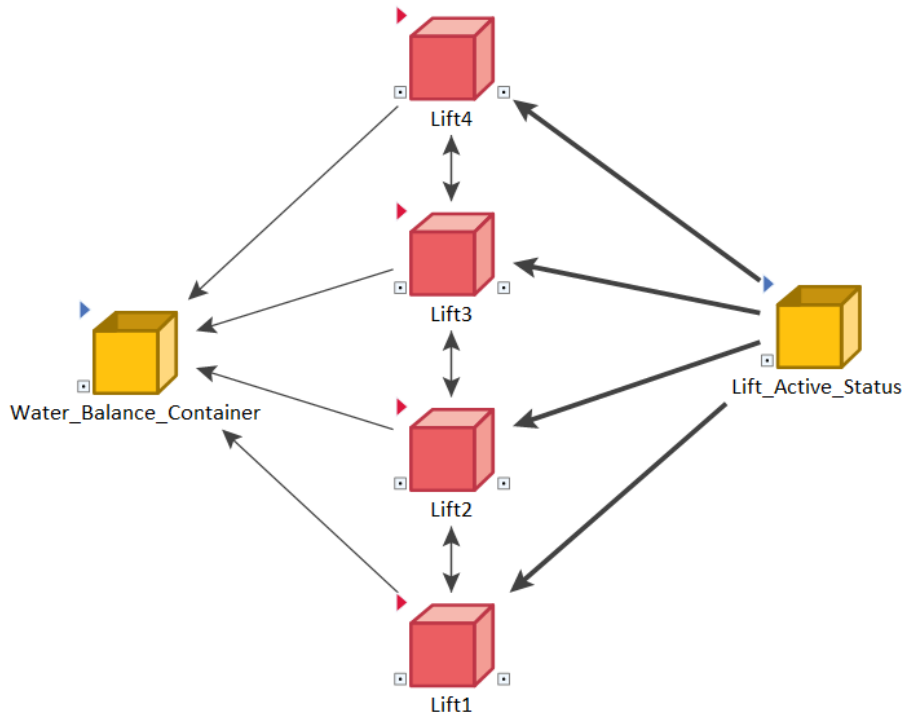


Figure A2 - 19: End_Dump

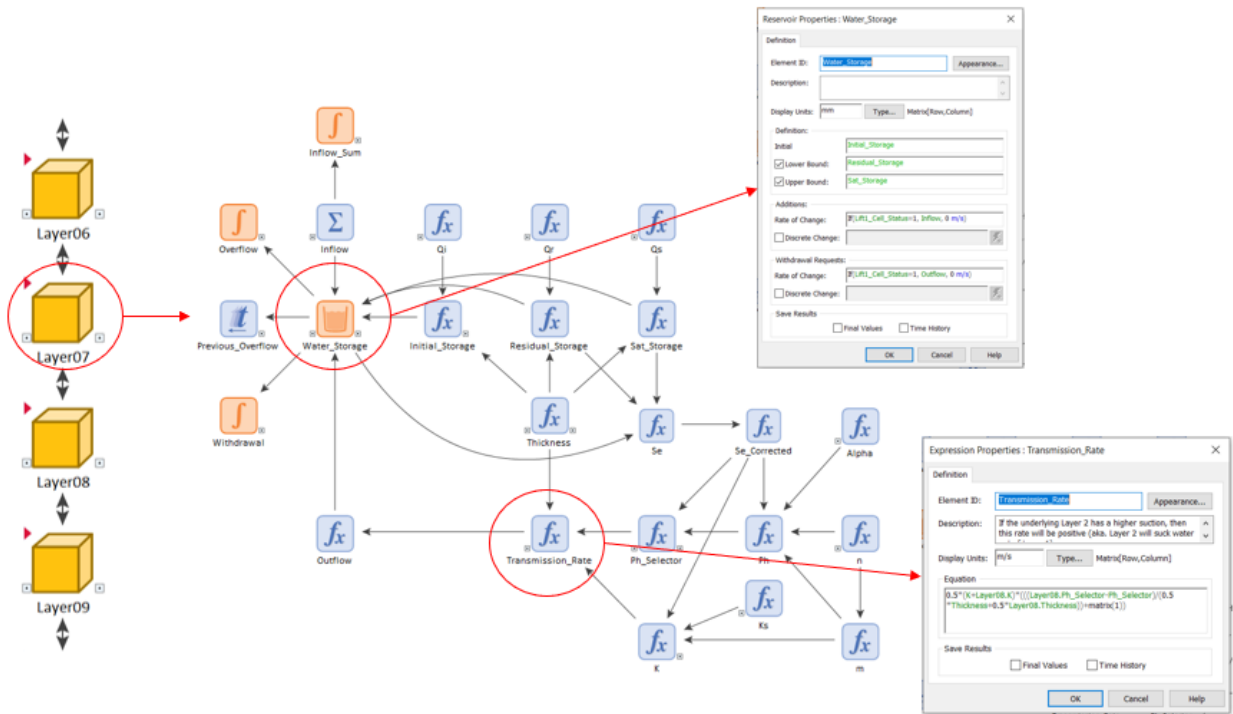


Figure A2 - 20: Example - Layer07

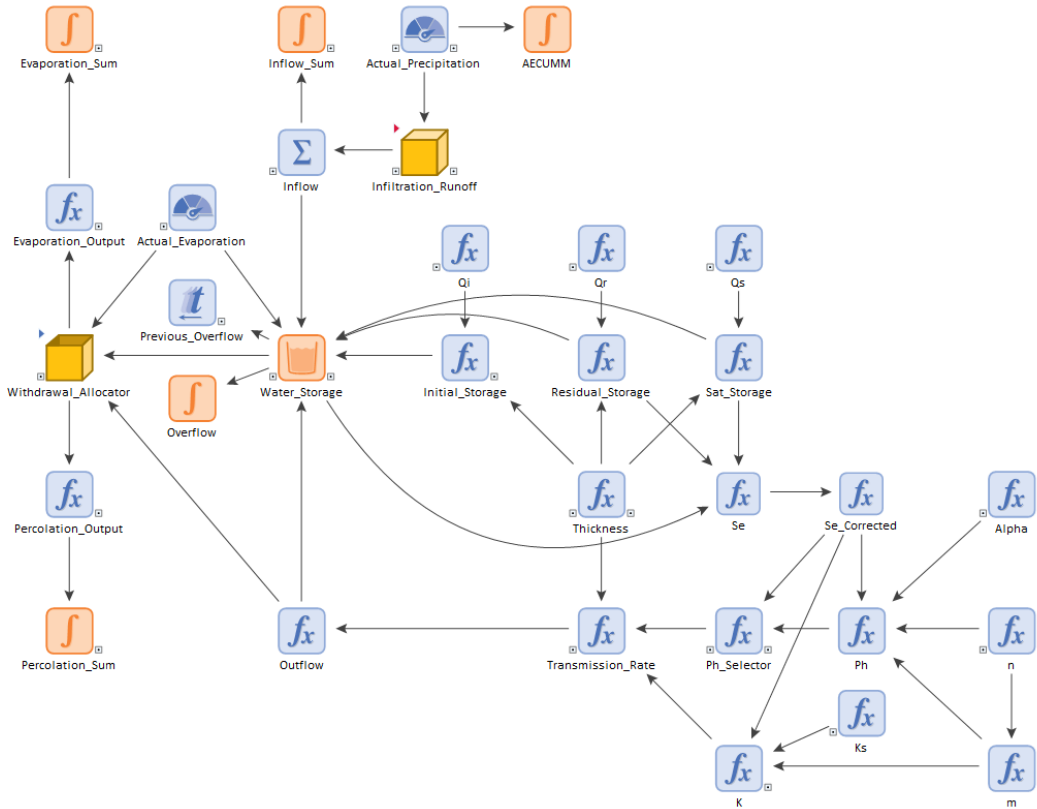


Figure A2 - 21: Layer_Top

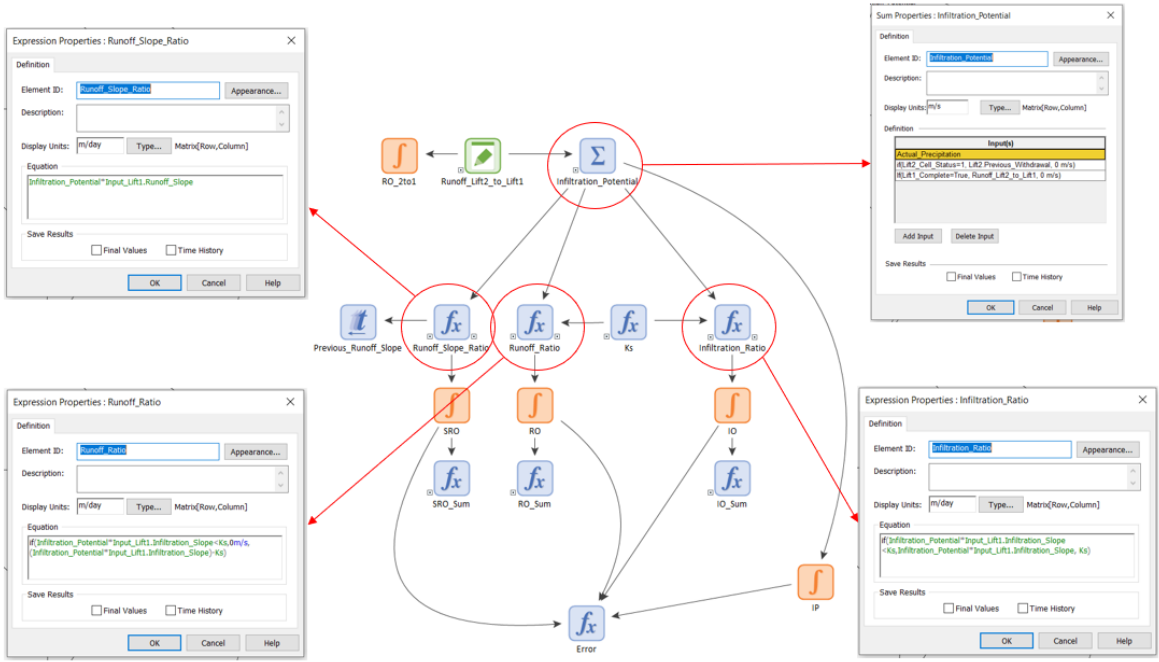


Figure A2 - 22: Infiltration_Runoff

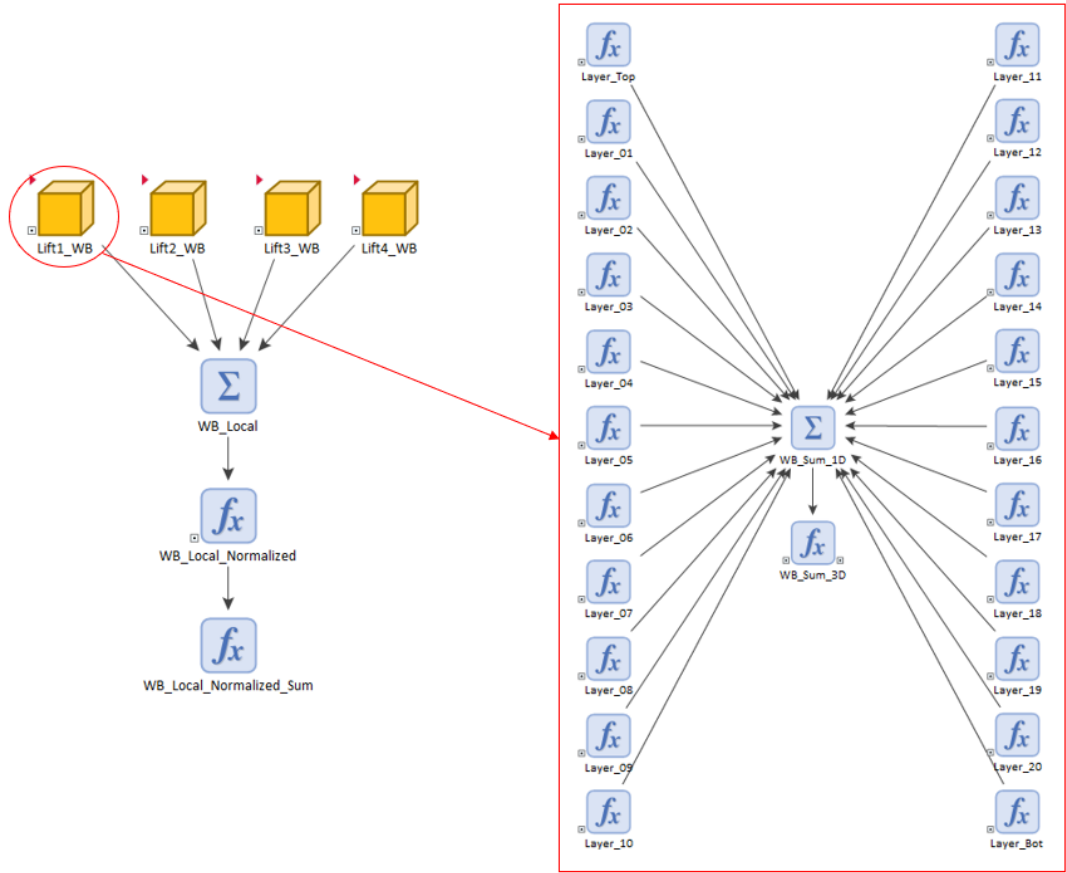


Figure A2 - 25: Water_Balance_Container

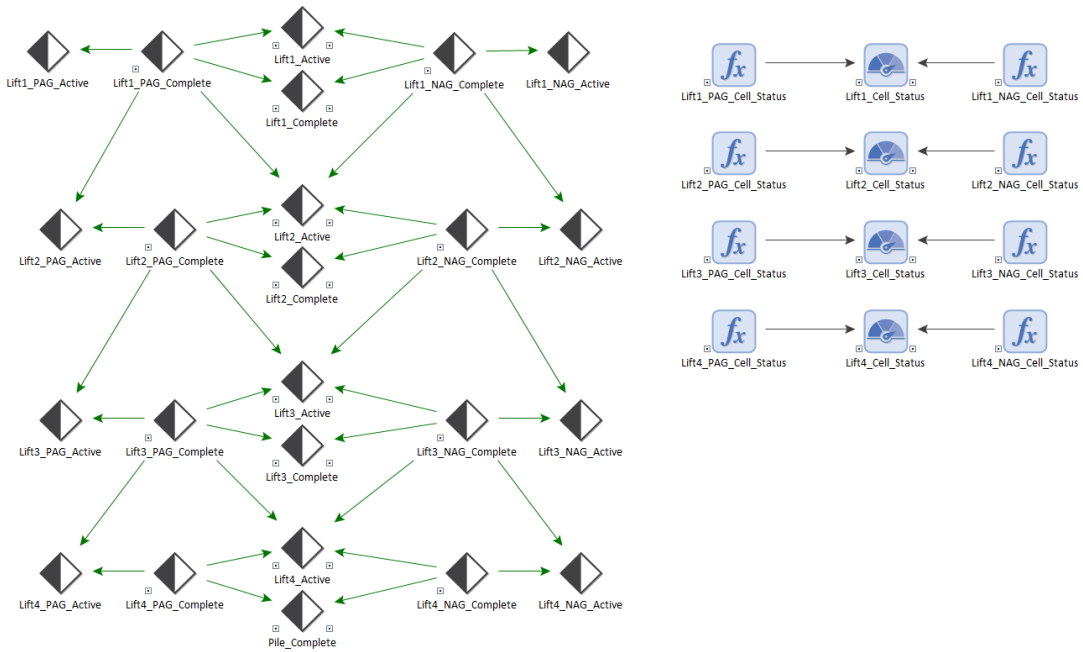


Figure A2 - 26: Lift_Active_Status

Output Container

The output container pulls climate information from each lift to sum global pile totals for precipitation, evaporation, runoff, water storage, and seepage.

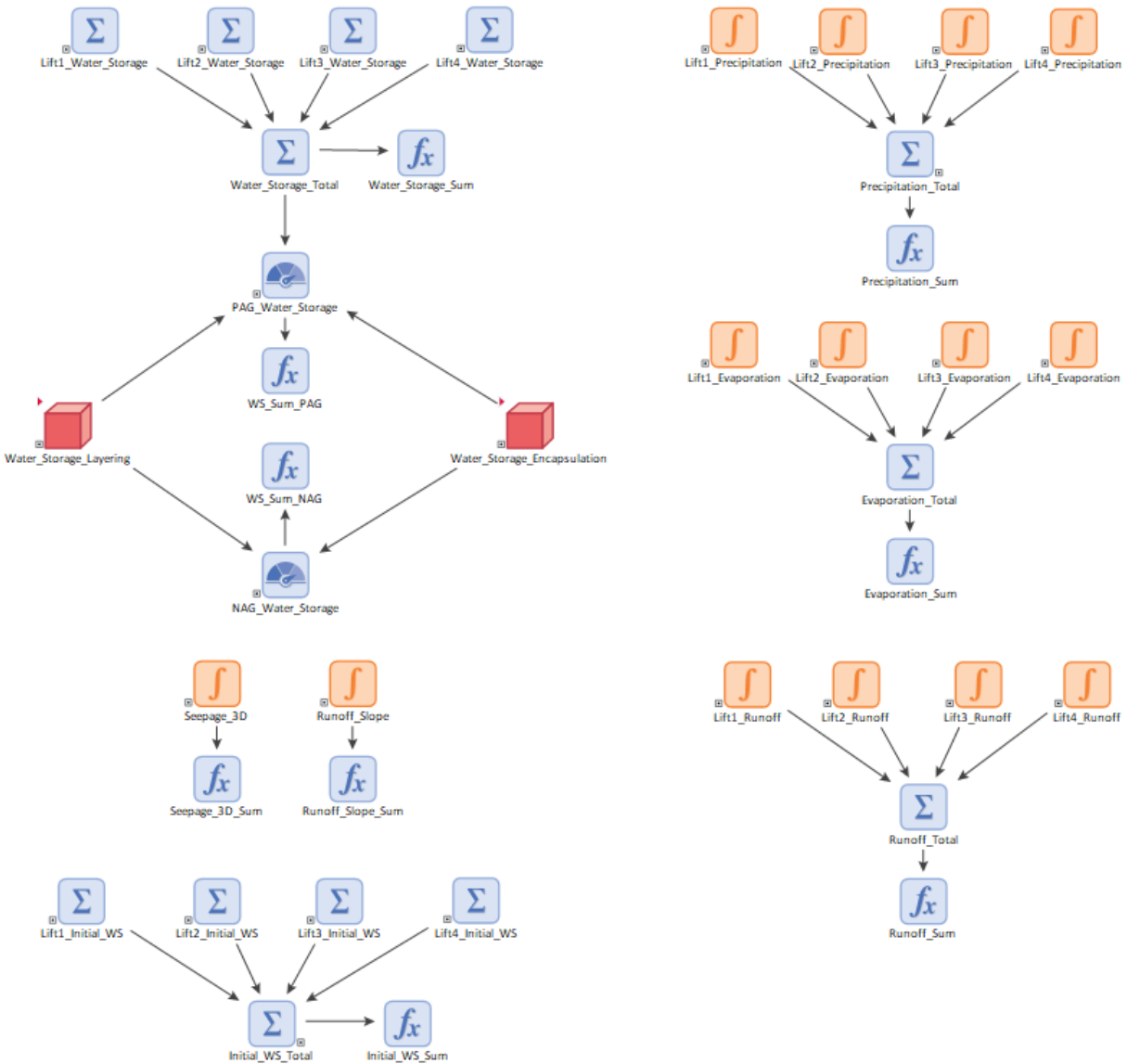


Figure A2 - 27: Output_Container

APPENDIX 3 – MODEL USER GUIDE

This appendix complements the descriptions of user interface in Chapter 3 on the set up and input procedures of the simulation. Below is a step-by-step guide to setting up the Goldsim model inputs and simulation settings.

Step 1: Waste Rock Deposition

Two dumping methods, end-dumping and paddock dumping can be simulated, which requires the user to choose either the WR Model-End Dump or WR Model-Paddock Dump model file.

Step 2: Pile Geometry

Pile geometry is inputted through an excel input file, the user inputs the surface area and height for each lift in the pile (Figure A3 - 1), the model then determines the required cell area and volume. The user is then required to input a construction sequence coupled with a PAG and NAG placement plan to simulate the ARD mitigation options: PAG separation, layering, and encapsulation (Figure A3 - 2). Each lift has two matrices: PAG Placement and NAG Placement, with “0” indicating no material (PAG/NAG), and positive numbers indicating the construction sequence of PAG/NAG. Using this input, the Excel file calculates the total volume of material (PAG or NAG) produced when the construction cell is full. The inputs from the excel file are imported into GoldSim using spreadsheet elements.

	Surface Area (m ²)	Height (m)	# of Cells Open to Atmosphere	Cell Area (m ²)	Total Area of Cells (m ²)	Volume (m ³)
Lift 4 Surface			2			
Lift 4 Slope			10			
Lift 3 Surface			18			
Lift 3 Slope			26			
Lift 2 Surface			34			
Lift 2 Slope			42			
Lift 1 Surface			50			
Lift 1 Slope			58			

Figure A3 - 1: Lift Area and Height Input Table

Row	1	2	3	4	5	6	7	8	9	10	11	12	13	14	15	16
1	1	16	31	46	61	76	91	106	121	136	151	166	181	196	211	226
2	2	17	32	47	62	77	92	107	122	137	152	167	182	197	212	227
3	3	18	33	48	63	78	93	108	123	138	153	168	183	198	213	228
4	4	19	34	49	64	79	94	109	124	139	154	169	184	199	214	229
5	5	20	35	50	65	80	95	110	125	140	155	170	185	200	215	230
6	6	21	36	51	66	81	96	111	126	141	156	171	186	201	216	231
7	7	22	37	52	67	82	97	112	127	142	157	172	187	202	217	232
8	8	23	38	53	68	83	98	113	128	143	158	173	188	203	218	233
9	9	24	39	54	69	84	99	114	129	144	159	174	189	204	219	234
10	10	25	40	55	70	85	100	115	130	145	160	175	190	205	220	235
11	11	26	41	56	71	86	101	116	131	146	161	176	191	206	221	236
12	12	27	42	57	72	87	102	117	132	147	162	177	192	207	222	237
13	13	28	43	58	73	88	103	118	133	148	163	178	193	208	223	238
14	14	29	44	59	74	89	104	119	134	149	164	179	194	209	224	239
15	15	30	45	60	75	90	105	120	135	150	165	180	195	210	225	240

Figure A3 - 2: Example Input of Construction Sequence of PAG Material

Within the GoldSim Input Dashboard (Figure A3 - 3), the user is required to indicate the vertical geometry of NAG and PAG for the layering case, with “0” for NAG and “1” for PAG. Lift 4 only has 10 layers and therefore 11 to 20 will have no impact on the model.

Model Inputs

Additional inputs can be found:
 - in "End_Dump_Inputs" Excel file for pile design
 - within model input container for constants and inputs that would require model updates if changed

[Go to Model Input Container](#)

Mitigation Method: PAG Separation Layering Encapsulation

Compacted Surface?

Year historical weather starts:

Latitude:

Model Run Start Month: July

Placement of PAG and NAG for Layering: (0=NAG, 1=PAG)

	Lift 1&2&3	Lift 4
1	0	0
2	0	0
3	0	0
4	0	0
5	0	0
6	0	1
7	0	1
8	0	1
9	0	1
10	0	1
11	1	0
12	1	0
13	1	0
14	1	0
15	1	0
16	1	0
17	1	0
18	1	0
19	1	0
20	1	0

[Back to Start](#)

Unsaturated Soil Parameters

	Soil E	Compacted	Soil D	Soil C	Soil B	Soil A
Van Genuchten - alpha [1/cm]	0.0886	0.0487	0.2938	0.42	0.8699	1.5404
Van Genuchten - n	2.95	4.14	1.94	1.82	1.65	1.58
Initial Volumetric Water Content	0.15	0.15	0.15	0.15	0.15	0.15
Residual Volumetric Water Content	0.069	0.069	0.102	0.078	0.109	0.138
Saturated Volumetric Water Content	0.38	0.24	0.38	0.38	0.38	0.38
Saturated Hydraulic Conductivity [m/s]	0.00013	0.0000415	0.00023	0.0004	0.00068	0.0013

Monthly Tonnage (PAG)

[tonne]	January	February	March	April	May	June	July	August	September	October	November	December
2019	0	0	0	0	0	0	7983	6861	0	3996	1898	5631
2020	17152	7425	67458	18592	110602	111316	61552	55596	59570	56812	58706	54920
2021	120171	120171	112420	100135	96905	96909	63729	63729	63729	91702	91702	91702
2022	90993	90993	90993	90023	90023	90023	53892	53892	53892	53892	53892	53892
2023	54480	54480	54480	54480	54480	54480	8032	8032	8032	8032	8032	8032
2024	6595	6595	6595	6595	6595	6595	0	0	0	0	0	0

Monthly Tonnage (NAG)

[tonne]	January	February	March	April	May	June	July	August	September	October	November	December
2019	0	0	0	0	0	0	46704	64851	160799	104272	120594	26715
2020	29690	27910	46118	44492	79884	66237	103990	93926	100636	102879	106308	99451
2021	110277	110277	103163	123828	119833	119833	159891	159891	159891	110160	110160	110160
2022	90336	90336	90336	89368	89368	89368	61285	61285	61285	61285	61285	61285
2023	61955	61955	61955	61955	61955	61955	7607	7607	7607	7607	7607	7607
2024	7757	7757	7757	7757	7757	7757	0	0	0	0	0	0

Monthly Tonnage (Overburden)

[tonne]	January	February	March	April	May	June	July	August	September	October	November	December
2019	0	0	0	0	0	0	7983	6861	0	3996	1898	5631
2020	17152	7425	67458	18592	110602	111316	61552	55596	59570	56812	58706	54920
2021	120171	120171	112420	100135	96905	96909	63729	63729	63729	91702	91702	91702
2022	90993	90993	90993	90023	90023	90023	53892	53892	53892	53892	53892	53892
2023	54480	54480	54480	54480	54480	54480	8032	8032	8032	8032	8032	8032
2024	6595	6595	6595	6595	6595	6595	0	0	0	0	0	0

Coefficient of Runoff from Slopes: Thickness of Top Layer:

Unit Weight of Waste Rock: Thickness of Bottom Layer:

[Outputs](#)

Figure A3 - 3: Input Dashboard – Layering Geometry

Step 4: Mitigation Method Selection

From the input dashboard within GoldSim (Figure A3 - 4), the user selects if the model will simulate the ARD mitigation option PAG separation, layering, or encapsulation; and if there is a compacted surface layer.

Model Inputs

Additional inputs can be found:
 - in "End_Dump_Inputs" Excel file for pile design
 - within model input container for constants and inputs that would require model updates if changed

[Go to Model Input Container](#)

Mitigation Method:

- PAG Separation
- Layering
- Encapsulation

Compacted Surface?

Year historical weather starts:

Latitude:

Model Run Start Month:

Placement of PAG and NAG for Layering:
(0=NAG, 1=PAG)

	Lift 1&2&3	Lift 4
1	0	0
2	0	0
3	0	0
4	0	0
5	0	0
6	0	1
7	0	1
8	0	1
9	0	1
10	0	1
11	1	0
12	1	0
13	1	0
14	1	0
15	1	0
16	1	0
17	1	0
18	1	0
19	1	0
20	1	0

[Back to Start](#)

Unsaturated Soil Parameters

	Soil E	Compacted	Soil D	Soil C	Soil B	Soil A
Van Genuchten - alpha [1/cm]	0.0886	0.0487	0.2938	0.42	0.8699	1.5404
Van Genuchten - n	2.95	4.14	1.94	1.82	1.65	1.58
Initial Volumetric Water Content	0.15	0.15	0.15	0.15	0.15	0.15
Residual Volumetric Water Content	0.069	0.069	0.102	0.078	0.109	0.138
Saturated Volumetric Water Content	0.38	0.24	0.38	0.38	0.38	0.38
Saturated Hydraulic Conductivity [m/s]	0.00013	0.0000415	0.00023	0.0004	0.00068	0.0013

Monthly Tonnage (PAG)

[tonne]	January	February	March	April	May	June	July	August	September	October	November	December
2019	0	0	0	0	0	0	7983	6861	0	3996	1898	5631
2020	17152	7425	67458	18592	110602	111316	61552	55596	59570	56812	58706	54920
2021	120171	120171	112420	100135	96905	96909	63729	63729	63729	91702	91702	91702
2022	90993	90993	90993	90023	90023	90023	53892	53892	53892	53892	53892	53892
2023	54480	54480	54480	54480	54480	54480	8032	8032	8032	8032	8032	8032
2024	6595	6595	6595	6595	6595	6595	0	0	0	0	0	0

Monthly Tonnage (NAG)

[tonne]	January	February	March	April	May	June	July	August	September	October	November	December
2019	0	0	0	0	0	0	46704	64851	160799	104272	120594	26715
2020	29690	27910	46118	44492	79884	66237	103990	93926	100636	102879	106308	99451
2021	110277	110277	103163	123828	119833	119833	159891	159891	159891	110160	110160	110160
2022	90336	90336	90336	89368	89368	89368	61285	61285	61285	61285	61285	61285
2023	61955	61955	61955	61955	61955	61955	7607	7607	7607	7607	7607	7607
2024	7757	7757	7757	7757	7757	7757	0	0	0	0	0	0

Monthly Tonnage (Overburden)

[tonne]	January	February	March	April	May	June	July	August	September	October	November	December
2019	0	0	0	0	0	0	7983	6861	0	3996	1898	5631
2020	17152	7425	67458	18592	110602	111316	61552	55596	59570	56812	58706	54920
2021	120171	120171	112420	100135	96905	96909	63729	63729	63729	91702	91702	91702
2022	90993	90993	90993	90023	90023	90023	53892	53892	53892	53892	53892	53892
2023	54480	54480	54480	54480	54480	54480	8032	8032	8032	8032	8032	8032
2024	6595	6595	6595	6595	6595	6595	0	0	0	0	0	0

Coefficient of Runoff from Slopes: Thickness of Top Layer:

Unit Weight of Waste Rock: Thickness of Bottom Layer:

[Outputs](#)

Figure A3 - 4: Input Dashboard – Mitigation Selection

Step 5: Unsaturated Soil Parameters

The user is required to input unsaturated soil parameters (Figure A3 - 5). In the end-dumping case five sets of soil parameters are needed, and only one in the paddock dumping case, with an additional set of soil parameters needed for a compacted surface layer. Chapter 4 identifies a

methodology for converting the homogeneous unsaturated soil parameters into a five layered system based on work by Barsi (2017).

Model Inputs

Additional inputs can be found:
 - in "End_Dump_Inputs" Excel file for pile design
 - within model input container for constants and inputs that would require model updates if changed

[Go to Model Input Container](#)

Mitigation Method: PAG Separation Layering Encapsulation

Compacted Surface?

Year historical weather starts:

Latitude:

Model Run Start Month: July

Placement of PAG and NAG for Layering: (0=NAG, 1=PAG)

	Lift 1&2&3	Lift 4
1	0	0
2	0	0
3	0	0
4	0	0
5	0	0
6	0	1
7	0	1
8	0	1
9	0	1
10	0	1
11	1	0
12	1	0
13	1	0
14	1	0
15	1	0
16	1	0
17	1	0
18	1	0
19	1	0
20	1	0

[Back to Start](#)

Unsaturated Soil Parameters

	Soil E	Compacted	Soil D	Soil C	Soil B	Soil A
Van Genuchten - alpha [1/cm]	0.0886	0.0487	0.2938	0.42	0.8699	1.5404
Van Genuchten - n	2.95	4.14	1.94	1.82	1.65	1.58
Initial Volumetric Water Content	0.15	0.15	0.15	0.15	0.15	0.15
Residual Volumetric Water Content	0.069	0.069	0.102	0.078	0.109	0.138
Saturated Volumetric Water Content	0.38	0.24	0.38	0.38	0.38	0.38
Saturated Hydraulic Conductivity [m/s]	0.00013	0.0000415	0.00023	0.0004	0.00068	0.0013

Monthly Tonnage (PAG)

[tonne]	January	February	March	April	May	June	July	August	September	October	November	December
2019	0	0	0	0	0	0	7983	6861	0	3996	1898	5631
2020	17152	7425	67458	18592	110602	111316	61552	55596	59570	56812	58706	54920
2021	120171	120171	112420	100135	96905	96909	63729	63729	63729	91702	91702	91702
2022	90993	90993	90993	90023	90023	90023	53892	53892	53892	53892	53892	53892
2023	54480	54480	54480	54480	54480	54480	8032	8032	8032	8032	8032	8032
2024	6595	6595	6595	6595	6595	6595	0	0	0	0	0	0

Monthly Tonnage (NAG)

[tonne]	January	February	March	April	May	June	July	August	September	October	November	December
2019	0	0	0	0	0	0	46704	64851	160799	104272	120594	26715
2020	29690	27910	46118	44492	79884	66237	103990	93926	100636	102879	106308	99451
2021	110277	110277	103163	123828	119833	119833	159891	159891	159891	110160	110160	110160
2022	90336	90336	90336	89368	89368	89368	61285	61285	61285	61285	61285	61285
2023	61955	61955	61955	61955	61955	61955	7607	7607	7607	7607	7607	7607
2024	7757	7757	7757	7757	7757	7757	0	0	0	0	0	0

Monthly Tonnage (Overburden)

[tonne]	January	February	March	April	May	June	July	August	September	October	November	December
2019	0	0	0	0	0	0	7983	6861	0	3996	1898	5631
2020	17152	7425	67458	18592	110602	111316	61552	55596	59570	56812	58706	54920
2021	120171	120171	112420	100135	96905	96909	63729	63729	63729	91702	91702	91702
2022	90993	90993	90993	90023	90023	90023	53892	53892	53892	53892	53892	53892
2023	54480	54480	54480	54480	54480	54480	8032	8032	8032	8032	8032	8032
2024	6595	6595	6595	6595	6595	6595	0	0	0	0	0	0

Coefficient of Runoff from Slopes: Thickness of Top Layer:

Unit Weight of Waste Rock: Thickness of Bottom Layer:

[Outputs](#)

Figure A3 - 5: Input Dashboard – Unsaturated Soil Parameters

Step 6: Mine Plan Inputs

The user is required to input the mine plan in monthly totals for the three streams, PAG, NAG, and overburden (Figure A3 - 6). Additional user inputs are the unit weight of waste rock which assumes the same average unit weight for both PAG and NAG waste rock. The thickness of top and bottom layers impact the evaporation and seepage calculations, and have been provided as in the dashboard to simplify the ability to perform sensitivity analysis on these inputs. The runoff from slopes input is an empirical fractor of water that runs off on the slope.

Model Inputs

Additional inputs can be found:
 - in "End_Dump_Inputs" Excel file for pile design
 - within model input container for constants and inputs that would require model updates if changed

[Go to Model Input Container](#)

Mitigation Method:

PAG Separation
 Layering
 Encapsulation

Compacted Surface?

Year historical weather starts:

1985

Latitude:

48.1

Model Run Start Month:

July

Placement of PAG and NAG for Layering:
 (0=NAG, 1=PAG)

	Lift 1&2&3	Lift 4
1	0	0
2	0	0
3	0	0
4	0	0
5	0	0
6	0	1
7	0	1
8	0	1
9	0	1
10	0	1
11	1	0
12	1	0
13	1	0
14	1	0
15	1	0
16	1	0
17	1	0
18	1	0
19	1	0
20	1	0

[Back to Start](#)

Unsaturated Soil Parameters

	Soil E	Compacted	Soil D	Soil C	Soil B	Soil A
Van Genuchten - alpha [1/cm]	0.0886	0.0487	0.2938	0.42	0.8699	1.5404
Van Genuchten - n	2.95	4.14	1.94	1.82	1.65	1.58
Initial Volumetric Water Content	0.15	0.15	0.15	0.15	0.15	0.15
Residual Volumetric Water Content	0.069	0.069	0.102	0.078	0.109	0.138
Saturated Volumetric Water Content	0.38	0.24	0.38	0.38	0.38	0.38
Saturated Hydraulic Conductivity [m/s]	0.00013	0.000415	0.00023	0.0004	0.00068	0.0013

Monthly Tonnage (PAG)

[tonne]	January	February	March	April	May	June	July	August	September	October	November	December
2019	0	0	0	0	0	0	7983	6861	0	3996	1898	5631
2020	17152	7425	67458	18592	110602	111316	61552	55596	59570	56812	58706	54920
2021	120171	120171	112420	100135	96905	96909	63729	63729	63729	91702	91702	91702
2022	90993	90993	90993	90023	90023	90023	53892	53892	53892	53892	53892	53892
2023	54480	54480	54480	54480	54480	54480	8032	8032	8032	8032	8032	8032
2024	6595	6595	6595	6595	6595	6595	0	0	0	0	0	0

Monthly Tonnage (NAG)

[tonne]	January	February	March	April	May	June	July	August	September	October	November	December
2019	0	0	0	0	0	0	46704	64851	160799	104272	120594	26715
2020	29690	27910	46118	44492	79884	66237	103990	93926	100636	102879	106308	99451
2021	110277	110277	103163	123828	119833	119833	159891	159891	159891	110160	110160	110160
2022	90336	90336	90336	89368	89368	89368	61285	61285	61285	61285	61285	61285
2023	61955	61955	61955	61955	61955	61955	7607	7607	7607	7607	7607	7607
2024	7757	7757	7757	7757	7757	7757	0	0	0	0	0	0

Monthly Tonnage (Overburden)

[tonne]	January	February	March	April	May	June	July	August	September	October	November	December
2019	0	0	0	0	0	0	7983	6861	0	3996	1898	5631
2020	17152	7425	67458	18592	110602	111316	61552	55596	59570	56812	58706	54920
2021	120171	120171	112420	100135	96905	96909	63729	63729	63729	91702	91702	91702
2022	90993	90993	90993	90023	90023	90023	53892	53892	53892	53892	53892	53892
2023	54480	54480	54480	54480	54480	54480	8032	8032	8032	8032	8032	8032
2024	6595	6595	6595	6595	6595	6595	0	0	0	0	0	0

Coefficient of Runoff from Slopes:

Thickness of Top Layer:

Unit Weight of Waste Rock:

Thickness of Bottom Layer:

[Outputs](#)

Figure A3 - 6. Input Dashboard – Mine Plan Inputs

Step 7: Climate Inputs

The user is able to influence high level climate inputs from the input dashboard including year historical weather starts, latitude, and model run start month (Figure A3 - 7).

Model Inputs

Additional inputs can be found:
 - in "End_Dump_Inputs" Excel file for pile design
 - within model input container for constants and inputs that would require model updates if changed

Mitigation Method: **PAG Separation**
 Layering
 Encapsulation

Compacted Surface?

Year historical weather starts:

Latitude:

Model Run Start Month:

Placement of PAG and NAG for Layering:
 (0=NAG, 1=PAG)

	Lift 1&2&3	Lift 4
1	0	0
2	0	0
3	0	0
4	0	0
5	0	0
6	0	1
7	0	1
8	0	1
9	0	1
10	0	1
11	1	0
12	1	0
13	1	0
14	1	0
15	1	0
16	1	0
17	1	0
18	1	0
19	1	0
20	1	0

Unsaturated Soil Parameters

	Soil E	Compacted	Soil D	Soil C	Soil B	Soil A
Van Genuchten - alpha [1/cm]	0.0886	0.0487	0.2938	0.42	0.8699	1.5404
Van Genuchten - n	2.95	4.14	1.94	1.82	1.65	1.58
Initial Volumetric Water Content	0.15	0.15	0.15	0.15	0.15	0.15
Residual Volumetric Water Content	0.069	0.069	0.102	0.078	0.109	0.138
Saturated Volumetric Water Content	0.38	0.24	0.38	0.38	0.38	0.38
Saturated Hydraulic Conductivity [m/s]	0.00013	0.000415	0.00023	0.0004	0.00068	0.0013

Monthly Tonnage (PAG)

[tonne]	January	February	March	April	May	June	July	August	September	October	November	December
2019	0	0	0	0	0	0	7983	6861	0	3996	1898	5631
2020	17152	7425	67458	18592	110602	111316	61552	55596	59570	56812	58706	54920
2021	120171	120171	112420	100135	96905	96909	63729	63729	63729	91702	91702	91702
2022	90993	90993	90993	90023	90023	90023	53892	53892	53892	53892	53892	53892
2023	54480	54480	54480	54480	54480	54480	8032	8032	8032	8032	8032	8032
2024	6595	6595	6595	6595	6595	6595	0	0	0	0	0	0

Monthly Tonnage (NAG)

[tonne]	January	February	March	April	May	June	July	August	September	October	November	December
2019	0	0	0	0	0	0	46704	64851	160799	104272	120594	26715
2020	29690	27910	46118	44492	79884	66237	103990	93926	100636	102879	106308	99451
2021	110277	110277	103163	123828	119833	119833	159891	159891	159891	110160	110160	110160
2022	90336	90336	90336	89368	89368	89368	61285	61285	61285	61285	61285	61285
2023	61955	61955	61955	61955	61955	61955	7607	7607	7607	7607	7607	7607
2024	7757	7757	7757	7757	7757	7757	0	0	0	0	0	0

Monthly Tonnage (Overburden)

[tonne]	January	February	March	April	May	June	July	August	September	October	November	December
2019	0	0	0	0	0	0	7983	6861	0	3996	1898	5631
2020	17152	7425	67458	18592	110602	111316	61552	55596	59570	56812	58706	54920
2021	120171	120171	112420	100135	96905	96909	63729	63729	63729	91702	91702	91702
2022	90993	90993	90993	90023	90023	90023	53892	53892	53892	53892	53892	53892
2023	54480	54480	54480	54480	54480	54480	8032	8032	8032	8032	8032	8032
2024	6595	6595	6595	6595	6595	6595	0	0	0	0	0	0

Coefficient of Runoff from Slopes: Thickness of Top Layer:

Unit Weight of Waste Rock: Thickness of Bottom Layer:

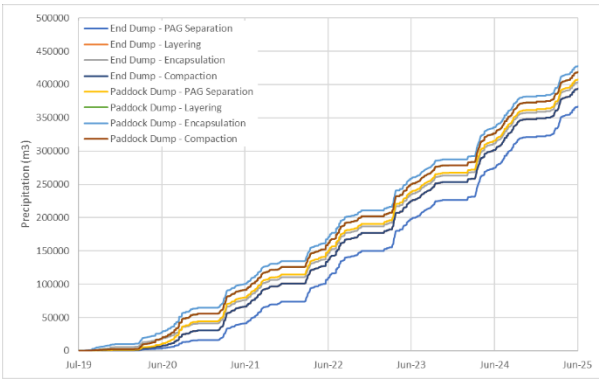
Figure A3 - 7. Input Dashboard – Climate Inputs

Step 8: Additional Inputs

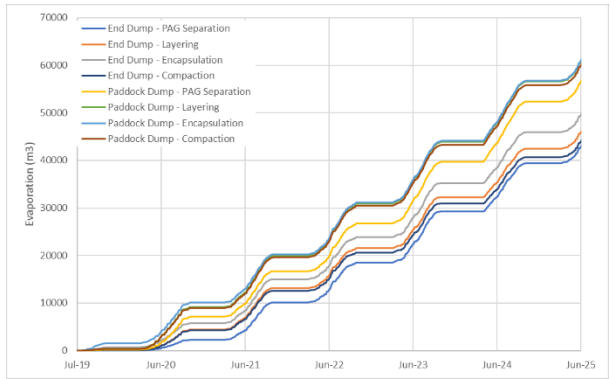
Step 1 to 7 has provided a general overview of the GoldSim model with available changeable inputs. There are additional inputs related to model selection that are buried within the GoldSim model that require additional effort to input within the current model. Users familiar with GoldSim modelling can use Chapter 3 and 4 as well as Appendix 2 as a guide for updating the GoldSim model to suit specific needs.

APPENIDX 4 – RESULTS FROM MODEL APPLICATION

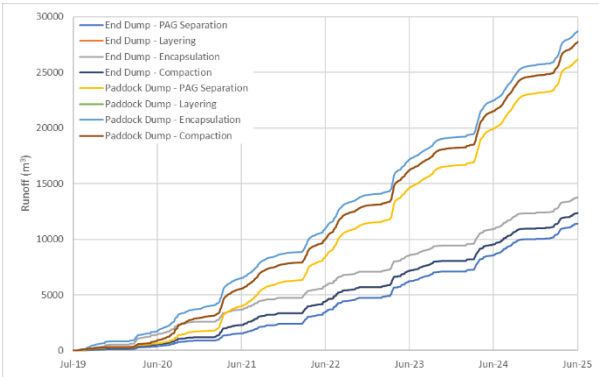
Table A4 - 1: Global Pile Behaviour – Construction (Year 0 to 6)



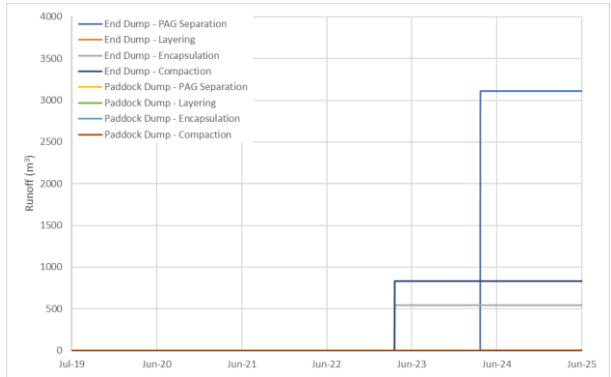
Precipitation on Pile (m³)



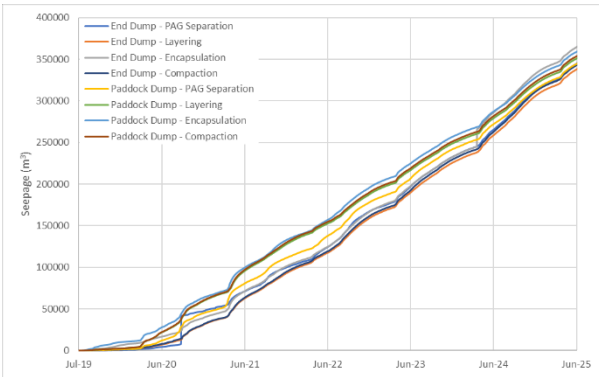
Evaporation from Pile (m³)



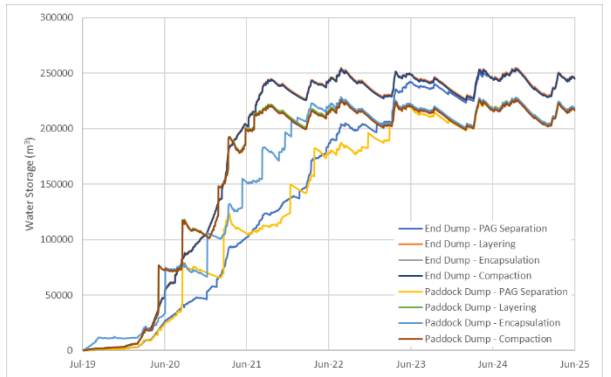
Lateral Runoff from Pile (m³)



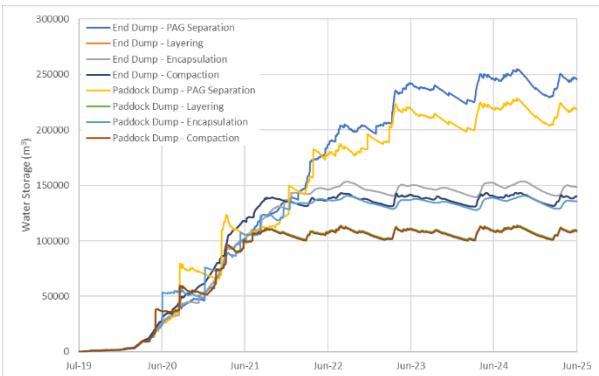
Vertical Runoff Lost from Pile (m³)



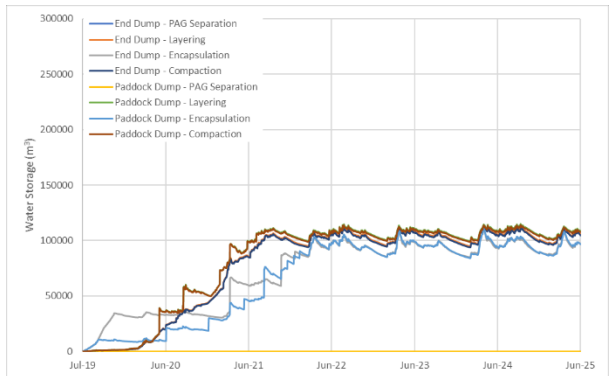
Seepage from Pile (m³)



Water Storage Within Pile (m³)

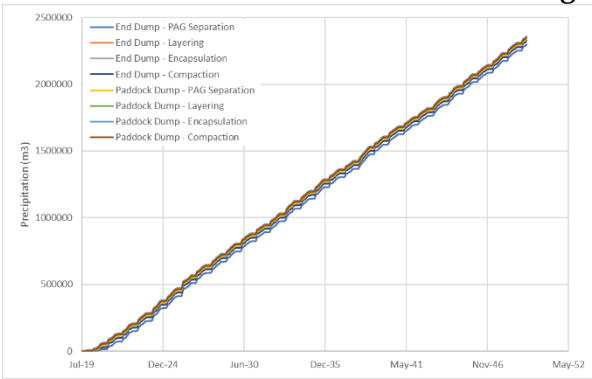


Water Storage Within Pile – PAG (m³)

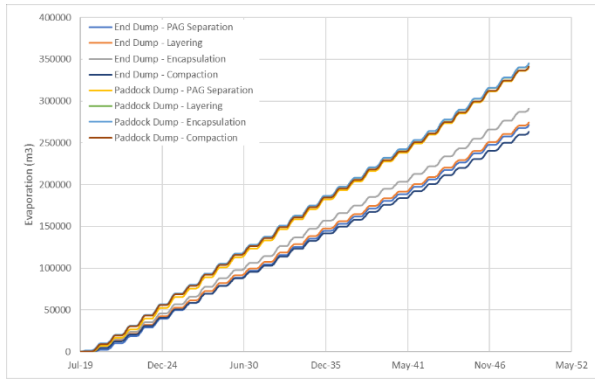


Water Storage Within Pile – NAG (m³)

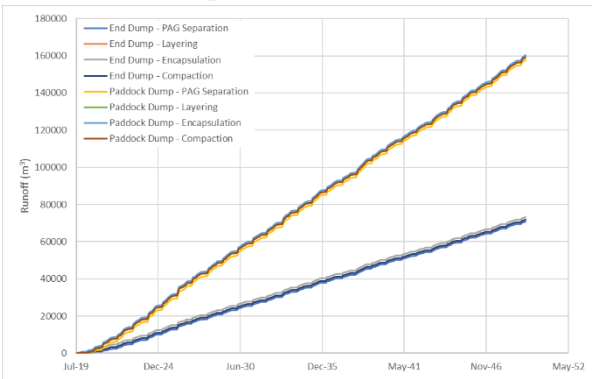
Table A4 - 2: Global Pile Behaviour – Longterm Behaviour (Year 0 to 50)



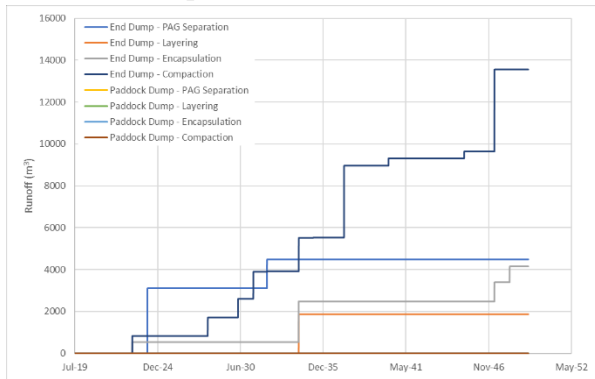
Precipitation on Pile (m³)



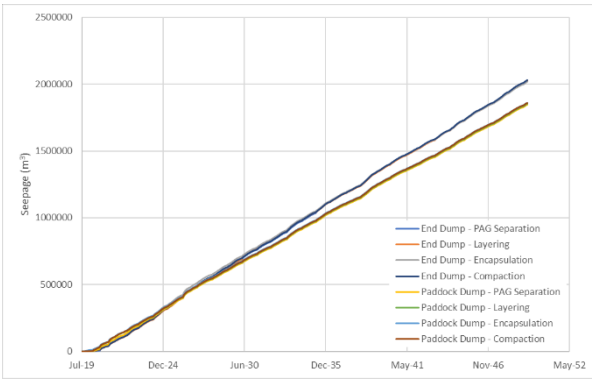
Evaporation from Pile (m³)



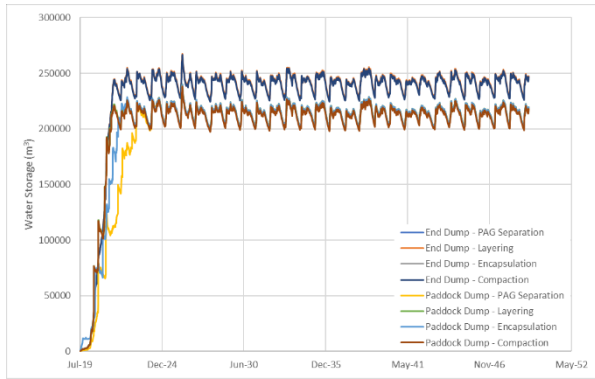
Lateral Runoff from Pile (m³)



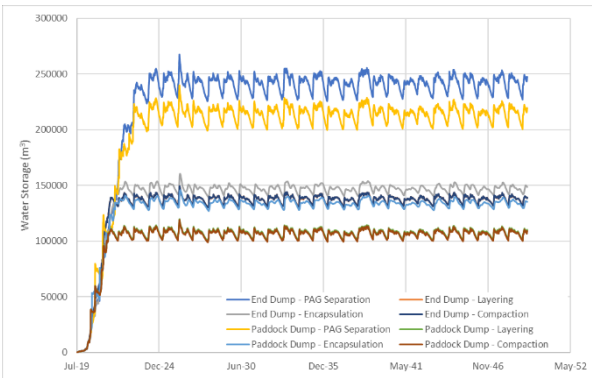
Vertical Runoff Lost from Pile (m³)



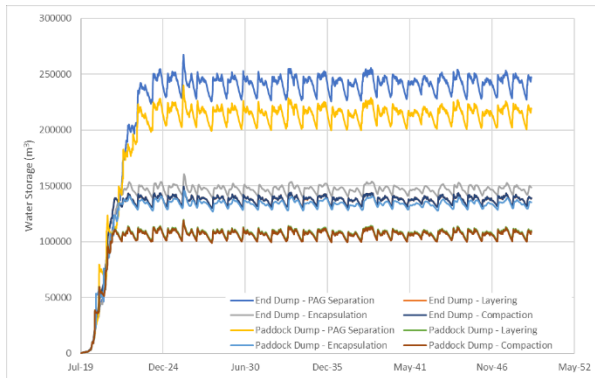
Seepage from Pile (m³)



Water Storage Within Pile (m³)

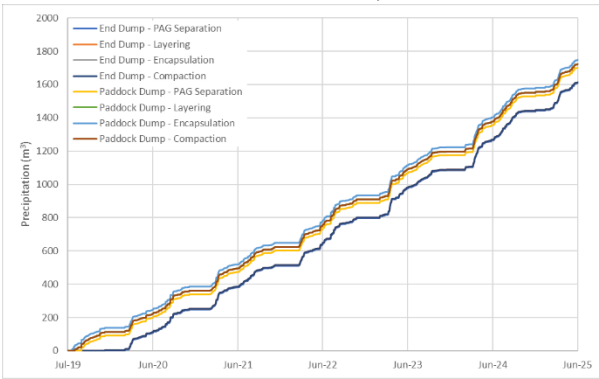


Water Storage Within Pile – PAG (m³)

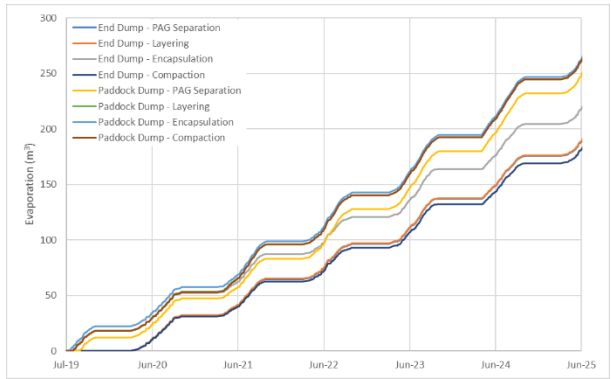


Water Storage Within Pile – NAG (m³)

Table A4 - 3: 3-D Column [2,2] – Construction (Year 0 to 6)

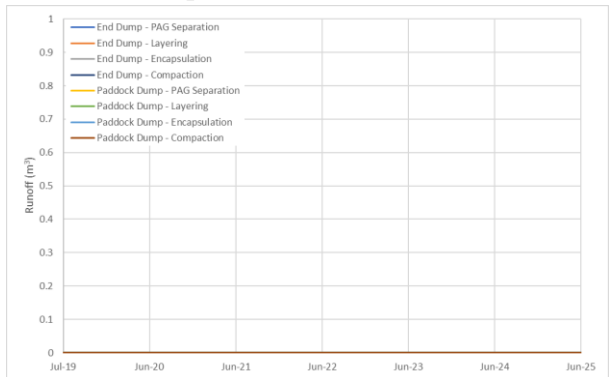


Precipitation on Pile (m³)



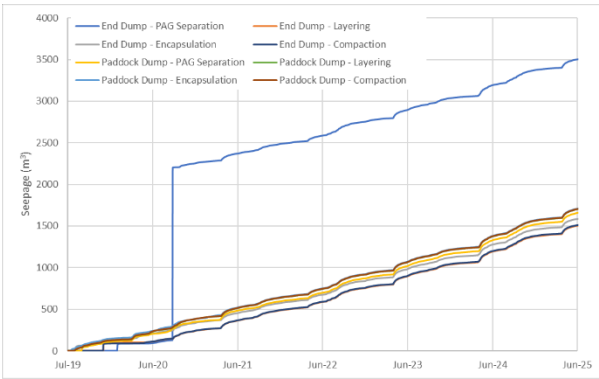
Evaporation from Pile (m³)

N/A

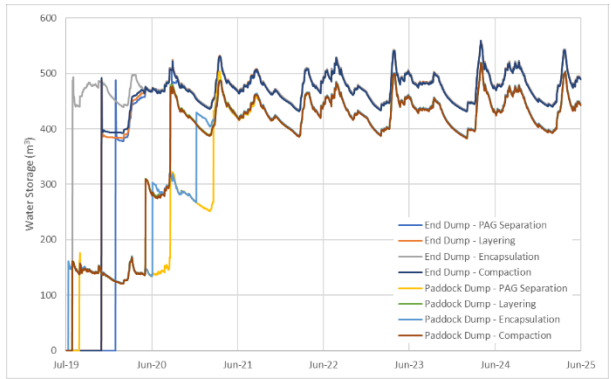


Lateral Runoff from Pile (m³)

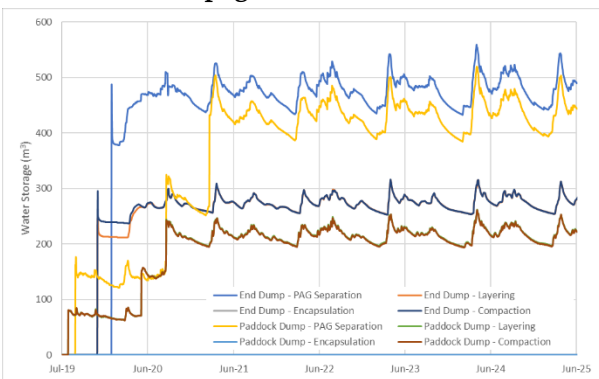
Vertical Runoff Lost from Pile (m³)



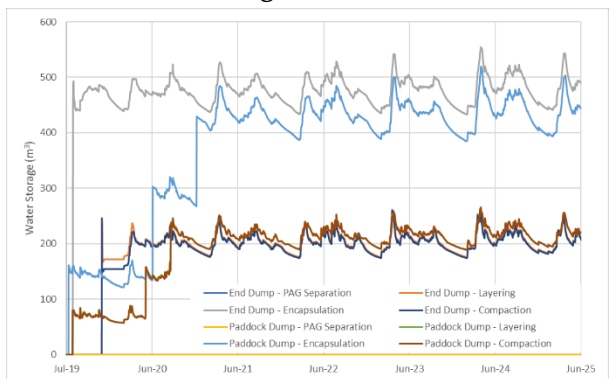
Seepage from Pile (m³)



Water Storage Within Pile (m³)

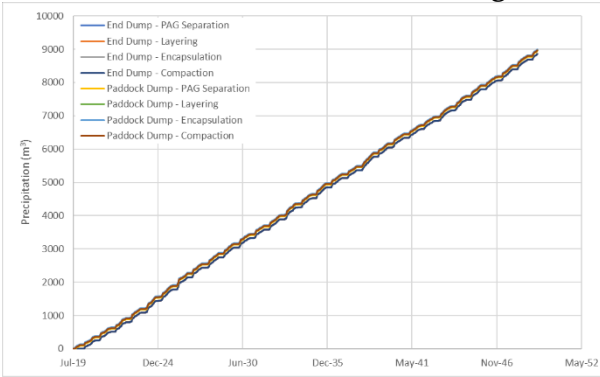


Water Storage Within Pile – PAG (m³)

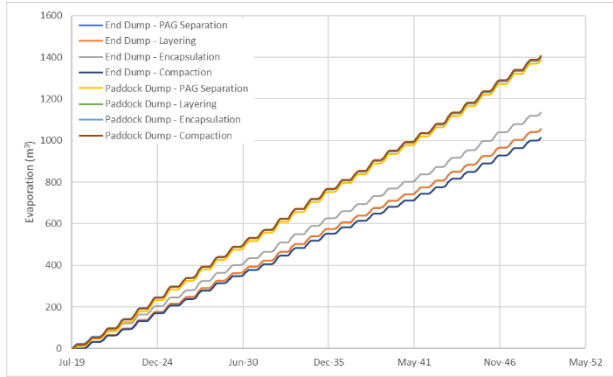


Water Storage Within Pile – NAG (m³)

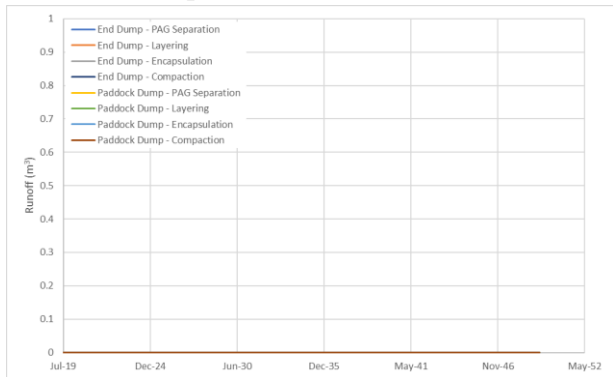
Table A4 - 4: 3-D Column [2,2] – Longterm Behaviour (Year 0 to 50)



Precipitation on Pile (m³)

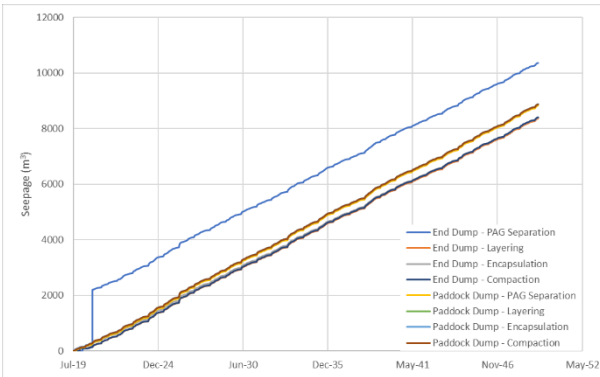


Evaporation from Pile (m³)

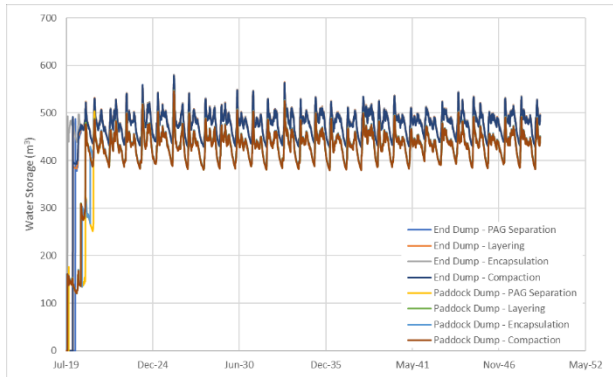


Lateral Runoff from Pile (m³)

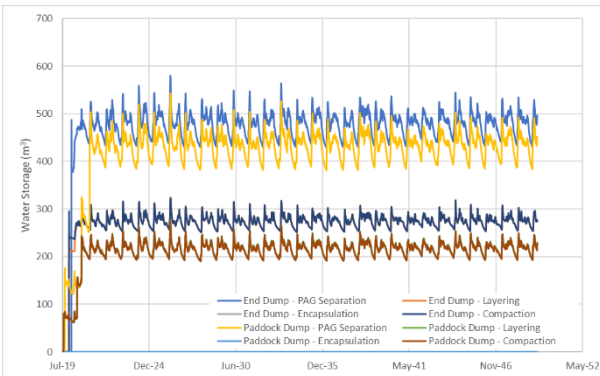
Vertical Runoff Lost from Pile (m³)



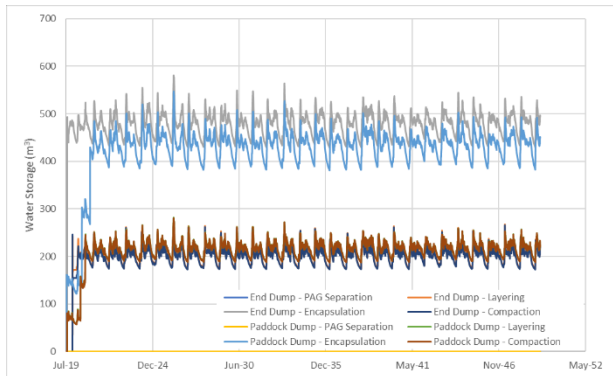
Seepage from Pile (m³)



Water Storage Within Pile (m³)

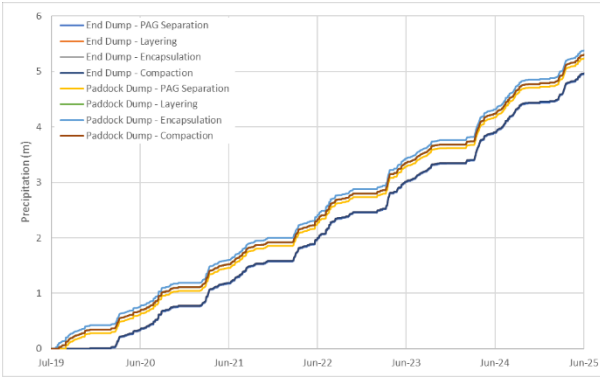


Water Storage Within Pile – PAG (m³)

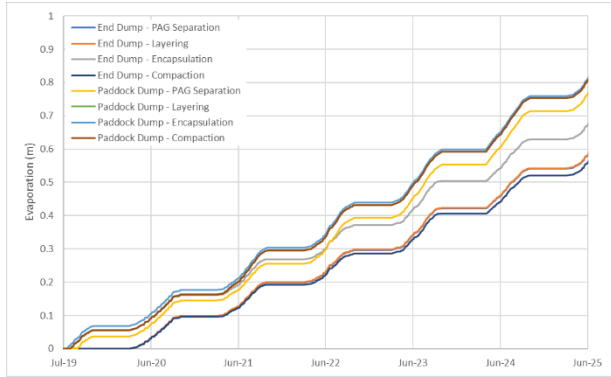


Water Storage Within Pile – NAG (m³)

Table A4 - 5: 1-D Column [2,2] – Construction (Year 0 to 6)

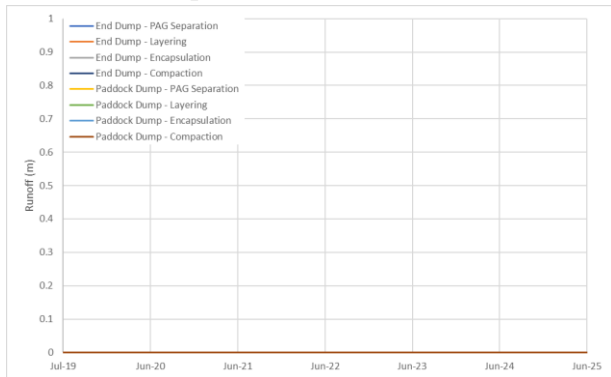


Precipitation on Pile (m)



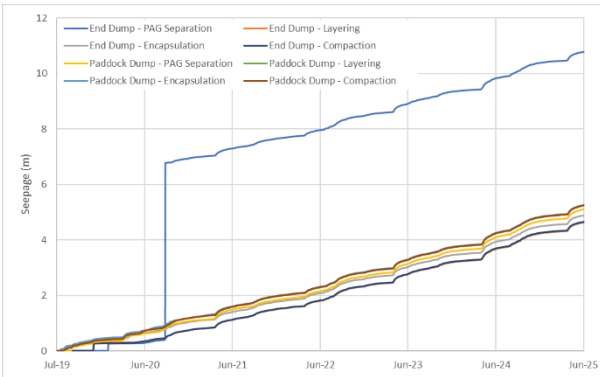
Evaporation from Pile (m)

N/A

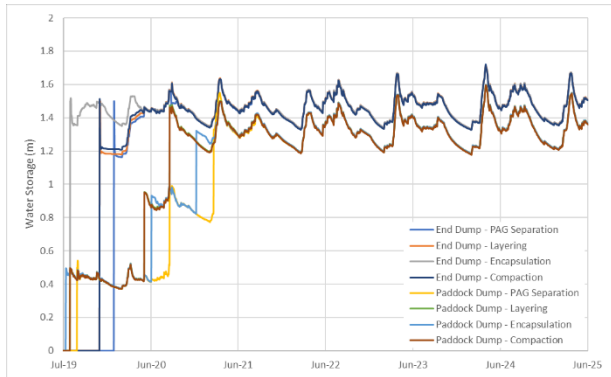


Vertical Runoff Lost from Pile (m)

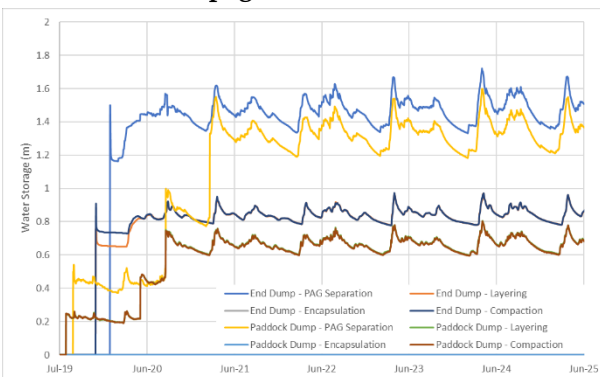
Lateral Runoff from Pile (m)



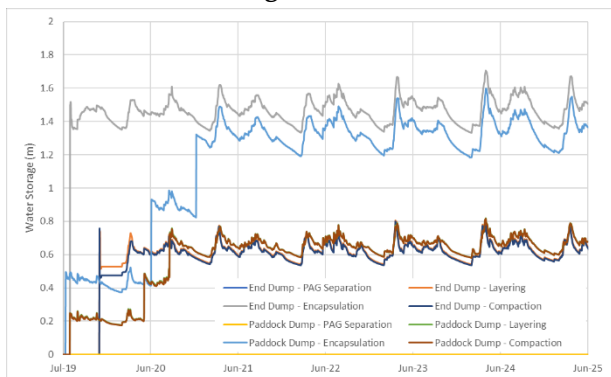
Seepage from Pile (m)



Water Storage Within Pile (m)

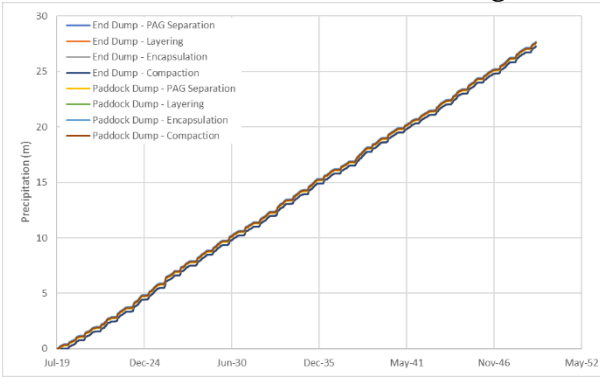


Water Storage Within Pile – PAG (m)

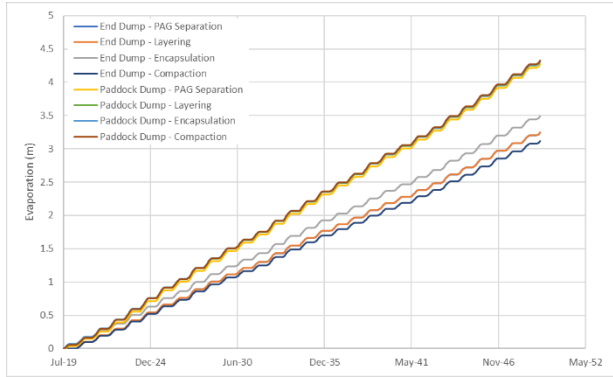


Water Storage Within Pile – NAG (m)

Table A4 - 6: 1-D Column [2,2] – Longterm Behaviour (Year 0 to 50)

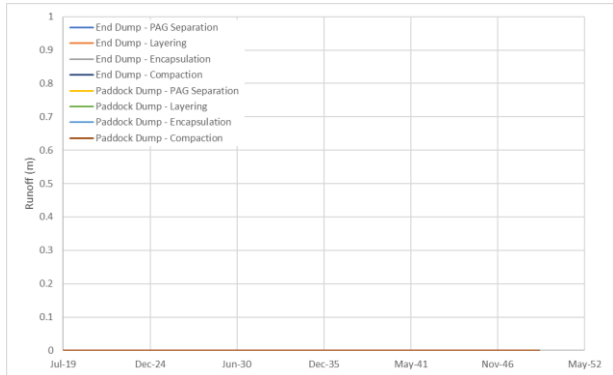


Precipitation on Pile (m)



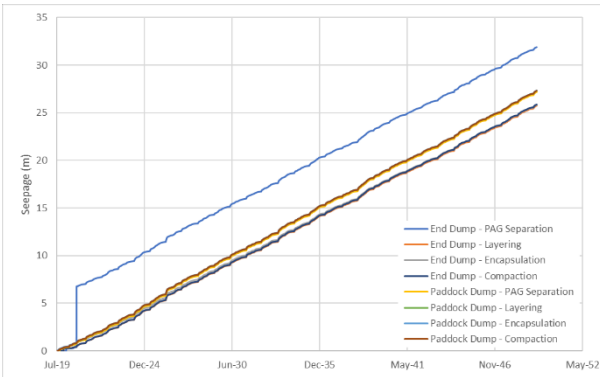
Evaporation from Pile (m)

N/A

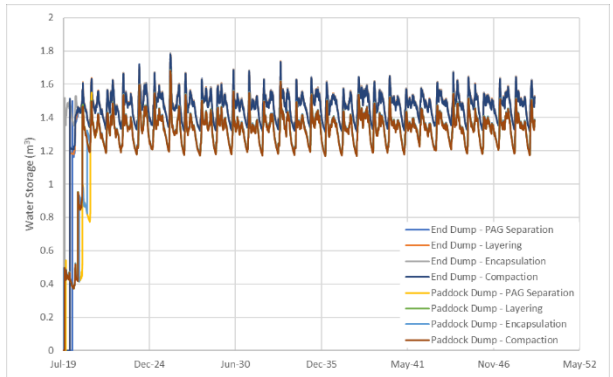


Lateral Runoff from Pile (m)

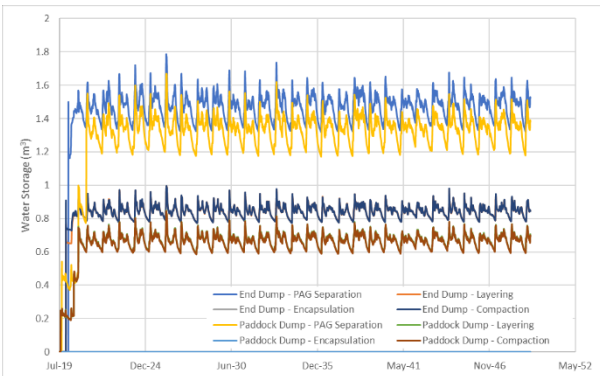
Vertical Runoff Lost from Pile (m)



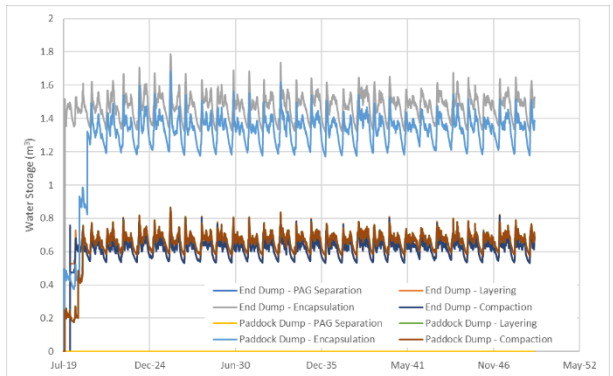
Seepage from Pile (m)



Water Storage Within Pile (m)

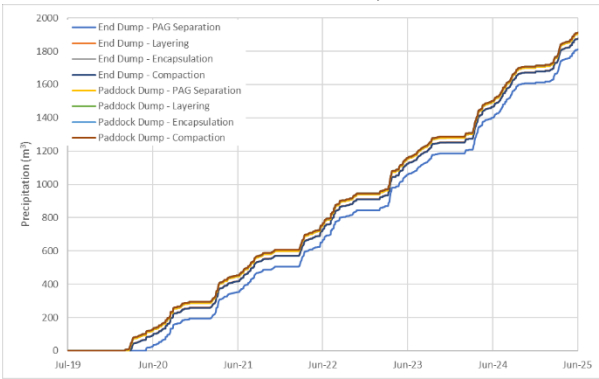


Water Storage Within Pile – PAG (m)

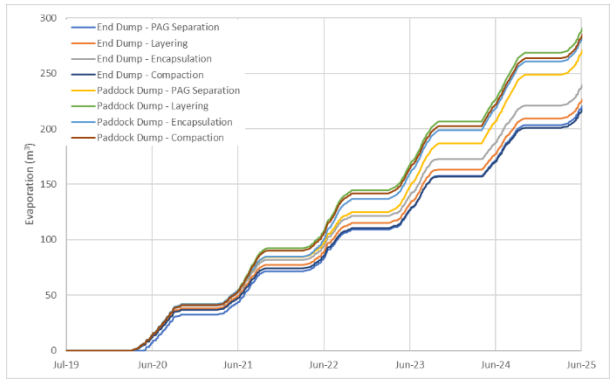


Water Storage Within Pile – NAG (m)

Table A4 - 7: 3-D Column [4,4] – Construction (Year 0 to 6)

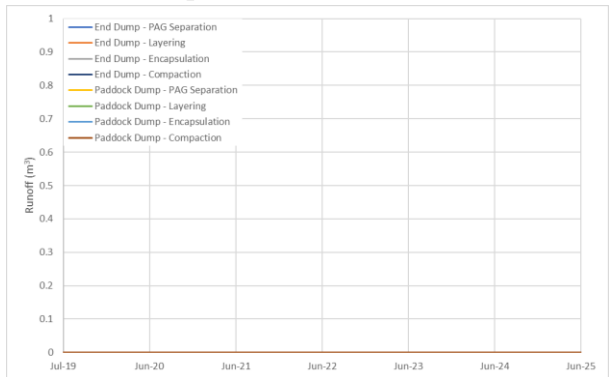


Precipitation on Pile (m³)



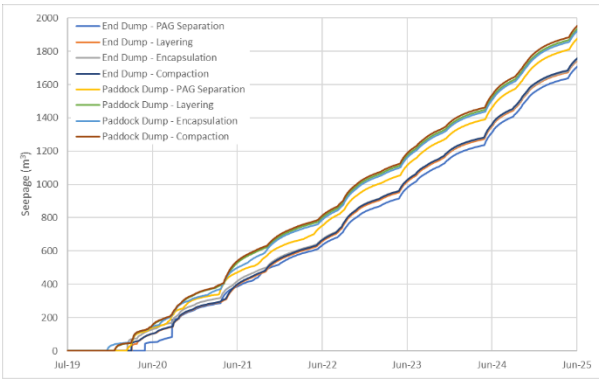
Evaporation from Pile (m³)

N/A

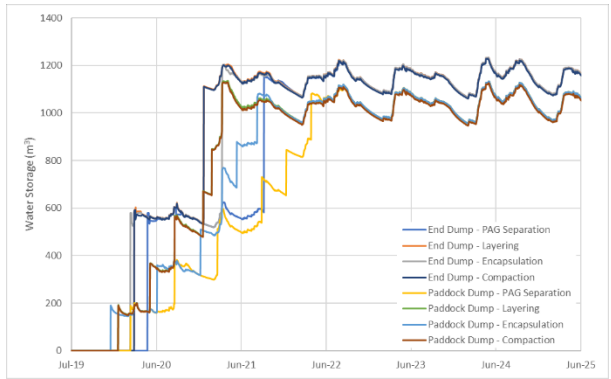


Lateral Runoff from Pile (m³)

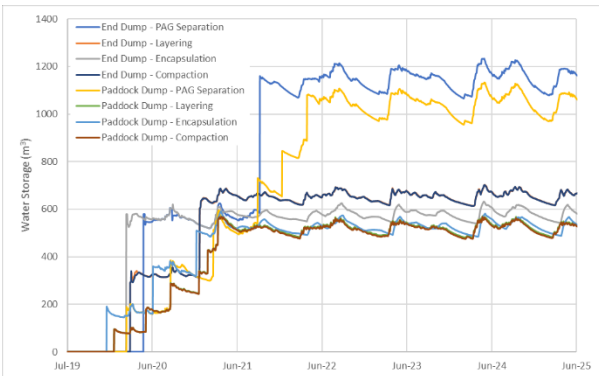
Vertical Runoff Lost from Pile (m³)



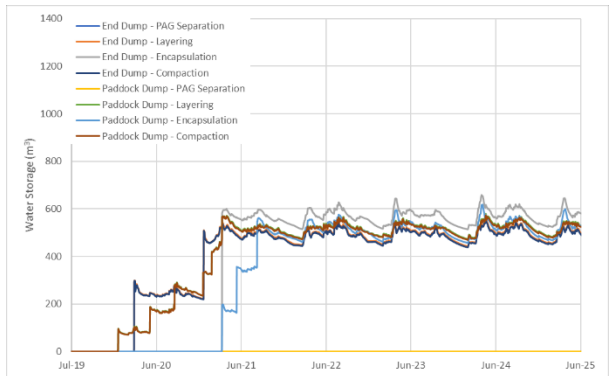
Seepage from Pile (m³)



Water Storage Within Pile (m³)

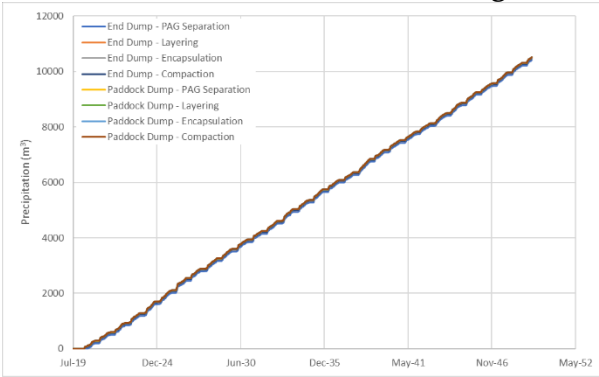


Water Storage Within Pile – PAG (m³)

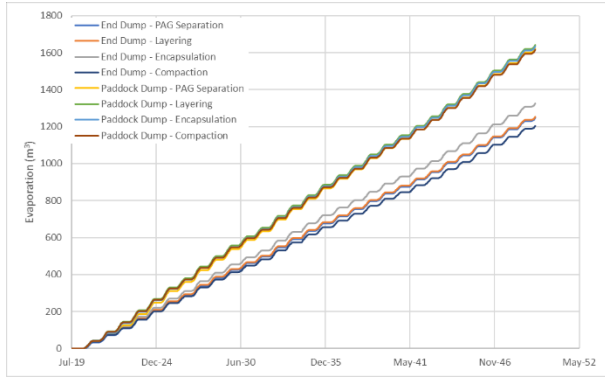


Water Storage Within Pile – NAG (m³)

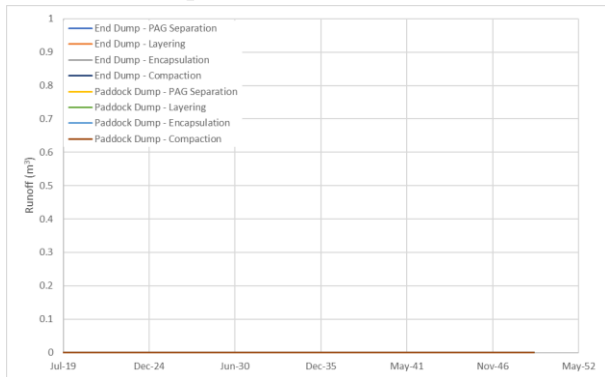
Table A4 - 8: 3-D Column [4,4] – Longterm Behaviour (Year 0 to 50)



Precipitation on Pile (m³)

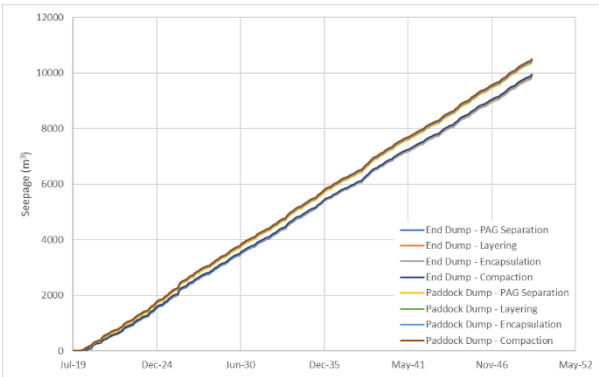


Evaporation from Pile (m³)

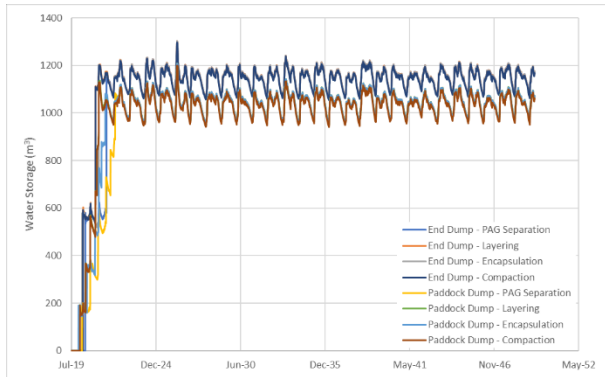


Lateral Runoff from Pile (m³)

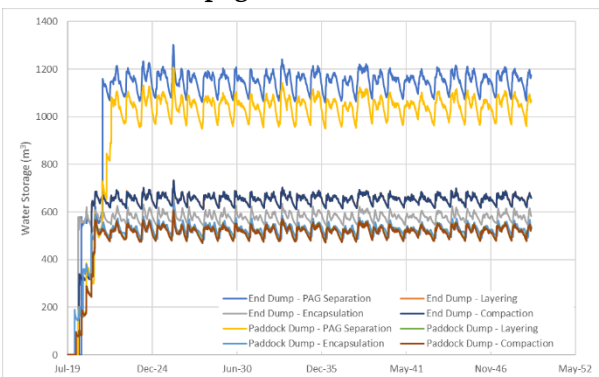
Vertical Runoff Lost from Pile (m³)



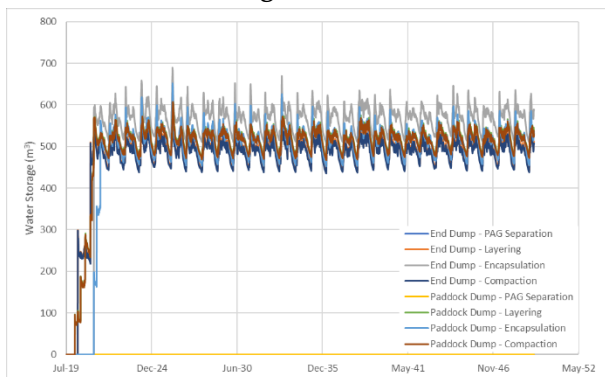
Seepage from Pile (m³)



Water Storage Within Pile (m³)

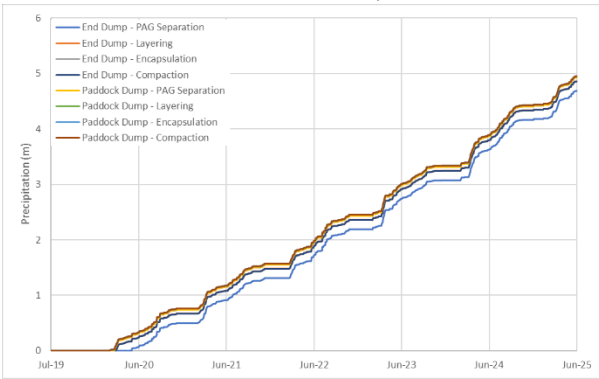


Water Storage Within Pile – PAG (m³)

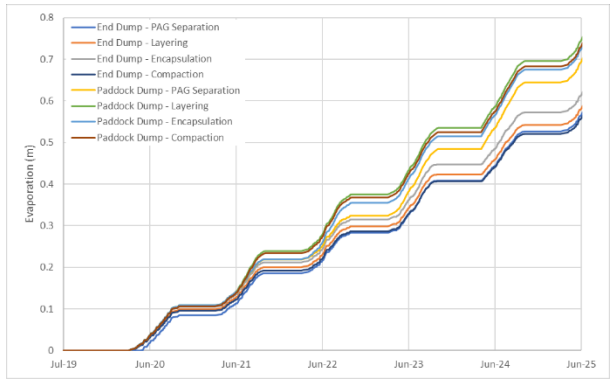


Water Storage Within Pile – NAG (m³)

Table A4 - 9: 1-D Column [4,4] – Construction (Year 0 to 6)

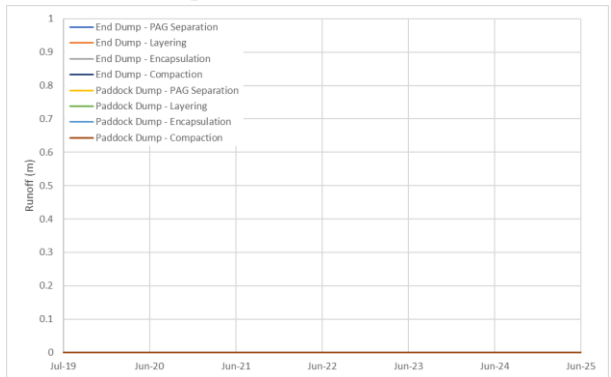


Precipitation on Pile (m)



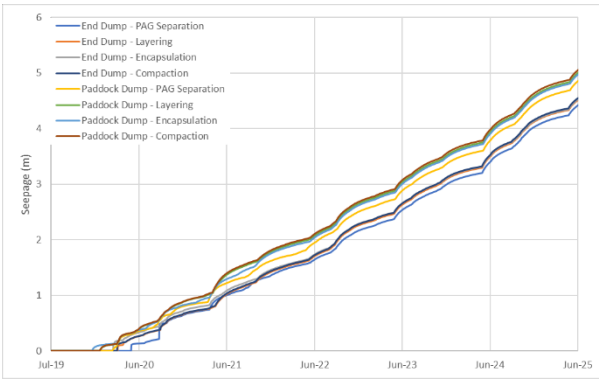
Evaporation from Pile (m)

N/A

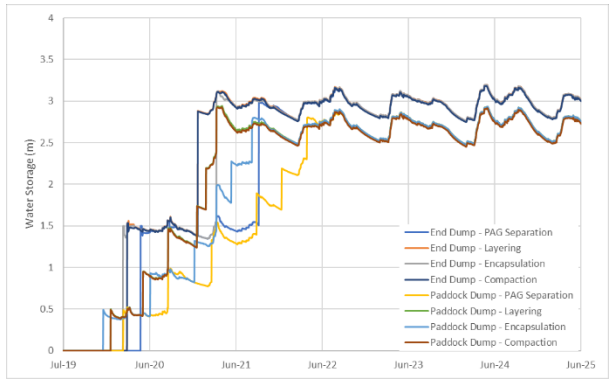


Lateral Runoff from Pile (m)

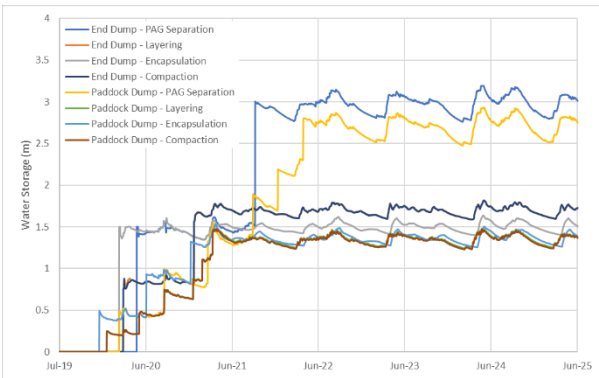
Vertical Runoff Lost from Pile (m)



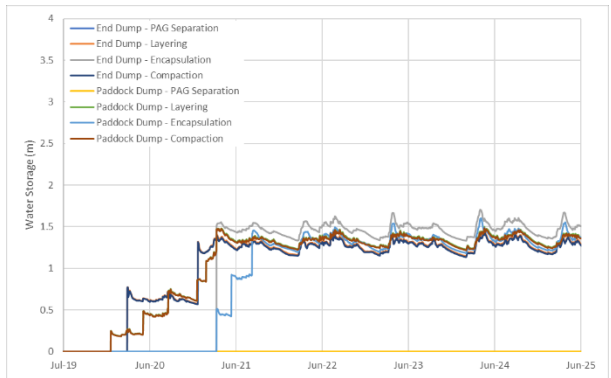
Seepage from Pile (m)



Water Storage Within Pile (m)

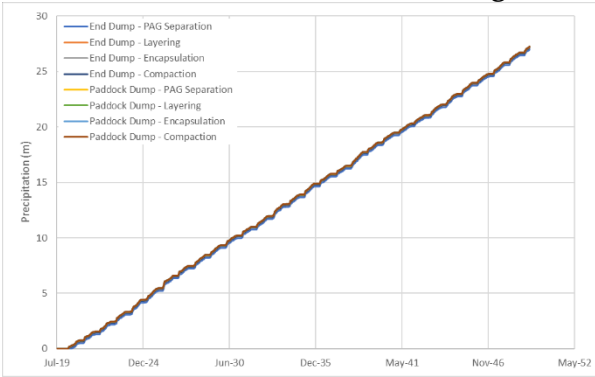


Water Storage Within Pile – PAG (m)

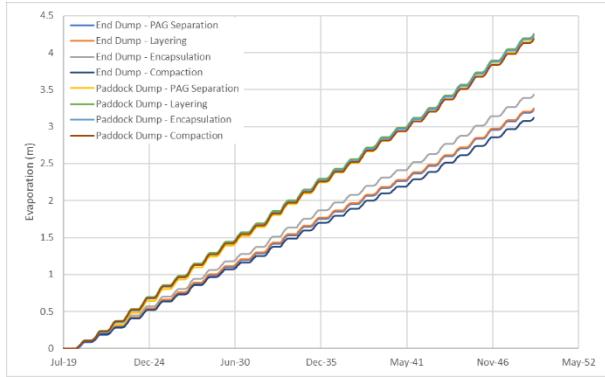


Water Storage Within Pile – NAG (m)

Table A4 - 10: 1-D Column [4,4] – Longterm Behaviour (Year 0 to 50)

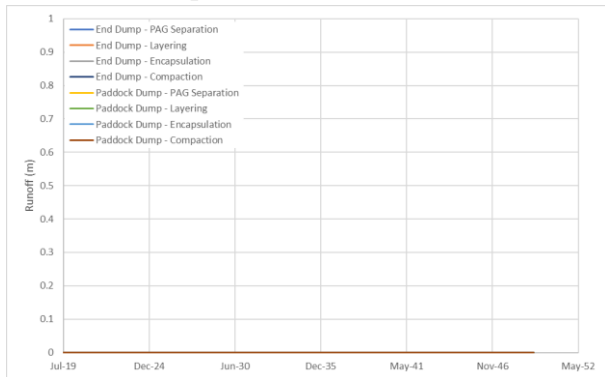


Precipitation on Pile (m)



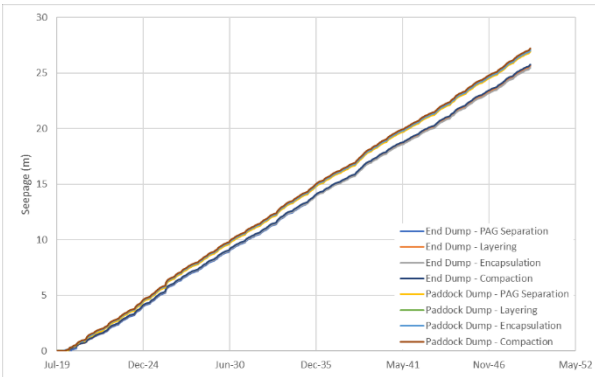
Evaporation from Pile (m)

N/A

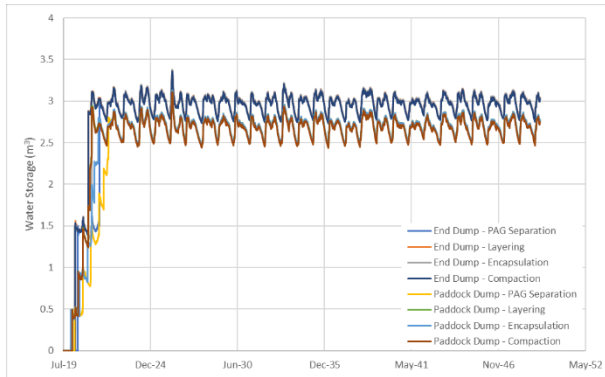


Lateral Runoff from Pile (m)

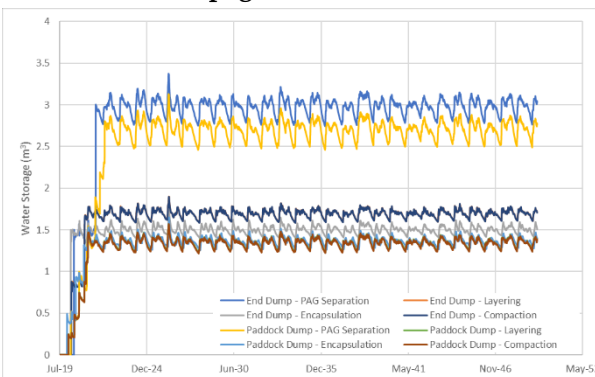
Vertical Runoff Lost from Pile (m)



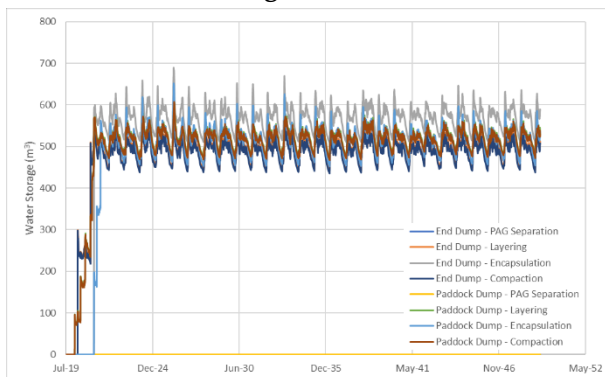
Seepage from Pile (m)



Water Storage Within Pile (m)

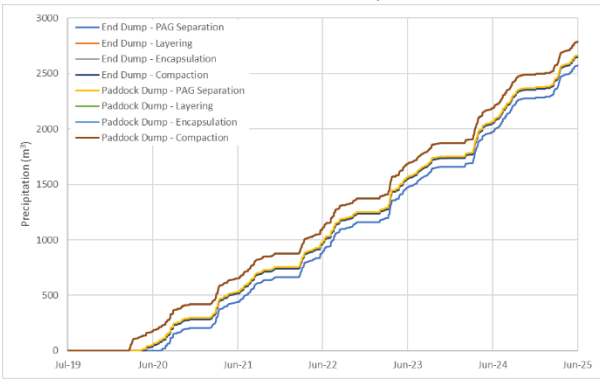


Water Storage Within Pile – PAG (m)

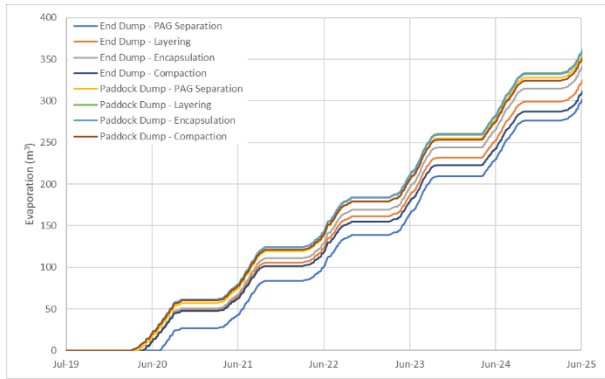


Water Storage Within Pile – NAG (m)

Table A4 - 11: 3-D Column [6,6] – Construction (Year 0 to 6)

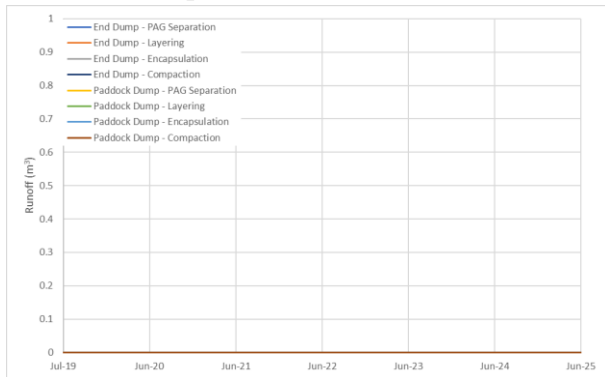


Precipitation on Pile (m³)



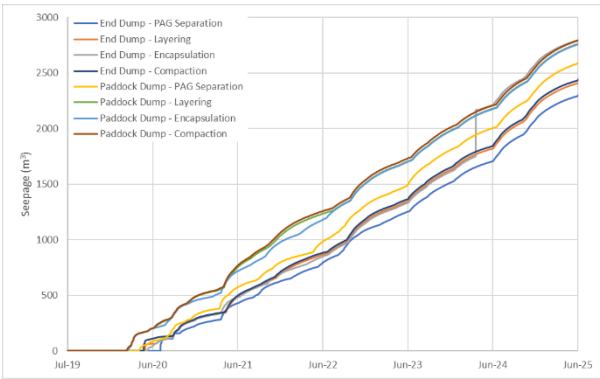
Evaporation from Pile (m³)

N/A

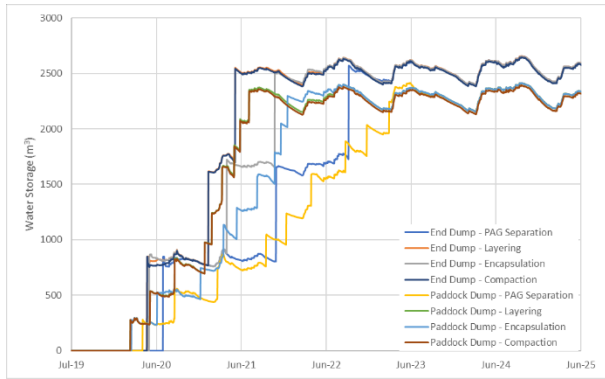


Lateral Runoff from Pile (m³)

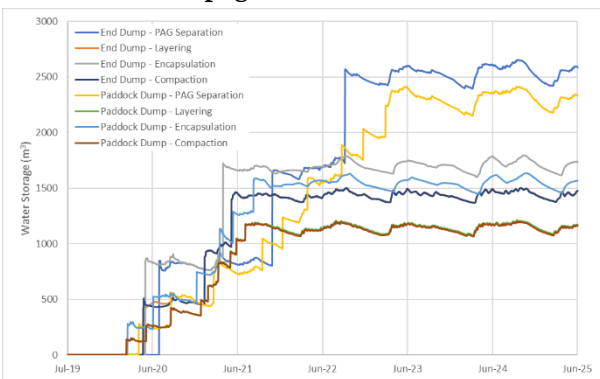
Vertical Runoff Lost from Pile (m³)



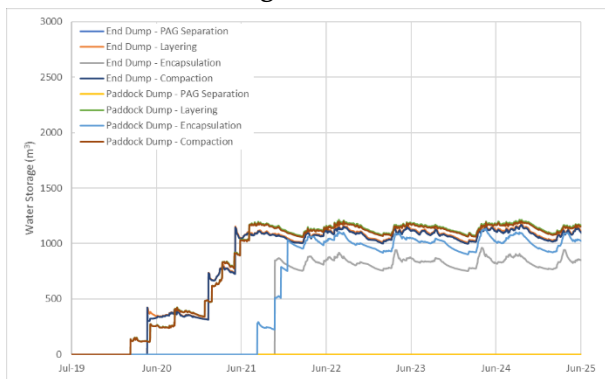
Seepage from Pile (m³)



Water Storage Within Pile (m³)

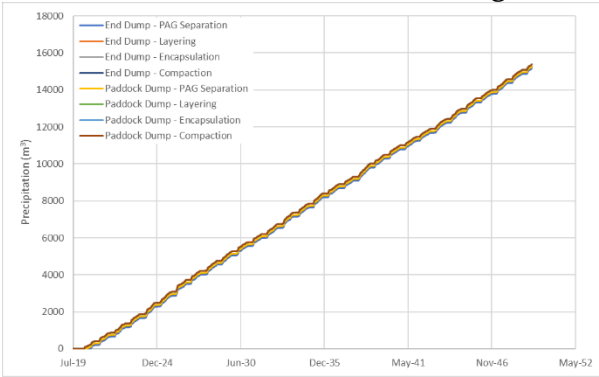


Water Storage Within Pile – PAG (m³)

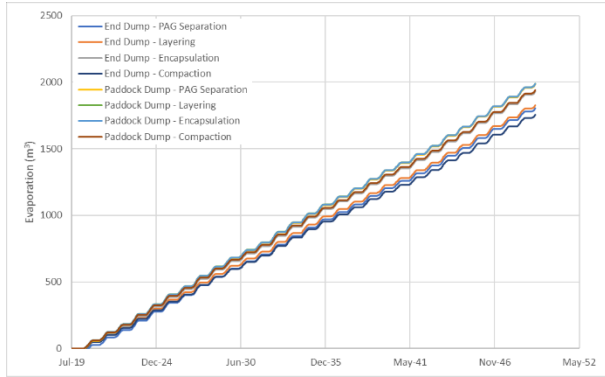


Water Storage Within Pile – NAG (m³)

Table A4 - 12: 3-D Column [6,6] – Longterm Behaviour (Year 0 to 50)

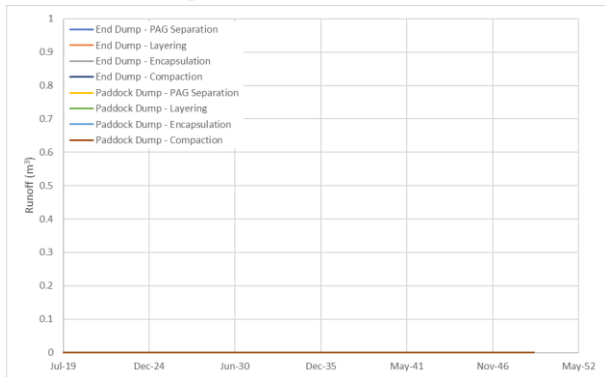


Precipitation on Pile (m³)



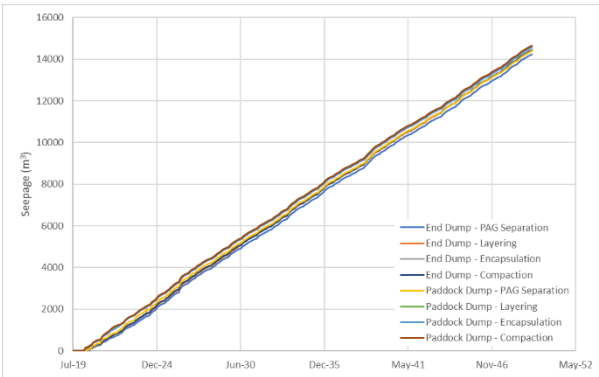
Evaporation from Pile (m³)

N/A

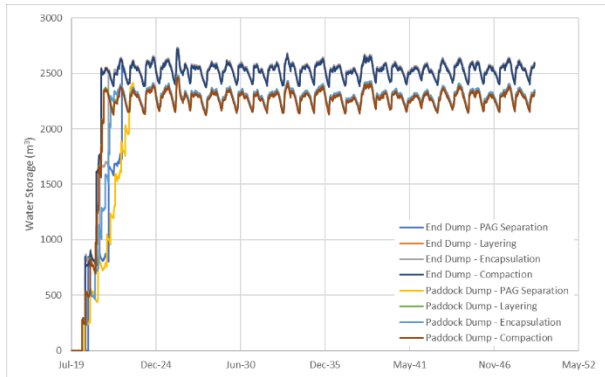


Lateral Runoff from Pile (m³)

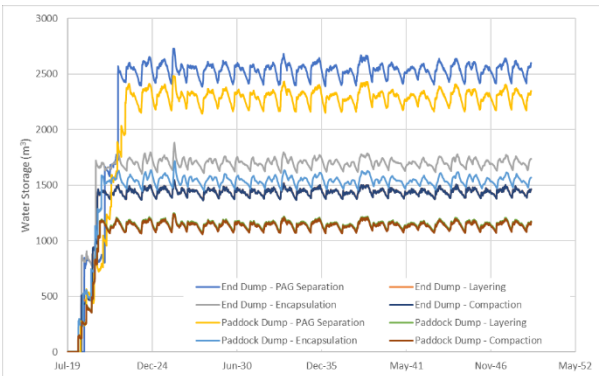
Vertical Runoff Lost from Pile (m³)



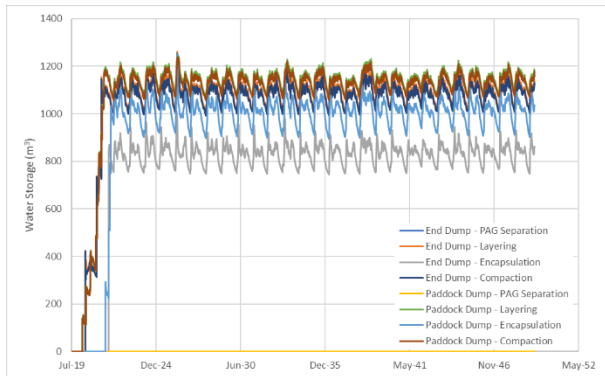
Seepage from Pile (m³)



Water Storage Within Pile (m³)

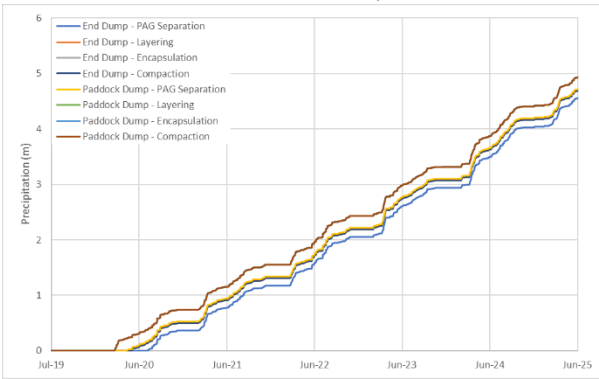


Water Storage Within Pile – PAG (m³)

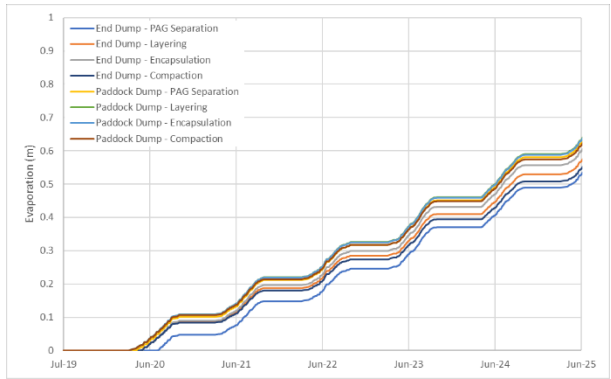


Water Storage Within Pile – NAG (m³)

Table A4 - 13: 1-D Column [6,6] – Construction (Year 0 to 6)

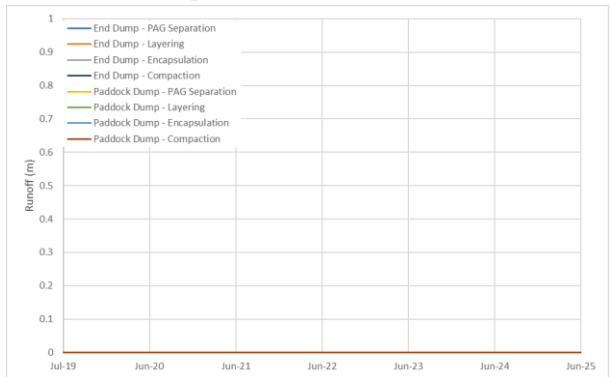


Precipitation on Pile (m)

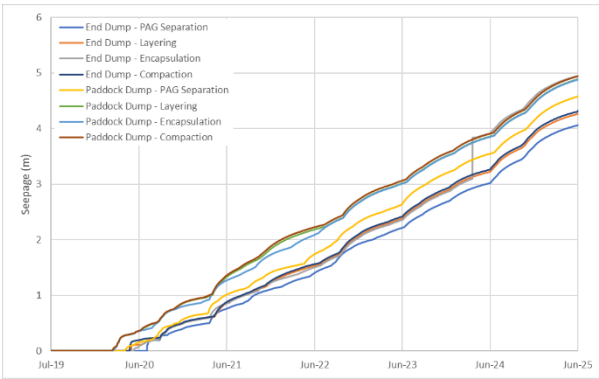


Evaporation from Pile (m)

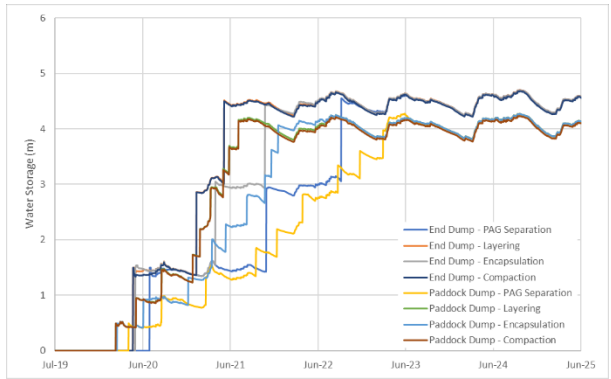
N/A



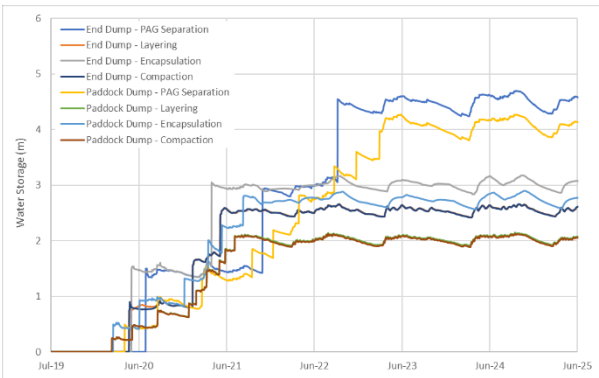
Vertical Runoff Lost from Pile (m)



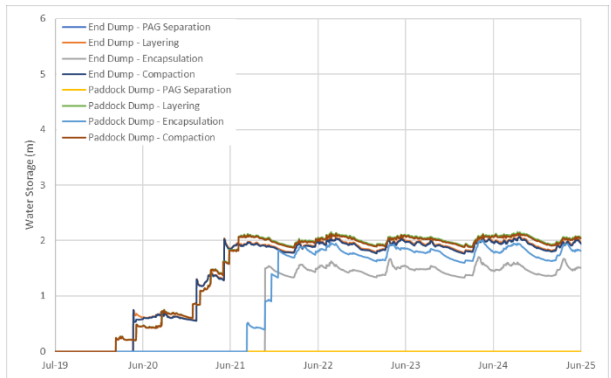
Seepage from Pile (m)



Water Storage Within Pile (m)

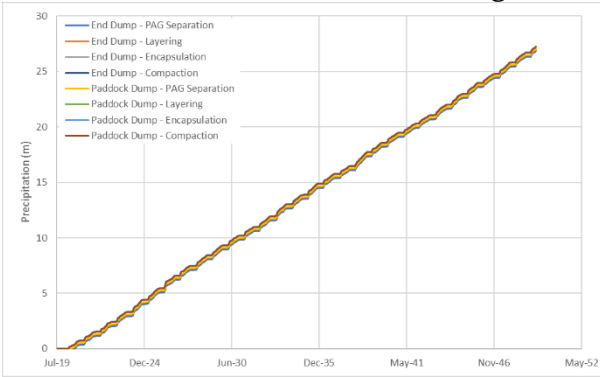


Water Storage Within Pile – PAG (m)

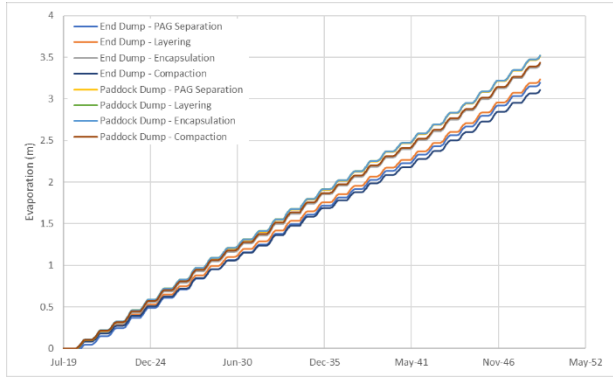


Water Storage Within Pile – NAG (m)

Table A4 - 14: 1-D Column [6,6] – Longterm Behaviour (Year 0 to 50)

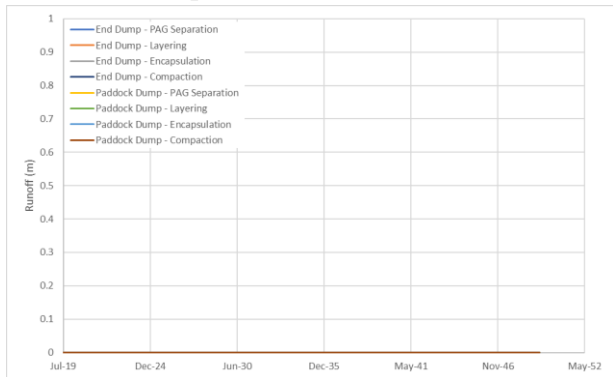


Precipitation on Pile (m)



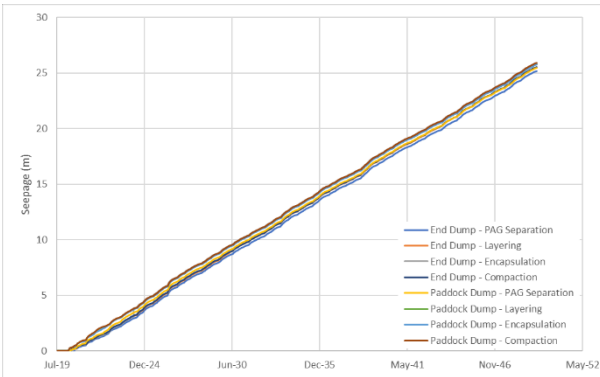
Evaporation from Pile (m)

N/A

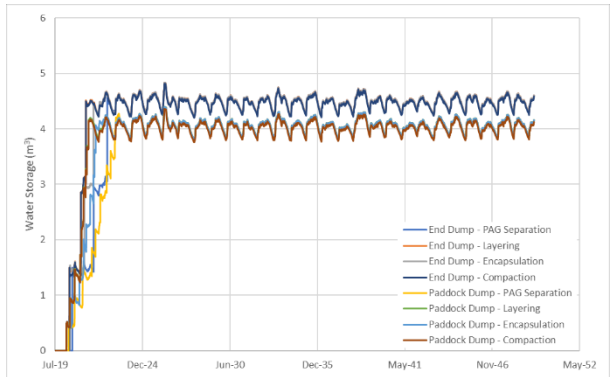


Lateral Runoff from Pile (m)

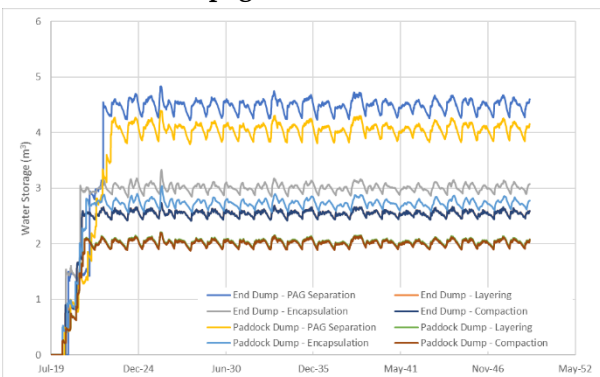
Vertical Runoff Lost from Pile (m)



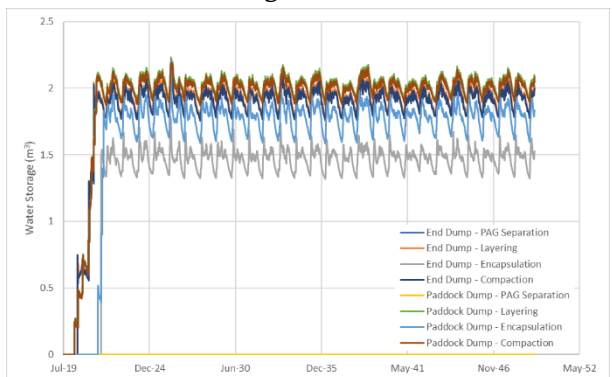
Seepage from Pile (m)



Water Storage Within Pile (m)

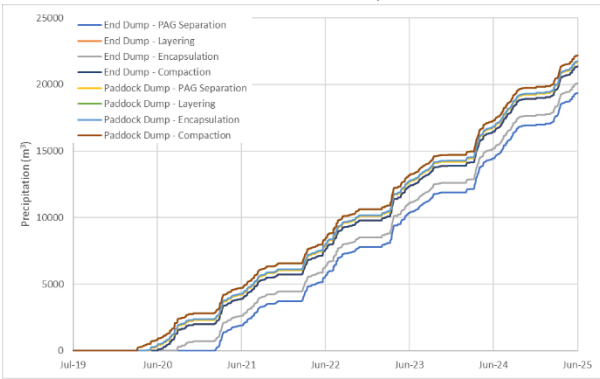


Water Storage Within Pile – PAG (m)

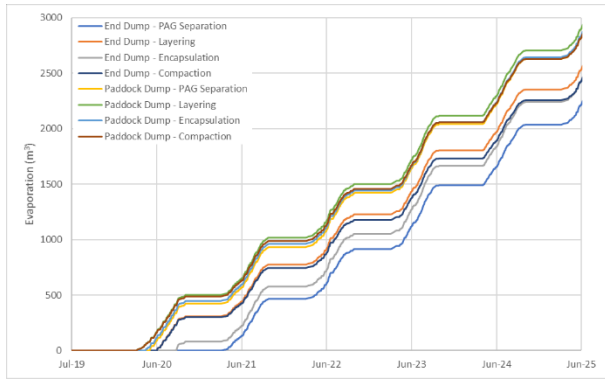


Water Storage Within Pile – NAG (m)

Table A4 - 15: 3-D Column [8,8] – Construction (Year 0 to 6)

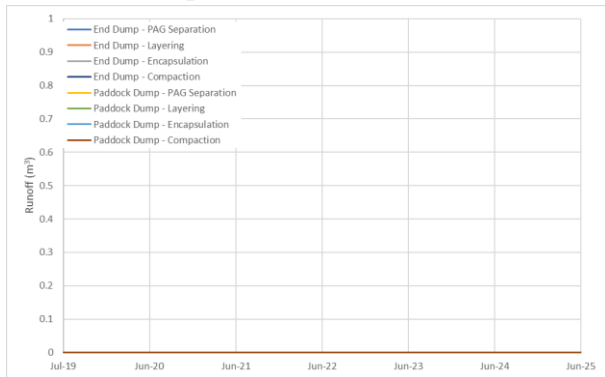


Precipitation on Pile (m³)



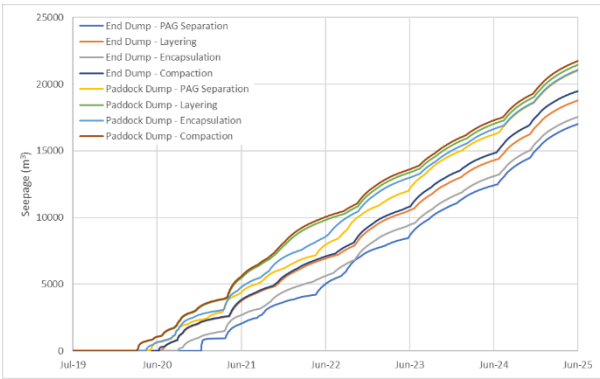
Evaporation from Pile (m³)

N/A

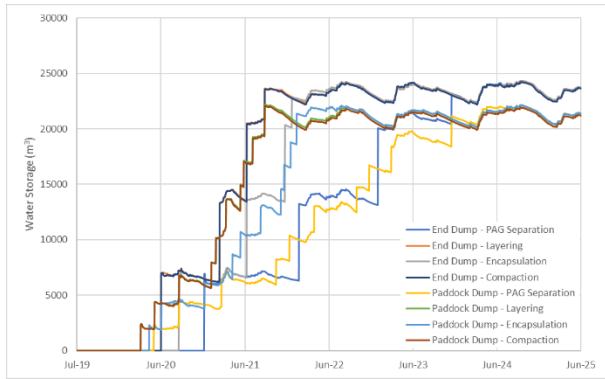


Lateral Runoff from Pile (m³)

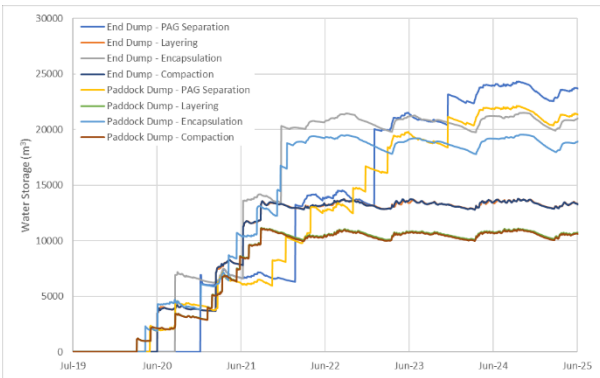
Vertical Runoff Lost from Pile (m³)



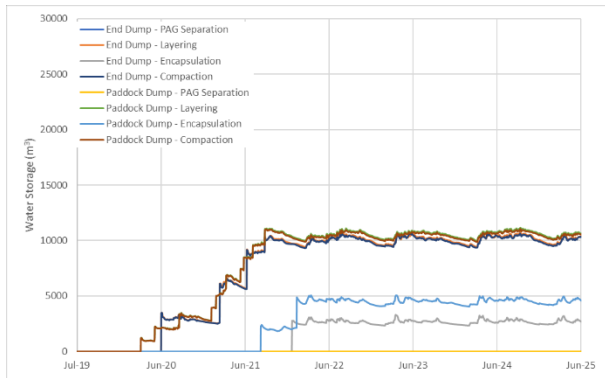
Seepage from Pile (m³)



Water Storage Within Pile (m³)

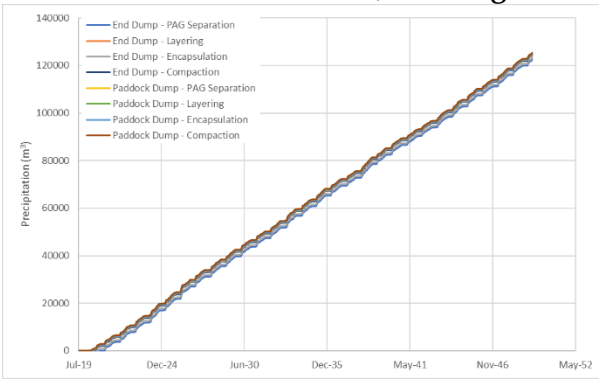


Water Storage Within Pile – PAG (m³)

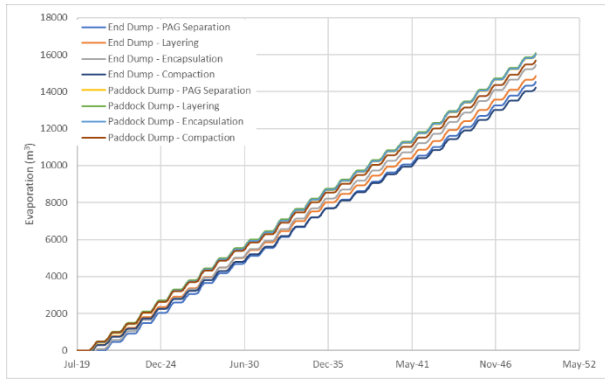


Water Storage Within Pile – NAG (m³)

Table A4 - 16: 3-D Column [8,8] – Longterm Behaviour (Year 0 to 50)

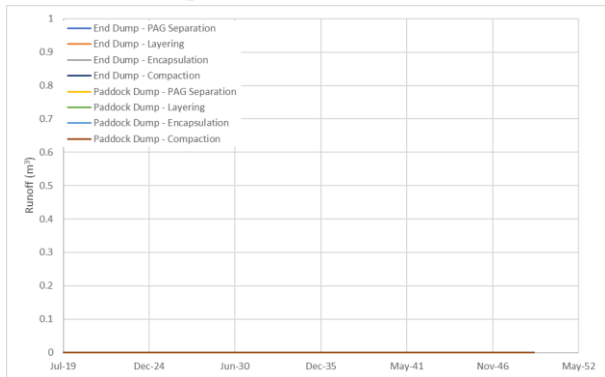


Precipitation on Pile (m³)



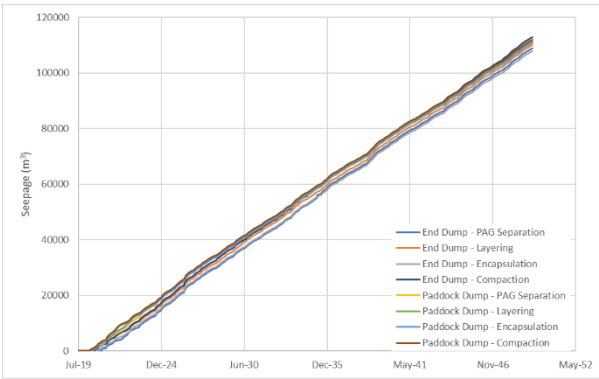
Evaporation from Pile (m³)

N/A

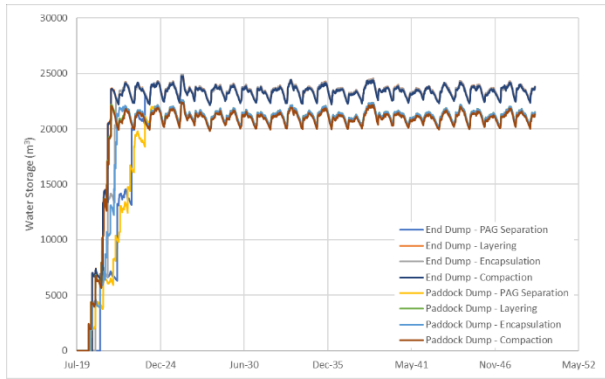


Lateral Runoff from Pile (m³)

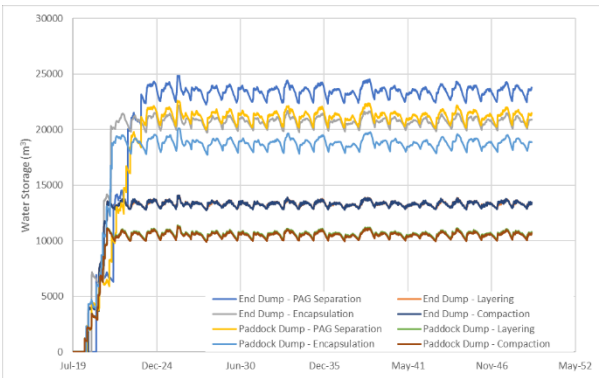
Vertical Runoff Lost from Pile (m³)



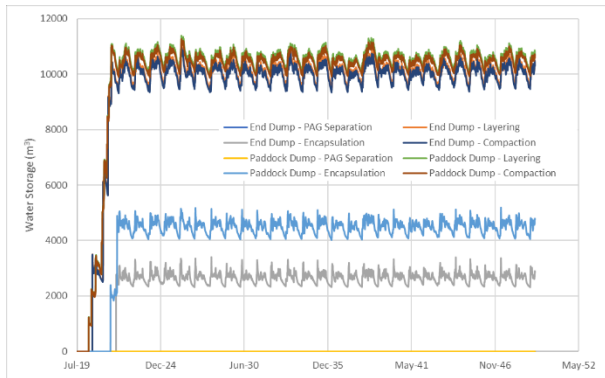
Seepage from Pile (m³)



Water Storage Within Pile (m³)

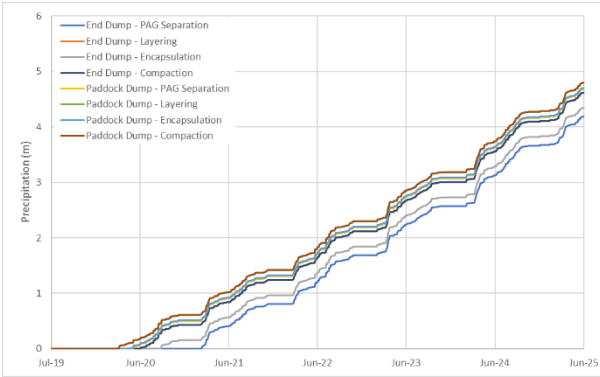


Water Storage Within Pile – PAG (m³)

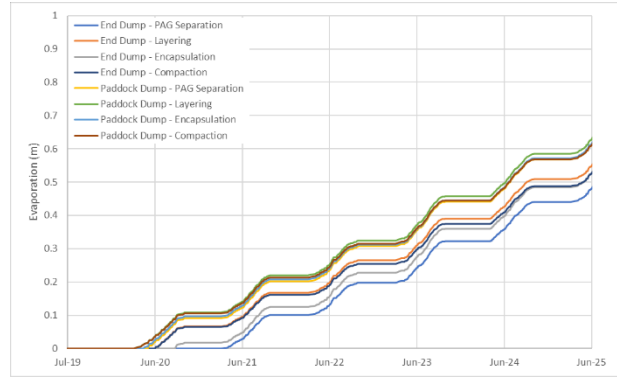


Water Storage Within Pile – NAG (m³)

Table A4 - 17: 1-D Column [8,8] – Construction (Year 0 to 6)

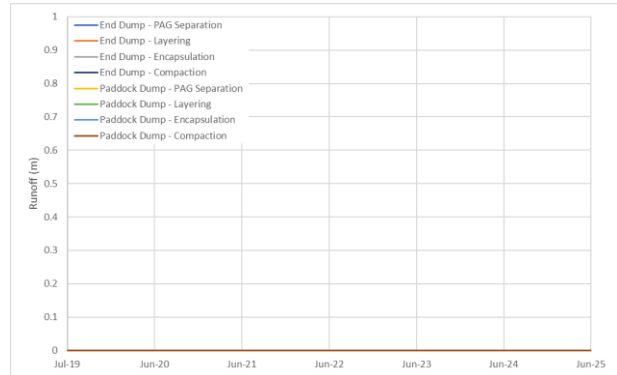


Precipitation on Pile (m)



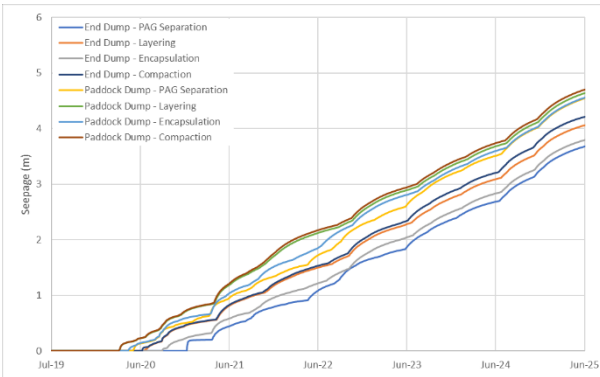
Evaporation from Pile (m)

N/A

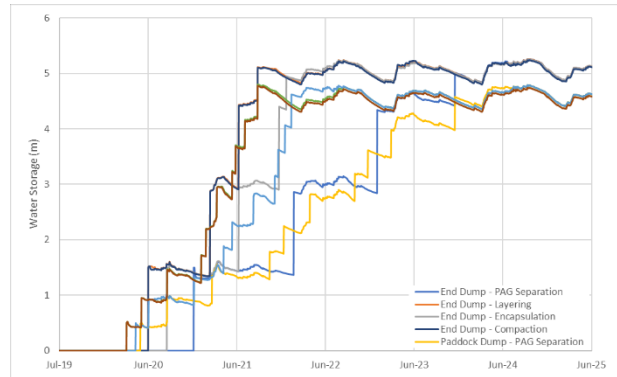


Lateral Runoff from Pile (m)

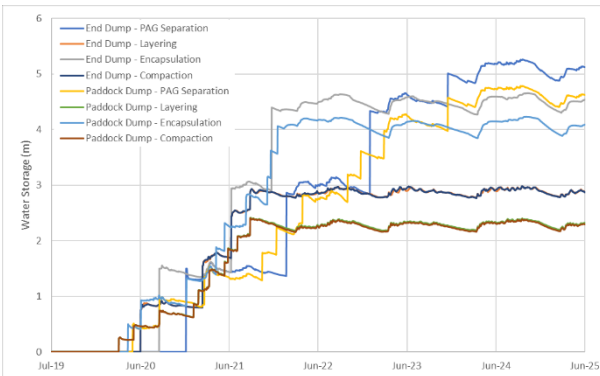
Vertical Runoff Lost from Pile (m)



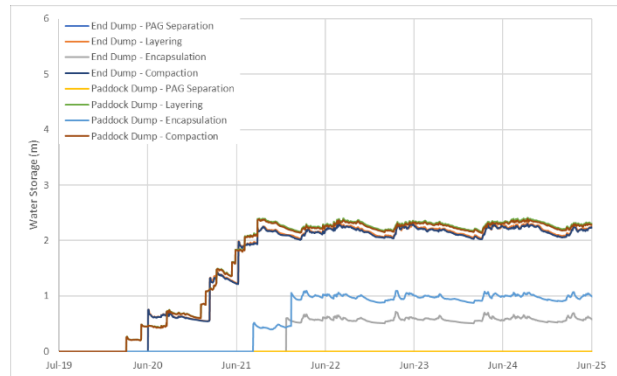
Seepage from Pile (m)



Water Storage Within Pile (m)

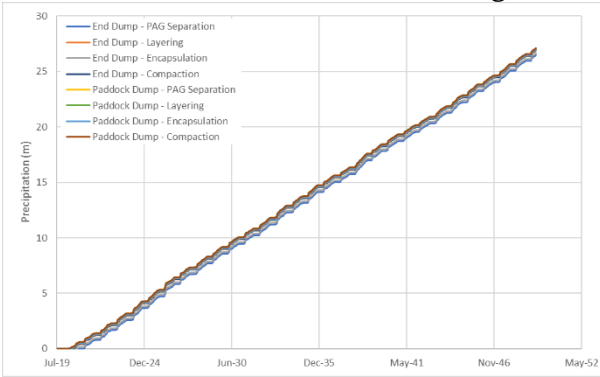


Water Storage Within Pile – PAG (m)

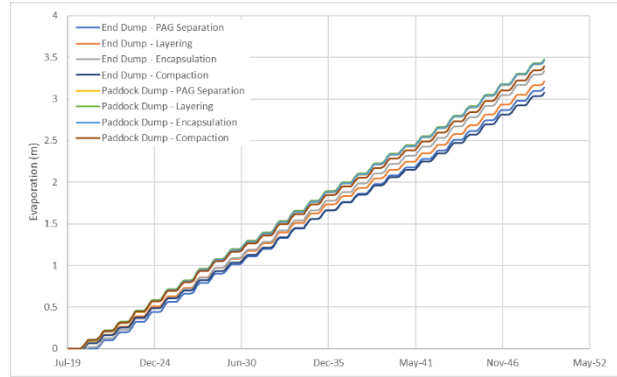


Water Storage Within Pile – NAG (m)

Table A4 - 18: 1-D Column [8,8] – Longterm Behaviour (Year 0 to 50)

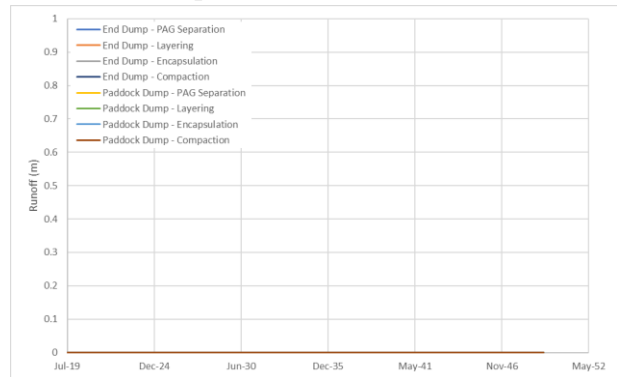


Precipitation on Pile (m)



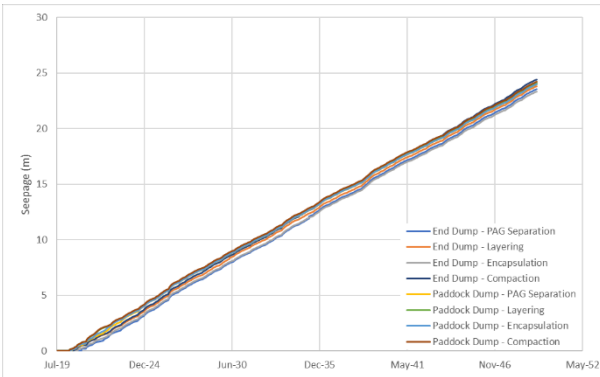
Evaporation from Pile (m)

N/A

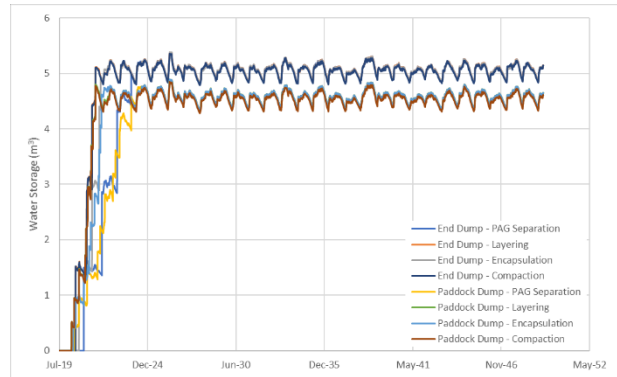


Lateral Runoff from Pile (m)

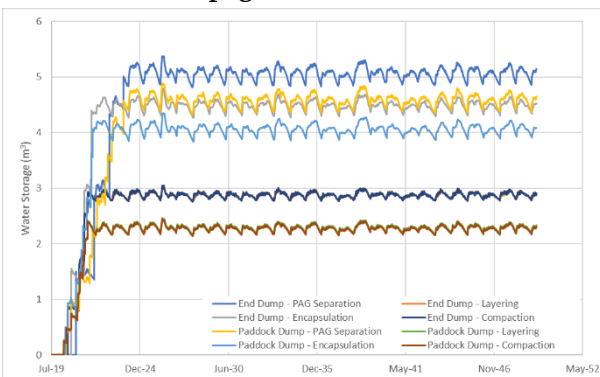
Vertical Runoff Lost from Pile (m)



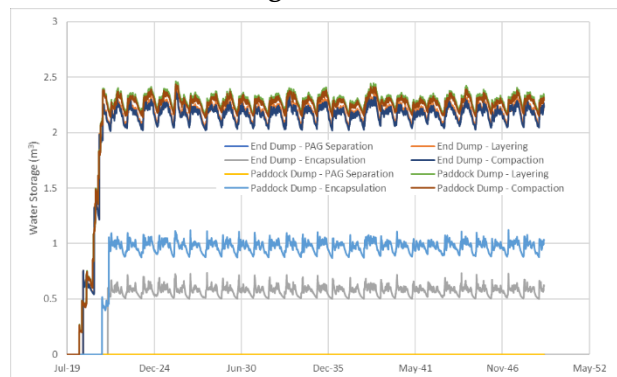
Seepage from Pile (m)



Water Storage Within Pile (m)



Water Storage Within Pile – PAG (m)



Water Storage Within Pile – NAG (m)